

The Influence of the Electrolyte on the Electrochemical Behavior of PTMA as Cathodic Electrode Material

Dissertation

(kumulativ)

zur Erlangung des akademischen Grades doctor rerum naturalium

(Dr. rer. nat)

vorgelegt dem Rat der Chemisch-Geowissenschaftlichen Fakultät der
Friedrich-Schiller-Universität Jena

von M.Sc. Patrick Gerlach

geboren am 04.05.1993 in Heilbad Heiligenstadt

Dissertation, Friedrich-Schiller-Universität Jena, 2022

Gutachter:

1. Prof. Dr. Andrea Balducci, Friedrich-Schiller-Universität Jena
2. Prof. Dr. Ulrich S. Schubert, Friedrich-Schiller-Universität Jena
3. Prof. Dr. David Mecerreyes, Universität des Baskenlandes (UPV/EHU)

Tag der Verteidigung: 05.01.2022

Danksagung

Mit der Fertigstellung dieser Dissertation endet ein prägender Teil meines bisherigen Lebens. Ich verbinde die letzten vier Jahre mit unzähligen schönen Momenten. Ich durfte mein Wissen erweitern, interessante Menschen treffen, neue Orte kennenlernen und bin mit meinen Aufgaben gewachsen. Ich danke daher Prof. Andrea Balducci für alle Möglichkeiten, die er mit in den letzten Jahren geboten hat. Zudem möchte ich ihm für viele hilfreiche wissenschaftliche Diskussionen und interessante Projekte, an denen ich mitwirken konnte, danken. Weiterhin danke Ich Prof. Ulrich S. Schubert für das Zweitgutachten meiner Dissertation.

Ich danke außerdem Lukas Medenbach und Simon Münch für ihre sehr hilfreichen wissenschaftlichen Meinungen zu meiner Arbeit. Dank gilt auch Jakob Krummacher und insbesondere Christoph Schütter, die ihre elektrochemische Erfahrung und ihr Wissen mit mir geteilt und mir somit den Einstieg in die Thematik meiner Promotion bereitet haben. Ebenso danke ich Saskia Sabrina Thieme für die großartige Organisation ohne die vieles in den letzten Jahren nicht möglich gewesen wäre. Ich danke zudem René Burges für die Polymersynthese und die Elektrodenfilme.

Ein großer Dank gilt der gesamten AG Balducci und Pietro Zaccagnini für das sehr gute Arbeitsklima, die interessanten Diskussionen, die Kaffeepausen und generell dafür, die Arbeit zu einem schönen Ort zu machen.

Weiterhin danke ich Lisann, die mich immer auf meinem Weg begleitet, für die emotionale Unterstützung in meinem Leben.

Ich danke außerdem meinen Eltern für ihre unendliche Unterstützung, ohne die ich nicht da stehen würde, wo ich heute bin.

Zuletzt danke ich meiner ganzen Familie und meinen Freunden für ihre positive Einstellung, Zuverlässigkeit, Hilfe und dafür mein Leben zu bereichern.

Selbstständigkeitserklärung

Ich erkläre, dass ich die vorliegende Arbeit selbständig und unter Verwendung der angegebenen Hilfsmittel, persönlichen Mitteilungen und Quellen angefertigt habe.

Jena, 01.07.2021

Ort, Datum

Unterschrift

Erklärung zu den Eigenanteilen/ Declaration of Authorship

| | | | | | |
|--|------------|----------|--|--|--|
| <p>P1: <i>A Critical Analysis about the Underestimated Role of the Electrolyte in Batteries Based on Organic Materials; ChemElectroChem, 7 (2020), 2364-2375.</i></p> <p><u>P. Gerlach</u>¹, A. Balducci²</p> | | | | | |
| Author | 1 | 2 | | | |
| Conceptual Contribution | • | • | | | |
| Literature research | • | | | | |
| Preparation of manuscript | • | | | | |
| Correction of manuscript | | • | | | |
| Proposal for crediting publication equivalents | 0.5 | | | | |

| | | | | | |
|---|------------|----------|----------|----------|----------|
| <p>P2: <i>The influence of the electrolyte composition on the electrochemical behaviour of cathodic materials for organic radical batteries; Journal of Power Sources 405 (2018), 142-149.</i></p> <p><u>P. Gerlach</u>¹, R. Burges², A. Lex-Balducci³, U. S. Schubert⁴, A. Balducci⁵</p> | | | | | |
| Author | 1 | 2 | 3 | 4 | 5 |
| Conceptual contribution | • | | | | • |
| Polymer synthesis | | • | | | |
| Electrode preparation | • | • | | | |
| Electrochemical tests | • | | | | |
| Data evaluation | • | | | | |
| Preparation of manuscript | • | | | | |
| Correction of manuscript | | | • | • | • |
| Proposal for crediting publication equivalents | 0.5 | | | | |

P3: *Influence of the salt concentration on the electrochemical performance of electrodes for polymeric batteries; Electrochimica Acta 306 (2019): 610-616.*
P. Gerlach¹, R. Burges², A. Lex-Balducci³, U. S. Schubert⁴, A. Balducci⁵

| Author | 1 | 2 | 3 | 4 | 5 |
|--|------------|---|---|---|---|
| Conceptual contribution | • | | | | • |
| Polymer synthesis | | • | | | |
| Electrode preparation | • | • | | | |
| Electrochemical tests | • | | | | |
| Data evaluation | • | | | | |
| Preparation of manuscript | • | | | | |
| Correction of manuscript | | | • | • | • |
| Proposal for crediting publication equivalents | 1.0 | | | | |

P4: *Aprotic and Protic Ionic Liquids as Electrolytes for Organic Radical Polymers; Journal of The Electrochemical Society 167 (2020): 120546.*
P. Gerlach¹, R. Burges², A. Lex-Balducci³, U. S. Schubert⁴, A. Balducci⁵

| Author | 1 | 2 | 3 | 4 | 5 |
|--|------------|---|---|---|---|
| Conceptual contribution | • | | | | • |
| Polymer synthesis | | • | | | |
| Electrode preparation | • | • | | | |
| Electrochemical tests | • | | | | |
| Data evaluation | • | | | | |
| Preparation of manuscript | • | | | | |
| Correction of manuscript | | | • | • | • |
| Proposal for crediting publication equivalents | 1.0 | | | | |

P5: *The influence of current density, rest time and electrolyte composition on the self-discharge of organic radical polymers; Electrochimica Acta 377 (2021): 138070.*
P. Gerlach¹, A. Balducci²

| Author | 1 | 2 | | | |
|--|------------|---|--|--|--|
| Conceptual contribution | • | • | | | |
| Electrochemical tests | • | | | | |
| Data evaluation | • | | | | |
| Preparation of manuscript | • | | | | |
| Correction of manuscript | | • | | | |
| Proposal for crediting publication equivalents | 1.0 | | | | |

Erklärung zu den Eigenanteilen des Promovenden sowie der weiteren Doktorandinnen/Doktoranden als Co-Autorinnen/-Autoren an den Publikationen und Zweitpublikationsrechten bei einer kumulativen Dissertation.

Für alle in dieser kumulativen Dissertation verwendeten Manuskripte liegen die notwendigen Genehmigungen der Verlage („Reprint permissions“) für die Zweitpublikation vor.

Die Co-Autorinnen/-Autoren der in dieser kumulativen Dissertation verwendeten Manuskripte sind sowohl über die Nutzung, als auch über die oben angegebenen Eigenanteile der weiteren Doktorandinnen/Doktoranden als Co-Autorinnen/-Autoren an den Publikationen und Zweitpublikationsrechten bei einer kumulativen Dissertation informiert und stimmen dem zu.

Die Anteile des Promovenden sowie der weiteren Doktorandinnen/Doktoranden als Co-Autorinnen/Co-Autoren an den Publikationen und Zweitpublikationsrechten bei einer kumulativen Dissertation sind in der Anlage aufgeführt.

Name des Promovenden/ Datum, Ort, Unterschrift des Promovenden

Ich bin mit der Abfassung der Dissertation als publikationsbasierte Dissertation, d.h. kumulativ, einverstanden und bestätige die vorstehenden Angaben.

Name Betreuer/ Datum, Ort, Unterschrift Betreuer

Abstract

For the realization of sustainable energy storage, technologies beyond the state-of-the-art lithium-ion battery are needed. One technology, which could be able to supplement the future electrochemical energy storage landscape in this regard are organic batteries, which use redox active organic molecules or polymers as electrode active materials. These redox materials include compounds like conducting polymers, carbonyls, organo-sulfurs or organic stable radicals and provide beneficial properties like a high theoretical gravimetric capacity, good safety, mechanical flexibility and producibility from abundant elements (C, H, O, N, S).

Especially the development of organic stable radical polymers received a lot of research interest in the last 20 years. These redox active materials excelled particularly in terms of rate capability and coulombic efficiency, when used in combination with a lithium-ion-based anode and electrolyte. One polymer, which has to be mentioned especially, is poly(2,2,6,6-tetramethyl-4-piperinidyl-N-oxyl methacrylate) (PTMA). PTMA, which has been thoroughly investigated as cathode material in a lithium-ion battery setup and became a standard material in organic battery research, provides a specific capacity near the theoretical value of 111 mAh g^{-1} , a stable redox potential of $3.6 \text{ V vs. Li}^+/\text{Li}$ and a high capacity retention at elevated current densities in state-of-the-art battery electrolytes such as 1 M LiPF_6 in EC/DMC. However, these electrolytes cause concerns in safety due to toxicity and flammability. Furthermore, the organic nature of these electrolytes promotes the dissolution of PTMA in the cell, which limits the cycle life and increases the self-discharge rate.

Although these problems are evident, for a long time there has been a lack of investigations addressing the important role of the electrolyte for PTMA and organic batteries in general. In fact, in consideration of the energy storage mechanism of PTMA, it is clear that electrolyte properties like ion concentration, conductivity and viscosity etc. will affect the electrochemical performance of PTMA-based electrodes in a major way. With respect to the existing approaches on electrolytes in this field, which have been pre-

sented in publication 1 (review article), it must be stated that more detailed studies towards the impact of the electrolyte on the electrochemical behavior of PTMA and other organic materials are necessary in order to optimize their performance in energy storage application.

Therefore, this thesis uses PTMA as a model active material and performs a systematic study on the influence of the electrolyte on the electrochemical behavior of PTMA-based electrodes. Thereby, in four different publications, special attention is paid to the influence of the electrolyte composition, the electrolyte concentration, the use of ionic liquids as electrolytes for PTMA and the self-discharge behavior of PTMA-based electrodes in different electrolytes.

The investigation of this topic starts with publication 2 in which PTMA is tested in a half-cell setup in combination with 3 different metal-free electrolytes, namely 1M 1-butyl-1-methylpyrrolidinium bis(trifluoromethylsulfonyl)imide (Pyr₁₄TFSI) in propylene carbonate (PC), tetraethylammonium bis(trifluoromethylsulfonyl)imide (Et₄NTFSI) in PC and neat Pyr₁₄TFSI, which is an ionic liquid. The results of this publication show a significant impact of the used conducting salt and the nature of the electrolyte on the performance of PTMA. In 1M Pyr₁₄TFSI in PC, PTMA delivers a high specific capacity of 100 mAh g⁻¹ as well as good rate capability. On the other hand, in 1M Et₄NTFSI in PC a far lower specific capacity is observed, although only the cation is changed in the system. Due to the low conductivity of pure Pyr₁₄TFSI, a reduction in capacity and rate capability is found for PTMA in this electrolyte. However, the high viscosity has a beneficial effect on the stability and self-discharge performance in comparison to the organic electrolytes. This is achieved due to the reduction of the dissolution of PTMA into this electrolyte. Furthermore, in this work hybrid devices containing a PTMA cathode and an activated carbon negative electrode are realized with 1M Pyr₁₄TFSI in PC as well as neat Pyr₁₄TFSI. Both systems are successfully cycled for 10000 cycles at a high current density of 10C. There, a beneficial effect of the ionic liquid-based electrolyte on the cycling stability is obtained as well.

After the investigation of the electrolyte composition on the electrochemical behavior of PTMA, publication 3 focusses on the impact of the electrolyte concentration. There PTMA is tested with 1, 2 and 3M 1-butyl-1-methylpyrrolidinium tetrafluoroborate

(Pyr₁₄BF₄) in PC. By doing so, a comparable performance is found for PTMA at low rates in all electrolytes, while at elevated currents the better transport of the low concentrated mixtures becomes evident. On the other side, the 3M electrolyte provides superior performance in terms of self-discharge of the electrodes. While in the 1M solution, the PTMA-based electrode is completely self-discharged after 4.5 days, in the 3M electrolyte residual charge is obtained even after 11 days of rest. The mechanism of this charge loss is found to be a diffusion-limited process probably due to dissolved active material, which works as redox shuttles in the electrolyte. Therefore, the increased viscosity of the 3M solution hinders this diffusion and thus reduced the charge loss in rest.

Since in publication 2 and 3 beneficial effects of high concentrated electrolytes on the electrochemical performance of PTMA have been found, PTMA is tested with two aprotic ionic liquids, namely Pyr₁₄TFSI and 1-butyl-1-methylpyrrolidinium bis(fluorosulfonyl)imide (Pyr₁₄FSI), and two protic ionic liquids, namely 1-butyl-pyrrolidinium bis(trifluoromethylsulfonyl)imide (Pyr_{H4}TFSI) and 1-butyl-pyrrolidinium bis(fluorosulfonyl)imide (Pyr_{H4}FSI), in publication 4. In this study, a good performance of PTMA-based electrodes in combination with aprotic ionic liquids is observed. Especially PTMA in Pyr₁₄FSI displays a high specific capacity of 74 mAh g⁻¹ (in comparison to other ionic liquids), good rate capability and a very stable cycling. This emphasizes once again the importance of the chosen ions in the electrolyte. However, PTMA in combination with protic ionic liquids as electrolyte shows a different picture. Here lower values of specific capacity and a general decomposition of the active material takes place during all presented experiments. This behavior is attributed to the interaction of PTMA and the proton present in Pyr_{H4}TFSI and Pyr_{H4}FSI, which leads to the degradation of the active groups. These interactions need to be clarified in future works.

Publication 5 represents the conceptual most sophisticated work shown in this thesis and elucidates the complex processes occurring during the self-discharge of PTMA. In order to do so this work utilizes a test schedule in which PTMA-based electrodes are charged at five different current densities (0.1C, 0.5C, 1C, 2C or 10C), rested for four different rest times (10 min, 1 h, 10 h or 24 h) and discharged at the corresponding current. This schedule results to a matrix of 20 capacity retention values and is applied to PTMA in organic electrolyte media (1M Pyr₁₄TFSI in PC) and ionic liquid electrolyte (pure

Pyr₁₄TFSI) to examine the influence of the electrolyte properties on the self-discharge behavior. Here it is found, that for PTMA in the two utilized electrolytes exist different threshold currents, which are appropriate to use, in order to achieve a stable charged state in the electrode. The value of this threshold current depends on the transport properties of the used electrolyte. When charging currents higher than this threshold are used, an unstable charged state is obtained. This is the cause of activation-controlled faradic reactions on the surface of the electrode followed by a charge redistribution process inside the electrode, which yields to a charge loss in the system. If the electrodes are charged with currents well below the threshold, the self-discharge is found to be diffusion-controlled again like examined in publication 3. Therewith it is clear that a careful selection of the electrolyte and fitting charging currents are necessary to minimize the self-discharge performance of PTMA.

The combined results of this thesis show that the electrochemical behavior of PTMA-based electrodes heavily depends on the electrolyte used in the system. Therefore, a careful selection of the electrolyte for every application is indispensable in order to optimize the performance of PTMA. While low concentrated electrolytes provide high capacity and rate capability, electrolytes with higher concentrations improve stability and self-discharge performance. This optimization is also possible for other organic battery materials and a deep investigation of the electrolyte/electrode interaction should be a standard in organic battery research. Furthermore, the electrolyte should be used as a tool for electrochemists to influence the processes occurring inside storage devices and illuminate corresponding mechanisms as proofed in the case of the self-discharge behavior of PTMA in this work.

Zusammenfassung

Für die Realisierung nachhaltiger Energiespeicher werden Technologien jenseits der modernen Lithium-Ionen-Batterie benötigt. Eine Technologie, welche die zukünftige elektrochemische Energiespeicherung in dieser Hinsicht ergänzen könnte, sind organische Batterien. Diese verwenden redoxaktive organische Moleküle oder Polymere als Elektrodenaktivmaterialien. Diese redoxaktiven Materialien umfassen Verbindungen wie leitfähige Polymere, Carbonyle, organische Schwefelverbindungen oder organische stabile Radikale und bieten nützliche Eigenschaften wie eine hohe theoretische gravimetrische Kapazität, hohe Sicherheit, mechanische Flexibilität und die Herstellung aus verfügbaren Elementen (C, H, O, N, S).

Besonders die Entwicklung von organischen stabilen radikalischen Polymeren hat in den letzten 20 Jahren ein großes Forschungsinteresse erfahren. Dort zeichneten sich diese redoxaktiven Materialien besonders durch ihre Ratenfestigkeit und coulombische Effizienz aus, wenn sie in Kombination mit einer Lithium-Ionen-basierten Anode und Elektrolyten eingesetzt wurden. Hier hervorzuheben ist Poly(2,2,6,6-tetramethyl-piperidinylnitroxyl-4-yl-methacrylat) (PTMA). PTMA, das eingehend als Kathodenmaterial im Lithium-Ionen-Batterieaufbau untersucht und zu einem Standardmaterial in der organischen Batterieforschung wurde, bietet eine spezifische Kapazität nahe dem theoretischen Wert von 111 mAh g^{-1} , ein stabiles Redoxpotential von $3,6 \text{ V vs. Li}^+/\text{Li}$ und eine hohe Kapazität bei hohen Stromdichten in modernen Batterieelektrolyten wie 1 M LiPF_6 in EC/DMC. Diese Elektrolyte verursachen jedoch Sicherheitsbedenken aufgrund von Toxizität und Entflammbarkeit. Darüber hinaus fördert die organische Natur dieser Elektrolyte die Löslichkeit von PTMA in der Zelle, was die Lebensdauer der Zelle begrenzt und die Selbstentladungsrate erhöht.

Obwohl diese Probleme offensichtlich sind, hat es lange Zeit an Untersuchungen gefehlt, die sich mit der wichtigen Rolle des Elektrolyten für PTMA und organische Batterien im Allgemeinen befasst haben. Es ist in Anbetracht des Energiespeichermechanismus von PTMA klar, dass Elektrolyteigenschaften wie Ionenkonzentration, Leitfähigkeit und Viskosität etc. die elektrochemische Leistung PTMA-basierter Elektroden maßgeblich beeinflussen. In Bezug auf die bestehenden Ansätze zu Elektrolyten in diesem Bereich, die in Publikation 1 (Übersichtsartikel) vorgestellt wurden, muss festgestellt werden, dass

detaillierte Studien zu den Auswirkungen des Elektrolyten auf das elektrochemische Verhalten von PTMA und anderen organischen Materialien notwendig sind, um deren Leistung in Energiespeicheranwendungen zu optimieren.

Daher wird in dieser Arbeit PTMA als Modellaktivmaterial verwendet und eine systematische Studie zum Einfluss des Elektrolyten auf das elektrochemische Verhalten von PTMA-basierten Elektroden durchgeführt. Dabei wird in vier verschiedenen Publikationen besonderes Augenmerk auf den Einfluss der Elektrolytzusammensetzung, der Elektrolytkonzentration, der Verwendung von ionischen Flüssigkeiten als Elektrolyte für PTMA und das Selbstentladeverhalten von PTMA-basierten Elektroden in verschiedenen Elektrolyten gelegt.

Die Untersuchung dieses Themas wird mit Veröffentlichung 2 begonnen, in der PTMA in einem Halbzellenaufbau in Kombination mit 3 verschiedenen metallfreien Elektrolyten getestet wird, 1M 1-Butyl-1-methylpyrrolidiniumbis(trifluoromethylsulfonyl)imid (Pyr₁₄TFSI) in Propylencarbonat (PC), Tetraethylammoniumbis(trifluoromethylsulfonyl)imid (Et₄NTFSI) in PC und reines Pyr₁₄TFSI, welches eine ionische Flüssigkeit ist. Die Ergebnisse dieser Veröffentlichung zeigen einen signifikanten Einfluss des verwendeten Leitsalzes und der Art des Elektrolyten auf die Leistung von PTMA. Im Einzelnen liefert PTMA in 1M Pyr₁₄TFSI in PC eine hohe spezifische Kapazität von 100 mAh g⁻¹ sowie eine gute Ratenfestigkeit. Dagegen wird in 1M Et₄NTFSI in PC eine deutlich geringere spezifische Kapazität beobachtet, obwohl nur das Kation im System verändert wird. Aufgrund der geringen Leitfähigkeit von reinem Pyr₁₄TFSI, wird für PTMA in diesem Elektrolyten eine reduzierte Kapazität und Ratenfestigkeit festgestellt. Allerdings wirkt sich die hohe Viskosität im Vergleich zu den organischen Elektrolyten positiv auf die Stabilität und das Selbstentladeverhalten aus. Dies wird durch die Verringerung der Löslichkeit von PTMA in diesem Elektrolyten erreicht. Des Weiteren werden in dieser Arbeit Hybridsysteme, welche eine PTMA-Kathode und eine negative Elektrode mit Aktivkohle enthalten, mit 1M Pyr₁₄TFSI in PC sowie mit reinem Pyr₁₄TFSI realisiert. Beide Systeme werden erfolgreich für 10000 Zyklen bei einer hohen Stromdichte von 10C zyklisiert. Dabei wird ebenfalls ein positiver Effekt der ionischen Flüssigkeit als Elektrolyt auf die Zyklenstabilität festgestellt.

Nach der Untersuchung der Elektrolytzusammensetzung auf das elektrochemische Verhalten von PTMA wird in Publikation 3 der Einfluss der Elektrolytkonzentration untersucht. Dort wird PTMA mit 1, 2 und 3M 1-Butyl-1-methylpyrrolidiniumtetrafluoroborat ($\text{Pyr}_{14}\text{BF}_4$) in PC getestet. Dabei wird für PTMA bei niedrigen Strömen in allen Elektrolyten ein vergleichbares Verhalten festgestellt, während bei höheren Strömen der bessere Transport der niedrig konzentrierten Mischungen deutlich wird. Auf der anderen Seite bietet der 3M Elektrolyt eine überlegene Leistung in Bezug auf die Selbstentladung der Elektroden. Während in der 1M Lösung die PTMA-basierte Elektrode nach 4,5 Tagen vollständig selbstentladen ist, wird im 3M Elektrolyten auch nach 11 Tagen Ruhezeit eine Restladung gemessen. Der Mechanismus dieses Ladungsverlustes erwies sich als diffusionslimitierter Prozess, der wahrscheinlich auf gelöstes Aktivmaterial zurückzuführen ist, welches als Redox-Shuttle im Elektrolyten wirkt. Daher behindert die erhöhte Viskosität der 3M Lösung diese Diffusion und reduziert somit den Ladungsverlust während der Ruhephase.

Da in Publikation 2 und 3 vorteilhafte Effekte von hochkonzentrierten Elektrolyten auf die elektrochemische Leistung von PTMA gefunden wurden, wird PTMA in Veröffentlichung 4 mit zwei aprotischen ionischen Flüssigkeiten, $\text{Pyr}_{14}\text{TFSI}$ und 1-Butyl-1-methylpyrrolidiniumbis(fluorosulfonyl)imid ($\text{Pyr}_{14}\text{FSI}$) und zwei protischen ionischen Flüssigkeiten, 1-Butyl-pyrrolidiniumbis(trifluoromethylsulfonyl)imid ($\text{Pyr}_{\text{H}4}\text{TFSI}$) und 1-Butyl-pyrrolidiniumbis(fluorosulfonyl)imid ($\text{Pyr}_{\text{H}4}\text{FSI}$) getestet. In dieser Studie wird eine gute Leistung von PTMA-basierten Elektroden in Kombination mit aprotischen ionischen Flüssigkeiten beobachtet. Insbesondere PTMA in $\text{Pyr}_{14}\text{FSI}$ zeigt eine hohe spezifische Kapazität von 74 mAh g^{-1} (im Vergleich zu anderen ionischen Flüssigkeiten), eine gute Ratenfestigkeit und hohe Stabilität. Dies unterstreicht einmal mehr die Bedeutung der gewählten Ionen im Elektrolyten. PTMA in Kombination mit protischen ionischen Flüssigkeiten als Elektrolyt zeigt jedoch ein anderes Bild. Hier kommt es bei allen gezeigten Experimenten zu niedrigeren Werten der spezifischen Kapazität und zu einer generellen Zersetzung des Aktivmaterials. Dieses Verhalten wird auf die Wechselwirkung von PTMA und dem in $\text{Pyr}_{\text{H}4}\text{TFSI}$ und $\text{Pyr}_{\text{H}4}\text{FSI}$ vorhandenen Proton zurückgeführt, die zum Abbau der aktiven Gruppen führt. Diese Wechselwirkungen müssen in zukünftigen Arbeiten aufgeklärt werden.

Publikation 5 stellt die konzeptionell anspruchsvollste Arbeit dieser Dissertation dar und klärt die komplexen Vorgänge bei der Selbstentladung von PTMA auf. Dazu wird ein Versuchsplan verwendet, bei dem PTMA-basierte Elektroden mit fünf verschiedenen Stromdichten (0,1C, 0,5C, 1C, 2C oder 10C) geladen, für vier verschiedene Ruhezeiten (10 min, 1 h, 10 h oder 24 h) geruht und mit entsprechendem Strom entladen wird. Dieses Schema resultiert in einer Matrix von 20 Kapazitätserhaltungswerten und wird auf PTMA in organischem Elektrolyten (1M Pyr14TFSI in PC) und in ionischer Flüssigkeit (reines Pyr14TFSI) angewandt, um den Einfluss der Elektrolyteigenschaften auf das Selbstentladungsverhalten zu untersuchen. Dabei wird festgestellt, dass für PTMA in den beiden verwendeten Elektrolyten unterschiedliche Schwellenströme existieren, die zu verwenden sind, um einen stabilen Ladezustand in der Elektrode zu erreichen. Der Wert dieses Schwellenstroms hängt von den Transporteigenschaften des verwendeten Elektrolyten ab. Bei der Verwendung von Ladeströmen, die höher als dieser Schwellenwert sind, wird ein instabiler Ladezustand erreicht. Dies ist die Ursache für aktivierungskontrollierte faradische Reaktionen an der Elektrodenoberfläche, gefolgt von einem Ladungsumverteilungsprozess im Inneren der Elektrode, der zu einem Ladungsverlust im System führt. Werden die Elektroden mit Strömen deutlich unterhalb der Schwelle aufgeladen, so zeigt sich die Selbstentladung wieder diffusionskontrolliert, wie in Veröffentlichung 3 festgestellt. Damit ist klar, dass eine sorgfältige Auswahl des Elektrolyten und passende Ladeströme notwendig ist, um die Selbstentladung von PTMA zu minimieren.

Die kombinierten Ergebnisse dieser Arbeit zeigen, dass das elektrochemische Verhalten von PTMA-basierten Elektroden stark von dem im System verwendeten Elektrolyten abhängt. Daher ist eine sorgfältige Auswahl des Elektrolyten für jede Anwendung unerlässlich, um die Leistung von PTMA zu optimieren. Während niedrig konzentrierte Elektrolyte eine hohe Kapazität und Ratenfestigkeit bieten, verbessern Elektrolyte mit höheren Konzentrationen die Stabilität und das Selbstentladungsverhalten. Diese Optimierung ist auch für andere organische Batteriematerialien möglich und eine tiefgehende Untersuchung der Elektrolyt/Elektroden-Interaktion sollte ein Standard in der organischen Batterieforschung sein. Darüber hinaus sollte der Elektrolyt als Werkzeug für Elektrochemiker genutzt werden, um die Vorgänge im Inneren von Speichergeräten zu beeinflussen und entsprechende Mechanismen zu beleuchten, wie im Fall des Selbstentladungsverhaltens von PTMA in dieser Arbeit bewiesen.

Table of Contents

| | |
|--|-----|
| Table of Contents..... | I |
| Figure Index | III |
| Table Index..... | IV |
| List of Abbreviations | V |
| 1 Introduction | 1 |
| 1.1 Motivation | 1 |
| 1.2 Energy Storage in Battery Systems | 3 |
| 1.3 Organic Redox Active Materials for Organic Batteries | 6 |
| 1.3.1 General Classification of ROMPs | 6 |
| 1.3.2 Possible Cell Configurations of ROMPs..... | 7 |
| 1.3.3 ROMP Classes..... | 10 |
| 1.4 A Detailed View on PTMA..... | 22 |
| 1.5 Publication 1: A Critical Analysis about the Underestimated Role of the Electrolyte in Batteries Based on Organic Materials..... | 25 |
| 1.5.1 The Importance of the Electrolyte for Organic Materials | 25 |
| 1.5.2 Electrolytes used in Organic Batteries..... | 29 |
| 1.5.3 Electrolytes used for PTMA | 33 |
| 1.6 Aim of the Work..... | 48 |
| 2 Results and Discussion | 49 |
| 2.1 Publication 2: The influence of the electrolyte composition on the electrochemical behaviour of cathodic materials for organic radical batteries | 49 |
| 2.2 Publication 3: Influence of the salt concentration on the electrochemical performance of electrodes for polymeric batteries..... | 61 |
| 2.3 Publication 4: Aprotic and Protic Ionic Liquids as Electrolytes for Organic Radical Polymers..... | 72 |

| | | |
|-----|---|------|
| 2.4 | Publication 5: The influence of current density, rest time and electrolyte composition on the self-discharge of organic radical polymers..... | 82 |
| 3 | Conclusion..... | 91 |
| 4 | Outlook | 94 |
| | References | VIII |
| | Appendix | XVII |

Figure Index

| | |
|---|-----------|
| <i>Figure 1: Increase of annual world energy consumption, reprinted with permission from reference [1]....</i> | <i>1</i> |
| <i>Figure 2: General battery cell setup with anode, cathode and electrolyte during discharge.</i> | <i>3</i> |
| <i>Figure 3: Possible cell configurations of all-organic storage devices.</i> | <i>7</i> |
| <i>Figure 4: Possible cell configurations of metal-ion-based organic storage devices.</i> | <i>8</i> |
| <i>Figure 5: Possible cell configurations of ROMPs in supercapacitors, dual ion batteries or hybrid devices. .</i> | <i>9</i> |
| <i>Figure 6: Electrochemical performance of a PTMA-based composite electrode in 1M Pyr₁₄BF₄ in PC: A) CV at a scan rate of 2 mV s⁻¹, B) Charge/discharge profile E vs. t at current density of 1C, C) Voltage profile E vs. Q at current density of 1C, D) Rate capability at current density of 0.2C to 50C, E) Cycling stability for 150 cycles at 1C, F) Self-discharge behavior E vs. t at a charge current density of 1C and 1 day of rest...</i> | <i>23</i> |
| <i>Figure 7: Number of published articles with the topic: “organic redox active electrode materials” and “electrolyte for organic redox active electrode materials” per year (derived from web of knowledge 18.03.2021).</i> | <i>28</i> |

Table Index

| | |
|--|-----------|
| <i>Table 1: Change of charge state of N-, P- and B-type organic materials.....</i> | <i>6</i> |
| <i>Table 2: ROMP classes with corresponding subgroups, examples and general redox reactions.....</i> | <i>11</i> |
| <i>Table 3: Examples for conducting polymers with typical values of potential and specific capacity.....</i> | <i>13</i> |
| <i>Table 4: Examples for carbonyl compounds with typical values of potential and specific capacity.....</i> | <i>16</i> |
| <i>Table 5: Examples for organosulfur compounds with typical values of potential and specific capacity. ..</i> | <i>19</i> |
| <i>Table 6: Examples for organic radical polymers with typical values of potential and specific capacity.</i> | <i>21</i> |
| <i>Table 7: Desired properties for electrolytes for modern EES.....</i> | <i>26</i> |
| <i>Table 8: Desired properties for solvents and ions to form efficient electrolytes.....</i> | <i>26</i> |

List of Abbreviations

| | |
|----------------------------------|---|
| AC | Activated carbon |
| ACN | Acetonitrile |
| AQ | Anthraquinone |
| BQ | 1,4-Benzoquinone |
| CC | Carbonyl compound |
| CP | Conducting polymer |
| CuTCNQ | Cuprous Tetracyano quinodimethane |
| CV | Cyclic voltammetry |
| DCA | Dichloroisocyanuric acid |
| DMC | Dimethyl carbonate |
| DMcT | 2,5-Dimercapto-1,3,4-thiadiazole |
| DMTS | Dimethyl trisulfide |
| DPD | Dilithium pyromellitic diimide |
| DS | Disulfide |
| EC | Ethylene carbonate |
| EES | Electrochemical energy storage |
| EMC | Ethyl methyl carbonate |
| EMIMTFSI | 1-Ethyl-3-methylimidazolium bis(trifluoromethylsulfonyl)imide |
| Et ₄ NBF ₄ | Tetraethylammonium tetrafluoroborate |
| Et ₄ NTFSI | Tetraethylammonium bis(trifluoromethylsulfonyl)imide |
| IL | Ionic liquid |
| LCO | Lithium cobalt oxide |
| LFP | Lithium iron phosphate |
| Li | Lithium |
| LIB | Lithium-ion battery |
| LiClO ₄ | Lithium perchlorate |
| LiPF ₆ | Lithium hexafluorophosphate |
| LiTFSI | Lithium bis(trifluoromethylsulfonyl)imide |
| LP30 | 1M LiPF ₆ in EC/DMC 1:1 |
| NMC | Lithium nickel manganese cobalt oxide |

| | |
|-----------------------------------|--|
| OB | Organic Battery |
| ORP | Organic radical polymer |
| OSC | Organosulfur compound |
| OSR | Organic stable radical |
| PAC | Polyacetylene |
| PAn | Polyaniline |
| PAQS | Poly(anthraquinonyl sulfide) |
| PC | Propylene carbonate |
| PDDTB | Poly(1,4-di(1,3-dithiolan-2-yl) benzene) |
| PDTDA | Poly-2,2-dithiodianiline |
| PDTTA | Poly(5,8-dihydro-1H,4H-2,3,6,7-tetrathia anthracene) |
| PEDOT | Poly(3,4-ethylenedioxythiophene) |
| PGS | Poly(galvinoxystyrene) |
| PI | Polyimide |
| PNTCDA | 1,4,5,8-naphthalenetetracarboxylic dianhydride-derived polyimide |
| PPDT | Poly(2-phenyl-1,3-dithiolane) |
| PPy | Polypyrrole |
| PROXYL | 2,2,5,5-Tetramethyl-1-pyrrolidine-N-oxyl |
| PS | Polysulfide |
| PTCDA | 3,4,9,10-Perylene tetracarboxylic acid dianhydride |
| PTEO | Poly(2,5,5-Tetramethyl-3-oxiranylpyrrolidine-N-oxyl ethyleneoxide) |
| PTH | Polythiophene |
| PTMA | Poly(2,2,6,6-tetramethyl piperidiny-N-oxyl-4-yl methacrylate) |
| PTPA | Polytripehnylamin |
| PVMPT | Poly(3-vinyl-N-methylphenothiazine) |
| Pyr _{H4} FSI | 1-Butyl-pyrrolidinium bis(fluorosulfonyl)imide |
| Pyr _{H4} TFSI | 1-Butyl-pyrrolidinium bis(trifluoromethylsulfonyl)imide |
| Pyr ₁₄ BF ₄ | 1-Butyl-1-methylpyrrolidinium tetrafluoroborate |
| Pyr ₁₄ FSI | 1-Butyl-1-methylpyrrolidinium bis(fluorosulfonyl)imide |
| Pyr ₁₄ TFSI | 1-Butyl-1-methylpyrrolidinium bis(trifluoromethylsulfonyl)imide |

| | |
|--------|--|
| ROMP | Redox active organic molecule or polymer |
| SCN | Succinonitrile |
| SEI | Solid electrolyte interface |
| TE | Thioether |
| TEGDME | Tetraethylene glycol dimethyl ether |
| TEMPO | 2,2,6,6-Tetramethyl piperidiny-N-oxyl |
| TETD | Tetraethylthiuram disulfide |

1 Introduction

1.1 Motivation

The rapid increase of the world population is accompanied by a proportionally growing energy consumption and CO₂ generation (see Figure 1) [1,2]. In order to limit the CO₂ production and therewith the greenhouse effect, it is evident that this high demand on energy should not be met by fossil fuels, but more and more by renewable resources like wind, biomass, solar, geothermal, hydropower and tidal [1]. Many of these energy sources are unsteady in supply. Therefore, it is necessary to store generated energy for later usage and grid stabilization. One possibility to do this is the use of electrochemical storage devices like batteries. The most advanced battery technology today is the lithium-ion battery (LIB), which excels in both energy and power density [3]. The state-of-the-art LIB consists of a graphite anode, a transition metal oxide cathode and a Li-salt like lithium hexafluorophosphate (LiPF₆) dissolved in a mixture of organic carbonates e.g. ethylene carbonate/ dimethyl carbonate (EC/DMC) as electrolyte [3,4]. However, this setup deals with two main problems.

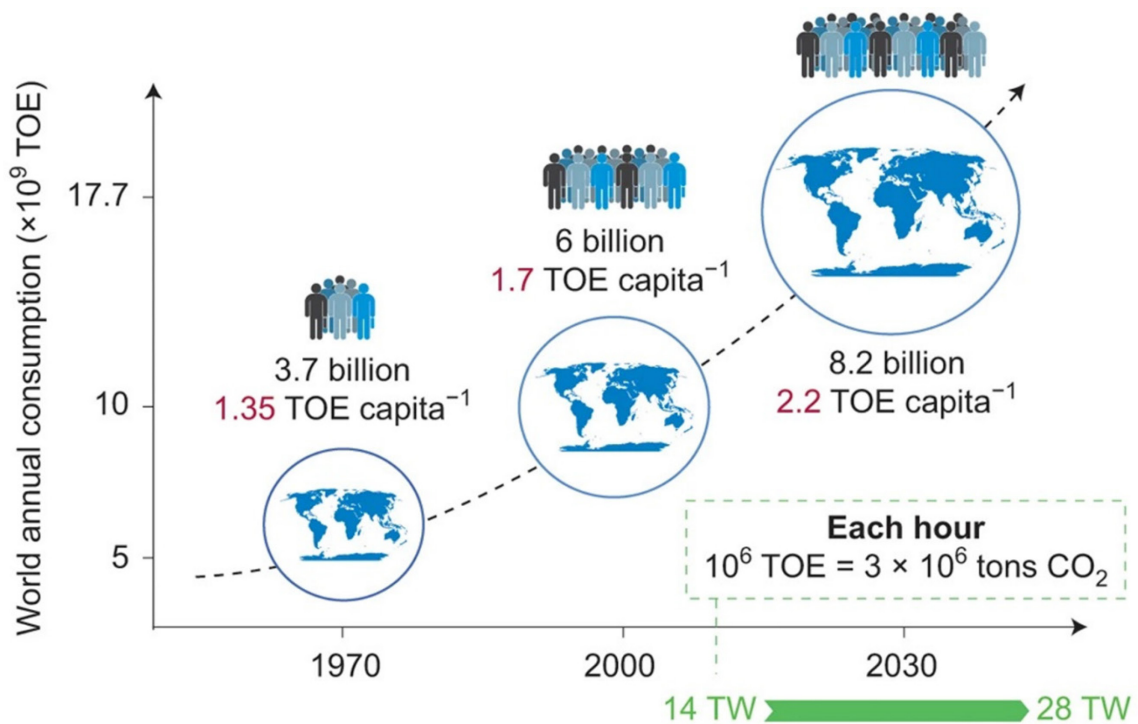


Figure 1: Increase of annual world energy consumption, reprinted with permission from reference [1].

Firstly, the established cathode active materials lithium nickel manganese cobalt oxide (NMC) and lithium cobalt oxide (LCO) rely on cobalt, which is on the list of critical raw materials [5–10]. Secondly, the utilized organic electrolytes are volatile and highly flammable, which makes them the source of serious safety risks [11]. Consequently, the introduction of new battery chemistries is of key interest for a sustainable energy supply. A battery concept, which could meet the requirements for this sustainable approach are organic batteries (OBs) utilizing redox active organic molecules or polymers (ROMPs) as electrode materials [11]. These materials perform electrochemical redox reactions and thereby can reversibly store and deliver charge. Due to their organic nature, ROMPs display very favorable properties in view of electrochemical energy storage and cell design. Among those are: a high theoretical gravimetric capacity, good safety, low cost, superior reaction kinetics, improved power, mechanical flexibility, property tailoring (e.g. redox potential, solubility, polarity), multi electron transfer reactions, abundant elements (C, H, O, N and S), production from renewable biomass resources and easy disposal [12–17]. However, up to date ROMPs were not able to penetrate the energy storage market in a major way, since there are still many drawbacks and challenges, which need to be overcome. In the future, limitations like a low volumetric capacity caused by the intrinsic low density of ROMPs, the dissolution of solid organic electrode material into liquid electrolytes (reduced cycling stability) and high self-discharge of some organic material classes need to be addressed [14,15,18–21].

The following introduction aims to provide an overview of materials, which have been used in OBs including the general classification of the compounds, the explanation of the exploited charge/discharge mechanisms and the consequent cell configurations in which organic materials are used. Afterwards, the general tasks of electrolytes in energy storage systems and the special role of the electrolyte in organic batteries are emphasized. This is followed by an overview of electrolytes, which have been investigated for the utilization with organic redox active materials. While doing so, a special focus will be set on organic stable radicals and especially poly(2,2,6,6-tetramethyl piperidinyll-N-oxyl-4-yl methacrylate) (PTMA), which is the main active electrode material of this work. However, at first a general introduction to the working principles of batteries is given.

1.2 Energy Storage in Battery Systems

Batteries are closed systems which convert chemical energy into electrical energy via the redox reactions at the two electrodes [22]. The electrode with the redox reaction at a lower redox potential is referred to as negative electrode (anode during discharge). The electrode where the redox reaction occurs at the higher redox potential is defined as positive electrode (cathode during discharge). Cathode and anode are connected by an external circuit. During the discharge process electrons move from the anode to the cathode through the external circuit. Therewith the anode is oxidized while the cathode is reduced.

Anode and cathode are ionically connected by an electrolyte, which assures the movement of ions between the electrodes and therewith charge compensation during the charge or discharge process. The importance of the electrolyte in this process is highlighted in section 1.5. The described processes during the discharge of a single battery cell are shown in Figure 2 [15].

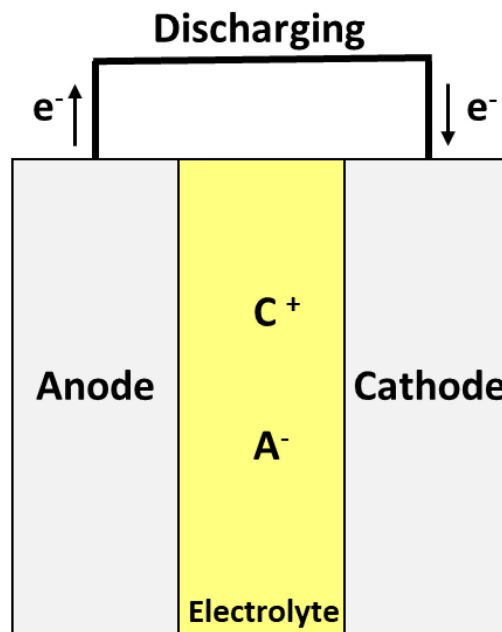


Figure 2: General battery cell setup with anode, cathode and electrolyte during discharge.

Important parameters utilized for the characterization of a battery system are considered and defined below.

Cell Voltage V or E [V]

$$V = V_C - V_A \quad (1)$$

V_C is the cathode potential and V_A is the anode potential. Both are given in V.

Theoretical capacity Q_{th} [mAh g⁻¹]

$$Q_{th} = \frac{n \times F}{M} \quad (2)$$

n is number of transferred electrons, F is the Faraday constant (96485 C mol⁻¹) and M is the molar mass of the electrode material (anode or cathode) in g mol⁻¹.

Specific capacity Q [mAh g⁻¹]

$$Q = \frac{i \times t}{m} \quad (3)$$

i is the applied current in mA, t is the time in h and m is the mass of the active material loaded on the electrode in g.

Energy E [Wh kg⁻¹]

$$E = Q \times V \quad (4)$$

The energy of a battery is the product of charge Q stored inside the system and the average voltage V at which the exploited redox reaction occurs.

Power P [W kg⁻¹]

$$P = i \times V = \frac{E}{t} \quad (5)$$

The power of a battery gives an information about how fast the energy of a battery can be stored or delivered.

Coulombic efficiency η [%]

$$\eta = \frac{Q_{Discharge}}{Q_{Charge}} \times 100 \% \quad (6)$$

The coulombic efficiency indicates the effectiveness of the charge/discharge process of a battery or electrode. This value should be near 100 % but can be decreased by parasitic processes or resistances in the cell.

C-Rate [C]

$$C - Rate = \frac{i}{i_{1h}} \quad (7)$$

In order to give information about how fast a battery or electrode is charged independent from the used active material, researchers use the C-rate. i_{1h} is the theoretical current, which is needed for the full charge of a system in 1 h. Therewith 1C corresponds to the current i applied to fully charge a battery or electrode in 1 h.

Cycling stability [mAh g⁻¹ or %]

The cycling stability describes the loss of specific capacity Q after a certain number of cycles in comparison to the initial capacity displayed by the same electrode or battery. The cycling stability can be given in mAh g⁻¹ or in %.

Self-Discharge [%]

The self-discharge of a battery is the spontaneous loss of charge due to parasitic reactions inside the cell during a rest period and is calculated analog to the coulombic efficiency.

1.3 Organic Redox Active Materials for Organic Batteries

1.3.1 General Classification of ROMPs

In general, ROMPs are organic materials (molecules or polymers), which can reversibly change their state of charge by exerting an electron transfer reaction of a redox active moiety (e.g. carbonyls, stable radicals, etc.) or by a doping process (conducting polymers) [11,23,24]. With this change of charge state energy can be stored or released in a cell with a ROMP-based electrode.

For a first classification, ROMPs can be divided into three different charge storage types, which are shown in Table 1. N-Type, which means during the charge/discharge process the compound alters between the electroneutral state (N) and the negative state (N⁻), P-type, where the active material moves from the neutral (P) to the positive state (P⁺), and bipolar materials (B), which can either be reduced or oxidized to both negative (B⁻) or positive (B⁺) state [12,25,26]. Depending on the used cell configuration, bipolar materials can be used as N- or P-type electrode materials. Nevertheless, due to their two possible reactions, the same bipolar material can be used as cathode as well as anode material in one cell. As highlighted in Table 1, the electrolyte of the electrochemical cell is deeply involved in the storage processes of all three ROMP types, since cations (C⁺) or anions (A⁻) are used for charge compensation. While doing so, in general any kind of ion is applicable for this charge compensation. This represents a significant difference between ROMPs and inorganic intercalation or insertion compounds in which the occurring storage process is highly dependent on the used ion (e.g. Li⁺ and Na⁺) [27,28].

Table 1: Change of charge state of N-, P- and B-type organic materials.

| Type | Redox Reaction |
|--------|---|
| N-type | $N + C^+ \xrightleftharpoons[+e]{-e} N^- C^+$ |
| P-type | $P + A^- \xrightleftharpoons[-e]{+e} P^+ A^-$ |
| B-type | $B \xrightleftharpoons[+e]{-e} B^- C^+ \quad B \xrightleftharpoons[-e]{+e} B^+ A^-$ |

1.3.2 Possible Cell Configurations of ROMPs

Considering the classification discussed in section 1.3.1, there are several possibilities to implement ROMPs in electrochemical storage systems [24,26].

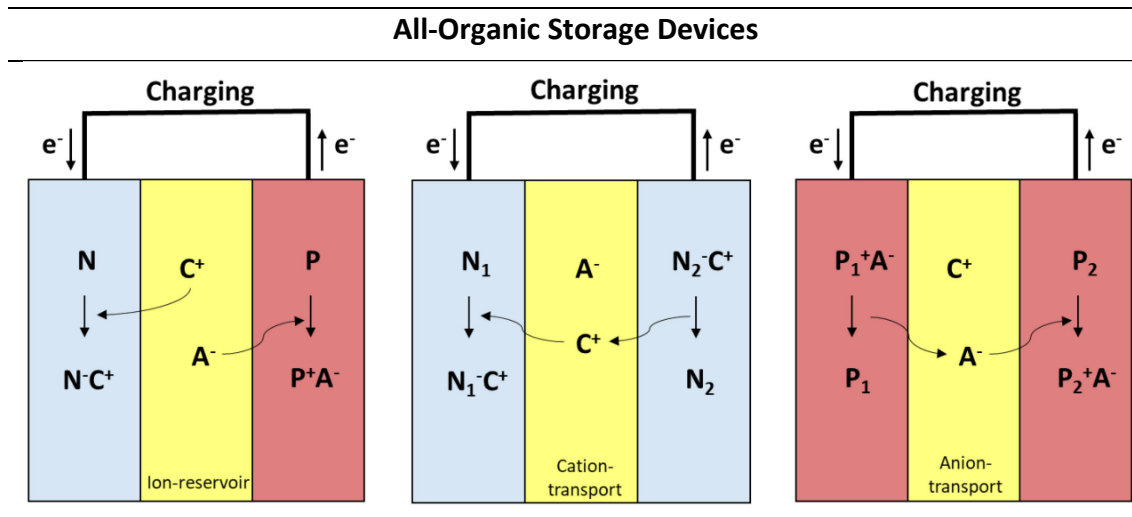


Figure 3: Possible cell configurations of all-organic storage devices.

In all-organic storage devices, ROMPs can be integrated in 3 different ways as featured in Figure 3. A first possible configuration is the obvious combination of an N-type and a P-type ROMP. In the discharged state, both materials are in the electroneutral state. During the charging process, the N-type ROMP N is reduced and moves to its electronegative state N^- . In this process, the charge compensation is assured by the insertion of cations from the electrolyte. In the meantime, the P-type ROMP is oxidized to the electropositive species and anions from the electrolyte are used for charge compensation in this electrode. For the discharge process the described processes are reversed. In this scenario the electrolyte functions as an ion-reservoir in which the salt concentration changes during cell cycling.

A second configuration is represented by the combination of two N-type materials operating at different reductive potentials. Here, in the discharged state one N-type ROMP is present in the electroneutral state (N_1), while the other one is in the electronegative state (N_2^-). Upon charging, N_2 is oxidized to the electroneutral state, while N_1 is reduced to the electronegative state. By that only the cation is needed for charge compensation and moves from one electrode to the other (N_2 to N_1). Therefore, the electrolyte acts as cation transport media in this case.

A third configuration is the combination of two p-type materials, which follows the same principles as the combination of two N-type materials. However, in this setup the anion moves between the two electrodes to provide charge compensation. Therefore, the electrolyte works as anion transport media.

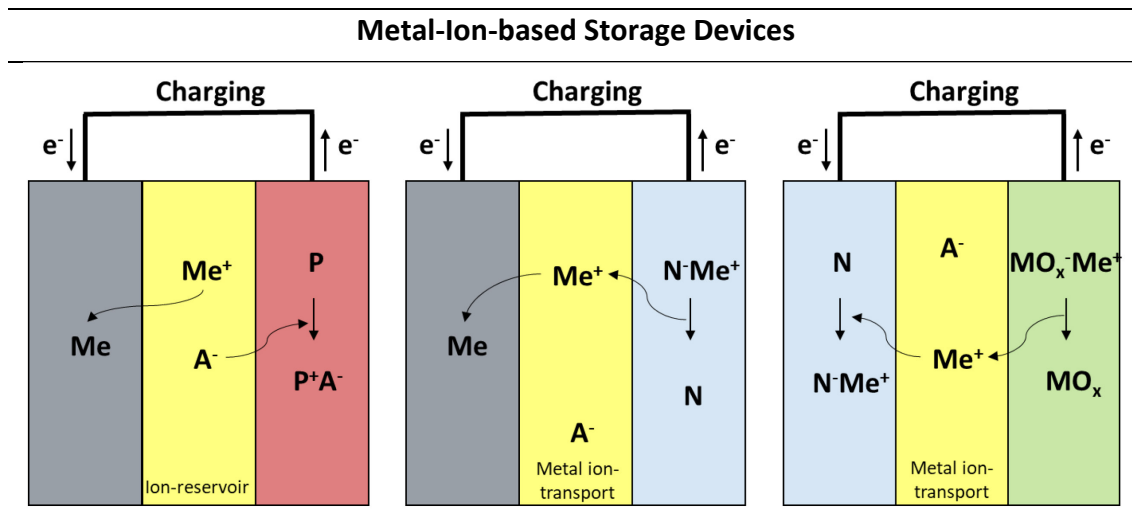


Figure 4: Possible cell configurations of metal-ion-based organic storage devices.

ROMPs can also be implemented in metal-ion-based storage devices. Figure 4 illustrates the possible cell configurations for these devices. A popular configuration is the combination of a metal-based anode (e.g. lithium, sodium, graphite etc.) with a P-type ROMP electrode, since this electrode combination results to the highest cell potentials for these devices. Upon charging the P-type is oxidized to the electropositive state with the subsequent insertion of anions provided by the electrolyte. In the meantime, metal-cations from the electrolyte are reduced at the metal electrode surface to the pure metal. Therewith, in total the concentration of ions in the electrolyte decreases while charging.

Furthermore, N-type ROMPs can be used in combination with metal-based anodes. In this cell configuration both electrodes utilize the metal-cations during cycling. While charging, the N-type is oxidized from the electronegative state to the neutral one. In this case, metal-cations are transported in the electrolyte from the N-type to the metal-based electrode, which is reduced during charging.

The same metal-ion transport process is displayed in the combination of N-type ROMPs with a metal oxide material (e.g. LCO, NMC, LFP). While charging, the metal-cations diffuse from the metal oxides, which are oxidized to the electroneutral state, to the N-type and inserted here.

Supercapacitors, Dual-Ion Batteries, Hybrid Devices

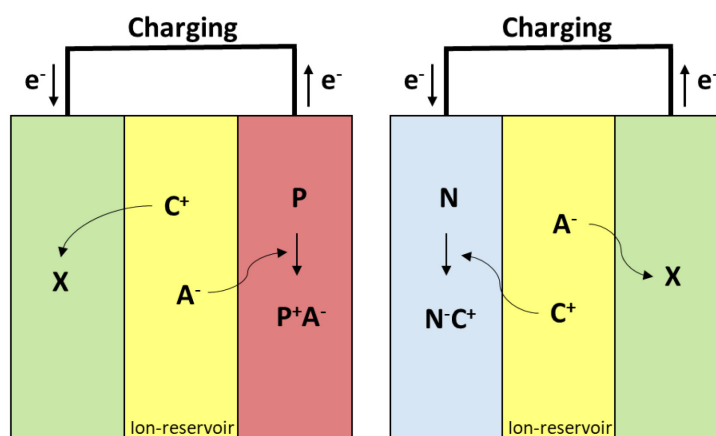


Figure 5: Possible cell configurations of ROMPs in supercapacitors, dual ion batteries or hybrid devices.

In order to achieve maximum cell voltage in supercapacitors, dual-ion batteries or hybrid devices, both P-type and N-type material should be in their electroneutral state at the discharged state of the electrochemical energy storage (EES) system. In this way, both P-type and N-type ROMPs alter from their electroneutral configuration to the positive or negative state upon cell charging. In the process, anions (P-type) or cations (N-type) are drawn from the electrolyte, while the counter ions are used in the other electrode. Hence, again the electrolyte acts as an ion-reservoir in these configurations.

Resulting from Figure 3, 4 and 5, the electrolyte utilized for ROMPs is an essential active component, which can work in principle in two different ways. Either it transports one ion type (cation or anion) from one electrode to the other during battery cycling (ion transport) or it stores and provides ions for charge compensation of generated charges in the active materials (ion-reservoir). As explained above, ROMPs itself have no need for any distinct ions (unlike LIBs) as long as the used electrolyte is able to provide charge compensation in the charge/discharge process. This means for the realization of OBs, researchers can select from a wide range of possible electrolyte mixtures.

1.3.3 ROMP Classes

The first prototype for an organic battery active material was proposed by Williams et. al. in 1969, where they combined dichloroisocyanuric acid (DCA) as cathode material with a lithium (Li) anode and 2M lithium perchlorate (LiClO_4) in methyl formate as electrolyte [29]. In the discharge of this primary battery system DCA is reduced to form the DCA anion and accept Li^+ for charge compensation (N-type reaction), while the lithium anode is oxidized. Therewith this battery was able to deliver a discharge capacity of 400 Wh kg^{-1} . However, an average discharge voltage of only 3.1 - 3.2 V, efficiencies of 60 – 70 %, solubility in the electrolyte and its primary nature made clear that this first proof of concept can only be the beginning for this new battery class.

In the following decades, researchers all over the globe presented new organic active materials. Many of those can today be assigned to a few ROMP main classes. These important classes are conducting polymers (CPs), carbonyl compounds (CCs), organosulfur compounds (OSCs) and organic stable radicals (OSRs) (see Table 2). These materials display different storage mechanisms, favorable properties, as well as intrinsic challenges, which will be presented and discussed in this section 1.3.3. Furthermore, exploited redox reactions for notable ROMP examples are given with corresponding key values of specific capacity and redox potential. Please note, that this section can only be an introduction to the field of ROMPs, as in the last decades researchers introduced an overwhelming number of materials.

Table 2: ROMP classes with corresponding subgroups, examples and general redox reactions.

| ROMP Class | Subgroups | Redox Reaction |
|-------------------------------|------------------|---|
| Conducting polymers | Polyacetylene | $\left(\text{---R---}\right)_n \xrightleftharpoons[+e^-]{\text{N-type}} \left(\text{---R---}\right)_n \xrightleftharpoons[-e^-]{\text{P-type}} \left(\text{---R---}\right)_n^+$ |
| | Polypyrrole | |
| | Polythiophene | |
| | Polyaniline | |
| Carbonyls | Quinones | $\text{R---C(=O)---R} \xrightleftharpoons[+e^-]{\text{N-type}} \text{R---C(O}^-\text{)---R}$ |
| | Carboxylates | |
| | Imides | |
| | Anhydrides | |
| Organosulfur compounds | Disulfides | $\text{R---S---S---R} \xrightleftharpoons[+2e^-]{\text{N-type}} \text{R---S}^-\text{---S}^-\text{---R}$ |
| | Thioethers | $\text{R---S---R} \xrightleftharpoons[-e^-]{\text{P-type}} \text{R---S}^+\text{---R}$ |
| Stable radicals | Nitroxyl radical | $\text{R---N}^{\cdot}\text{---R} \xrightleftharpoons[+e^-]{\text{N-type}} \text{R---N}^{\cdot}\text{---R} \xrightleftharpoons[-e^-]{\text{P-type}} \text{R---N}^+\text{---R}$ |
| | Phenoxy radical | $\text{Ar---}\dot{\text{O}} \xrightleftharpoons[+e^-]{\text{N-type}} \text{Ar---}\ddot{\text{O}}^-$ |

1.3.3.1 Conducting Polymers

First presented in 1977 with polyacetylene (PAC) [30], conducting polymers are among the first groups of organic active materials, which have been used for energy storage application [31–34]. After PAC, a variety of CP base structures has been presented by researchers. Some of the most investigated are polypyrrole (PPy), polythiophene (PTh) with its very prominent derivate poly(3,4-ethylenedioxythiophene) (PEDOT) and polyaniline (PAn) [35–42].

All conducting polymers have an overlap of adjacent π -orbitals in the polymer scaffold, which results in a semiconductor-like electronic band structure of valence and conduc-

tion band. Therewith the polymer can provide electronic conductivity through the scaffold. The charge storage within CPs relies on a highly delocalized doping process of the conjugated polymer backbone [43–45]. By oxidation (P-doping) or reduction (N-doping) of the CP delocalized positive charges (delocalized holes, P-type) or negative charges (delocalized electrons, N-type) are generated in the polymer. These charges are compensated by counter ions from the electrolyte (see Table 2). Therewith, CPs are electronically as well as ionically conductive.

This interesting storage mechanism via doping results in unique electrochemical storage properties for CPs.

As already discussed above, CPs provide high electronic conductivities in the doped state compared to other ROMP materials (e.g. up to 1500 S cm^{-1} for PEDOT) [46]. Furthermore, they provide favorable kinetics in the charge/discharge process resulting to high current rates [45,47].

On the other side, CPs also deal with serious intrinsic drawbacks. Due to the conjugated structure, the charge centers of CPs are not separated. This leads to an interaction of the redox centers and results in redox potentials dependent on the doping degree of the CP and, therewith, in a sloping cell voltage during cycling [15,24,48].

Additionally, although CPs can reach high specific capacities when fully doped (one electron or hole per monomer unit), these high doping degrees are seldom reached. Most works addressing CPs speak of maximum doping degrees of 0.3 – 0.5 or even lower [12,15,49]. In this regard, also higher doping is possible, however, at high doping stages a destabilization of the polymer backbone is taking place and side reactions of the CP with other cell components like the electrolyte can occur [50–52]. In the following, key features and properties of some prominent CPs are presented in order to give examples and numbers for the above given information. Furthermore, the utilized storage mechanisms are shown to illustrate the processes and reactions during charge/discharge.

Table 3: Examples for conducting polymers with typical values of potential and specific capacity.

| Material | Potential V vs. Li ⁺ /Li | Specific Capacity (mAh g ⁻¹) | Reference |
|---------------|--|---|------------|
| Polyacetylene | 3-4 | - 340/ + 48 | [53]/ [54] |
| | | | |
| Polypyrrole | 3-4 | 82 | [45] |
| | | | |
| Polythiophene | 3.1-4 | 82 | [45] |
| | | | |
| PEDOT | 2.7-4.2 | 30-70 | [45] |
| | | | |
| Polyaniline | 3-4 | 100-147 | [45] |
| | | | |

1.3.3.2 Carbonyl Compounds

Due to their early discovery in 1969 and pioneering works presenting very promising features for EES application, CCs like quinones, imides, anhydrides and carboxylates are among the most popular ROMPs [29,55].

CCs store charge in the molecular structure via the reduction of the C=O moiety to form a radical anion, which assigns the CCs to the N-type materials (see Table 2) [13]. Often two or more carbonyl groups have conjugated structures, which leads to the subsequent recombination of the generated radicals to form intramolecular bonds as seen in quinones [13,56]. This process results to multivalent anions. The negative charges of the anions are compensated by cations from the electrolyte (Li^+ or other metal-ions in most cases) [57]. Since the described charge storage process relies on a very distinct redox reaction of a redox active moiety in the groups, CCs (unlike CPs) show very stable redox potentials in energy storage application [25]. However, due to the separate redox centers CCs also display very low conductivities, which calls for conductive additives in electrode fabrication [58].

Although they are N-type ROMPs, CCs have been mostly investigated as cathode materials in combination with a lithium anode [59–63]. Other approaches include the use of sodium, all-organic systems or at rarest other metals like aluminum [64–67]. In the case of all-organic devices, CCs can also be used as anode materials together with a P-type ROMP.

In 1971 Alt et. al. were able to present very basic carbonyl structures like 1,4-benzoquinone (BQ), which displays a redox potential of 2.7 V vs. Li^+/Li and a remarkable theoretical capacity of 496 mAh g^{-1} [14,55]. Also other carbonyl structures, like anthraquinone (AQ), display a high capacity of 257 mAh g^{-1} , since in these compounds a lot of charge is stored per molecular weight [68]. This results to high theoretical capacities. However, due to their organic nature, these small carbonyls tend to show strong dissolution in the standard organic LIB electrolytes, limiting the cycling stability of the EES system in which they are used [58,68]. Attempts to address this problem is the polymerization of small CCs. One successful example for this is poly(anthraquinonyl sulfide) (PAQS), which is a polymeric derivate of AQ. It delivers a reversible specific capacity of 220 mAh g^{-1} with redox potentials at 1.5 and 2 V vs. Na^+/Na [64]. With the polymerization of the AQ a

significant higher structural stability and therewith cycling stability is achieved for PAQS, which results to a cycling stability near 100 % over 200 cycles at 5C in an organic electrolyte [64]. However, this improvement in stability comes at the price of a reduced specific capacity, since a large amount of redox inactive mass is incorporated into the active material.

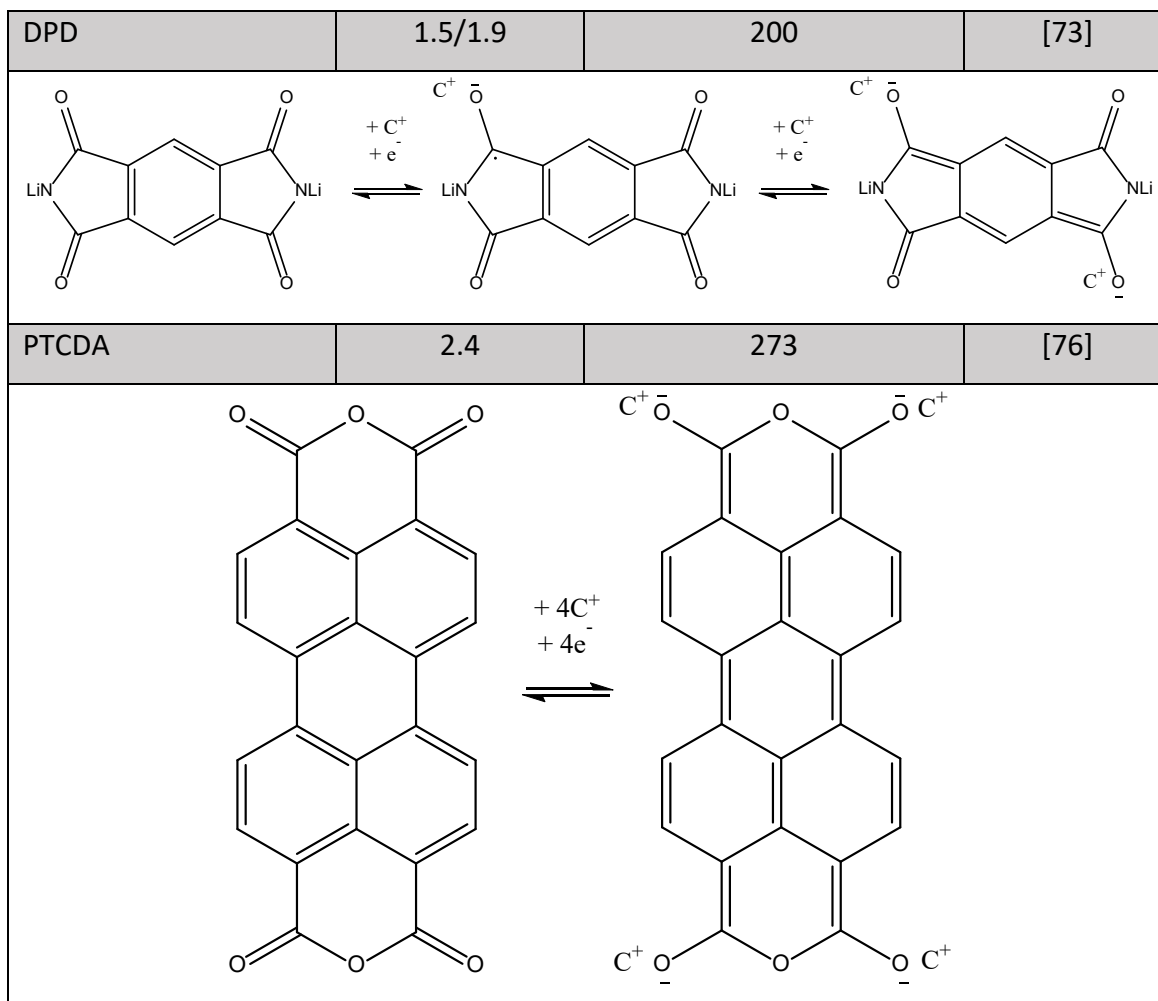
Another approach to reduce the dissolution of these materials consist of the tuning of the polarity of the active materials, which is done for example in the case of carboxylates (mostly lithium salts e.g. dilithium terephthalate, DLT) [13,69–72]. With this concept, ionic groups are introduced into small redox active molecules to increase the polarity of the compound. This aims to reduce the solubility in organic electrolytes.

Imides like dilithium pyromellitic diimide (DPD) or naphthalene diimide can also be used as N-type carbonyl compounds [25,73]. These materials can react in a two-step reduction (reduction with two electrons in each step) of which only the first is reversible and stabilized by the aromatic ring structure. The second reduction leads to decomposition of the redox system [74]. Therefore, in terms of energy storage only the first step is relevant. In order to achieve increased cycling stability also imides are polymerized to form the redox active material class of polyimides [75].

Another class of CCs are anhydrides like 3,4,9,10-perylene tetracarboxylic acid dianhydride (PTCDA), which can be understood as oxygen analogues of imides [76]. In this system upon the generation of the lithium enolate during charging, a conjugated system is formed in the perylene ring. A strong dissolution of PTCDA in 1M LiPF₆ in EC/DMC can be prevented by embedding the active material in a sulfide polymer structure. Therewith, a stable capacity can be achieved for 300 cycles [76].

Table 4: Examples for carbonyl compounds with typical values of potential and specific capacity.

| Material | Potential V vs. Li ⁺ /Li | Specific Capacity (mAh g ⁻¹) | Reference |
|---------------|--|---|-----------|
| Benzoquinone | 2.7 | 496 | [14,55] |
| | | | |
| Anthraquinone | 2.7 | 257 | [68] |
| | | | |
| PAQS | 1.8 | 220 | [64] |
| | | | |
| DLT | 0.8/1.4 | 300 | [70] |
| | | | |



1.3.3.3 Organosulfur Compounds

Organosulfur compounds, which are usable for organic energy storage applications can be divided into disulfides and polysulfides (DSs/PSs) as well as thioethers (TEs), which fundamentally differ in their redox mechanisms [14].

The redox reaction occurring in DSs/PSs involves the reversible breakage of the S-S bonds after the uptake of two electrons (N-type, see Table 2), which includes the charge compensation with two cations (again mostly metal-ions). During the reverse reaction, the S-S bonds are formed again.

The first who presented this concept was the group of Visco et al. in 1988 with the introduction of a molten tetraethylthiuram disulfide (TETD) electrode together with sodium [77]. This concept allows to use lower operative temperatures than the usual molten Na/S batteries [78]. Unfortunately, the reaction kinetics of the bond breakage and recombination are slow, which yields to a poor rate performance of the material shown

by a large peak separation in the cyclic voltammogram (CV) at a scan rate of 50 mV s^{-1} [79]. Due to the bad kinetics a lithium cell utilizing a solution of TETD was only able to deliver 36 % of its theoretical capacity of 181 mAh g^{-1} at low current [68,80].

After the investigation of small disulfide molecules like TETD or 2,5-dimercapto-1,3,4-thiadiazole (DMCT) [81], the incorporation of disulfides in polymer structures has been considered. This can be done on the one hand with the sulfides in the main chain like with DMCT mixed with PAn, which increases the kinetics of DMCT and leads to a capacity of 362 mAh g^{-1} [13,82]. On the other hand this is possible with disulfides in the side chain like with poly-2,2-dithiodianiline PDTDA [81] or poly(5,8-dihydro-1H,4H-2,3,6,7-tetrathia anthracene) PDDTA, which exhibits a high specific capacity of 422 mAh g^{-1} and an improved cycling stability [83].

Another approach to increase the capacity of disulfides is the introduction of more S-atoms, which results in the term of polysulfides like dimethyl trisulfide (DMTS) [84,85]. This approach introduces more redox active centers and combines the concept of classical polysulfide electrodes with organic polymers.

Unlike di- and polysulfides, the redox reaction of thioethers does not involve bond breakage, but an oxidation at the C-S-C thioether, which yields to a cationic radical sulfur group (P-type) [13]. The first thioethers have been presented by Zhang et al. in 2007 [86]. In this work the two polymers poly(2-phenyl-1,3-dithiolane) (PPDT) and poly(1,4-di(1,3-dithiolan-2-yl)benzene) (PDDTB) were synthesized and used as cathode materials in combination with a lithium anode. Especially PDDTB exhibited a high specific capacity of 378 mAh g^{-1} at two charge plateaus of 2.2 V vs. Li^+/Li . Other examples for thioethers are thianthrene-functionalized polynorborene [87] or poly(3-vinyl-N-methylphenothiazine) PVMPT [88–90].

Table 5: Examples for organosulfur compounds with typical values of potential and specific capacity.

| Material | Potential V vs. Li ⁺ /Li | Specific Capacity (mAh g ⁻¹) | Reference |
|----------|--|---|-----------|
| TETD | 2.7 | 65(181) | [80] |
| | | | |
| DMTS | 2.1 | 720 | [85] |
| | | | |
| PDDTB | 2.2 | 378 | [86] |
| | | | |

1.3.3.4 Organic Stable Radicals

Organic radicals in electrochemical energy storage application consist of a polymer backbone with radical groups attached to it, which can undergo redox reactions. In order to accumulate a sufficiently stable amount of those radicals into a polymer backbone, the unpaired electron needs to be inert towards other cell components like the electrolyte or towards the recombination with adjacent radicals [91,92]. This can be done either thermodynamically by delocalization of the radical electron or kinetically by isolation of the unpaired electron in the structure via bulky substituents [93]. Groups attached to

the polymer scaffold, which are used in this concept, are nitroxyl, phenoxy and hydrazyl [92]. Due to the stabilization of the radical this group of ROMPs is described as organic stable radicals or organic radical polymers (ORPs).

ORPs store charge via the transfer of the unpaired electron in the radical group (reduction for N-type, oxidation for P-type, see Table 2) [93]. Due to the simplicity of this electron transfer the rate of this reaction is usually very fast [91,94], which provides high power in EES application. Furthermore, since no significant change in the configuration of the polymer or pendent groups occurs during charge/discharge, they also provide high cycling stability [91].

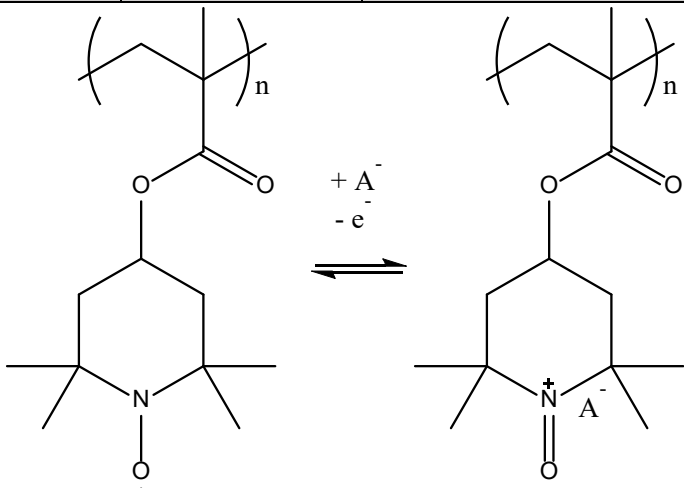
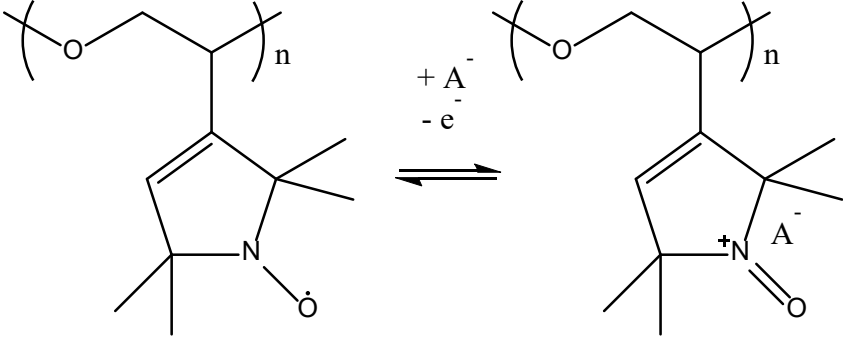
Nitroxyl radicals are the first ORPs, which have been introduced for EES by the pioneering work of Nakahara et al. in 2002 [95]. In this important work, which at the time revived the interest of researchers in the field of ROMPS, the redox active group 2,2,6,6-tetramethyl piperidiny-N-oxyl (TEMPO) was attached to a poly(methacrylate) polymer to form the ORP poly(2,2,6,6-tetramethyl piperidiny-N-oxyl-4-yl methacrylate) (PTMA). In this work and in following studies, PTMA proofed a specific capacity close to the theoretical value of 111 mAh g⁻¹ with a stable redox potential of 3.6 V vs. Li⁺/Li, high cycling stability, a coulombic efficiency near 100 % and high rate capability [20,95–104]. The main drawback of PTMA-based electrodes is their high self-discharge rate, which limits the application in real EES systems [20,102,105–107]. Nevertheless, PTMA can currently be regarded as the state-of-the-art ORP. Note that PTMA is only used as P-type material, as only the oxidation of the nitroxyl to the oxoammonium cation is reversible. The described N-type reaction to the aminoxyl anion is irreversible [92].

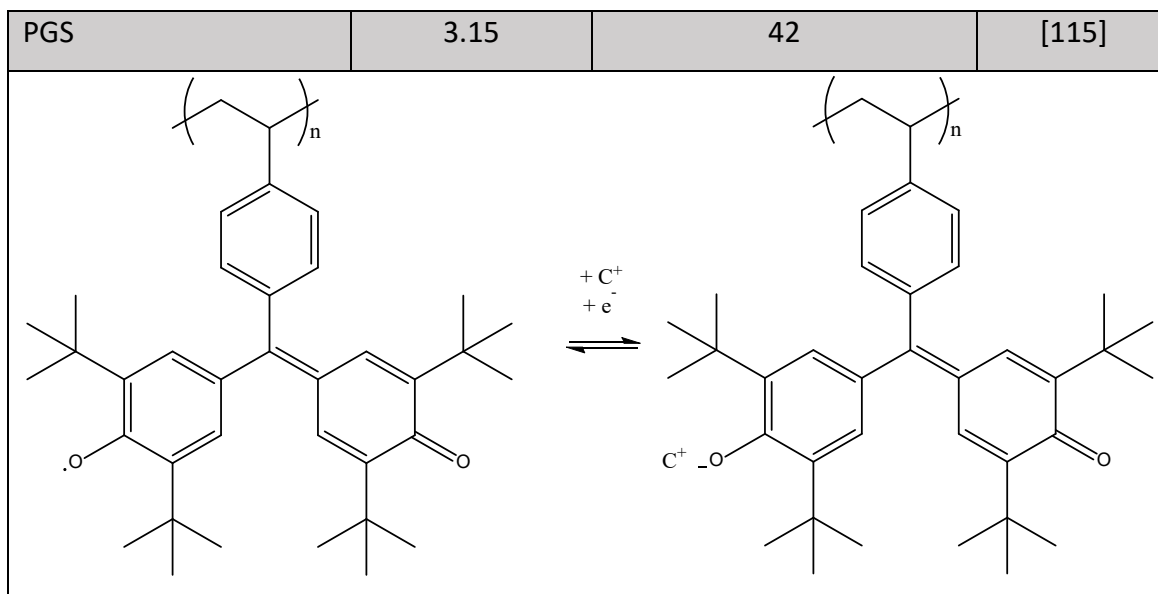
A popular alternative nitroxyl radical group to TEMPO is 2,2,5,5-tetramethyl-1-pyrrolidine-N-oxyl (PROXYL), which is represented for example in the poly(2,2,5,5-tetramethyl-3-oxiranyl pyrrolidine-N-oxyl ethyleneoxide) (PTEO), which is able to deliver a specific capacity of 146 mAh g⁻¹ at 3.5 V vs. Li⁺/Li [108].

Although the vast majority of ORPs is related to the use of nitroxyl groups [109–111], there are other examples like phenoxy radicals, which operate as N-type materials with the reduction to the phenolate (see Table 2) [112–114]. The most prominent repre-

sentative among phenoxyis is the galvinoxyl active group utilized for example in poly(galvinoxylstyrene) (PGS), which displays a specific capacity of 42 mAh g⁻¹ at a redox potential of 3.15 V vs. Li⁺/Li [112,115].

Table 6: Examples for organic radical polymers with typical values of potential and specific capacity.

| Material | Potential V vs. Li ⁺ /Li | Specific Capacity (mAh g ⁻¹) | Reference |
|--|--|---|-----------|
| PTMA | 3.6 | 111 | [20] |
|  | | | |
| PTEO | 3.5 | 146 | [108] |
|  | | | |



1.4 A Detailed View on PTMA

This thesis performs a detailed analysis on the performance of PTMA in dependence of the utilized electrolyte media. Since 2002, PTMA became one of the standard ORPs in OB research. Section 1.3.3.4 already explained the redox mechanism exploited in PTMA and gave an overview of the performance of PTMA in current literature. The values given there, however, are mostly reported for the PTMA cathodes in combination with a lithium-based anode and the standard electrolyte 1M LiPF₆ in EC/DMC in a coin cell setup. The Swagelok type cell setup utilized in the results and discussion part (section 2) of this work differs significantly from this cell design (see Appendix A1) and has been maintained for the entire number of publications presented in section 2 in order to ensure comparability of the results. Therefore, it is important for the reader to get an insight into the general performance of PTMA in the utilized setup of this work.

To provide this insight, Figure 6 illustrates an overview of the electrochemical behavior of a PTMA composite electrode in combination with the alternative electrolyte 1M 1-butyl-1-methylpyrrolidinium tetrafluoroborate (Pyr₁₄BF₄) in PC. This aims to introduce the characteristics of the active material PTMA to the reader and to give a standard to compare to the results of the following publications of this work.

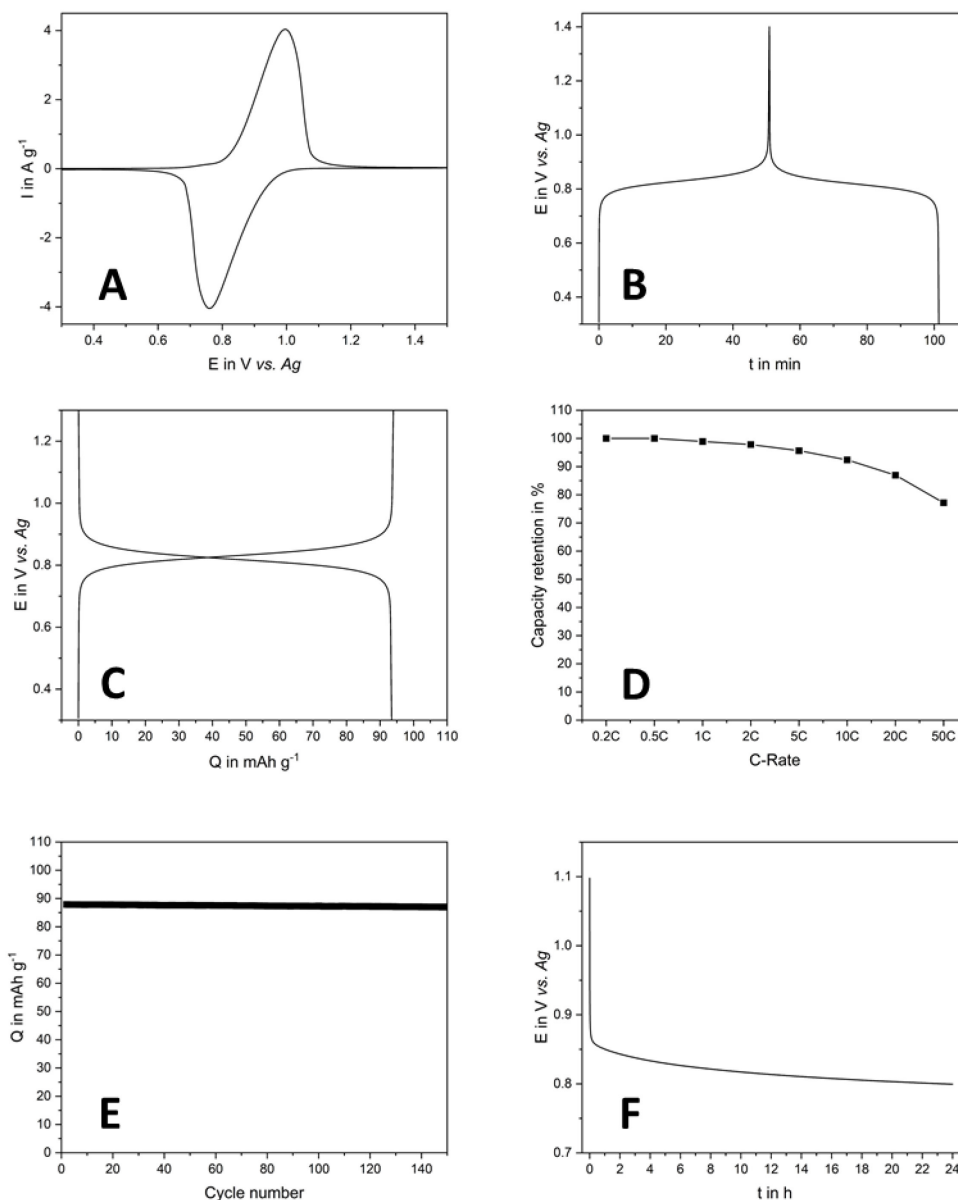


Figure 6: Electrochemical performance of a PTMA-based composite electrode in 1M Pyr₁₄BF₄ in PC: A) CV at a scan rate of 2 mV s⁻¹, B) Charge/discharge profile E vs. t at current density of 1C, C) Voltage profile E vs. Q at current density of 1C, D) Rate capability at current density of 0.2C to 50C, E) Cycling stability for 150 cycles at 1C, F) Self-discharge behavior E vs. t at a charge current density of 1C and 1 day of rest.

Figure 6A displays the cyclic voltammogram of a PTMA-based composite electrode in 1M Pyr₁₄BF₄ in PC at a scan rate of 2 mV s⁻¹. In this graph PTMA exerts one reversible redox peak couple with only minor peak separation of oxidation and reduction also at relatively high scan rate. This can be accounted to the fast one electron exchange reaction described in 1.3.3.4. The average redox potential of the reaction can be found at

0.85 V vs. Ag (3.85 V vs. Li⁺/Li), which is 0.25 V higher than the standard value given in literature [20].

Figure 6B presents the charge/discharge profile (cell potential E vs. time t) of a PTMA-based electrode in 1M Pyr₁₄BF₄ in PC cycled between 0.3 and 1.4 V vs. Ag with a current density of 1C (the calculation of 1C is based on the theoretical capacity of PTMA of 111 mAh g⁻¹). As visible in Figure 6B, PTMA shows a very distinct stable redox plateau at 0.85 V vs. Ag for both charge and discharge process. With a current of 1C a full cycle of the electrode (charge and discharge process) should last 120 min when 100 % of the theoretical capacity is accessible. In this graph, the cycle ends at 102 min, which corresponds to 85 % of the expected value. The coulombic efficiency, however, is near 100 %.

Figure 6C presents the charge/discharge behavior of a PTMA-based electrode in 1M Pyr₁₄BF₄ in PC as well. In this case the cell potential E is not plotted with respect to the time, but the specific capacity Q displayed by the cell. The redox potential is located at 0.85 V vs. Ag. The discharge capacity is observed at 93 mAh g⁻¹, which is 84 % of the theoretical capacity. The reduced capacity can be explained by the lower conductivity of 1M Pyr₁₄BF₄ in PC (8.36 mS cm⁻¹ at 20°C) compared to the values of the standard of 1M LiPF₆ in EC/DMC. The coulombic efficiency is close to 100 %.

Figure 6D shows the rate capability of a PTMA-based electrode in 1M Pyr₁₄BF₄ in PC from 0.2C to 50C, which highlights the ability of the active material to work at elevated currents. At 50C, PTMA still displays 77 % of the capacity received at 0.2C, which once again emphasizes the fast kinetics of this organic stable radical.

Figure 6E presents the cycling stability of PTMA in 1M Pyr₁₄BF₄ in PC over 150 charge/discharge cycles at a current density of 1C. In the graph a very stable discharge capacity at 87 mAh g⁻¹ is found for the whole measurement period, which indicates a negligible decomposition of the PTMA electrode in this system.

Figure 6F displays the self-discharge behavior of PTMA in 1M Pyr₁₄BF₄ in PC after charging at 1C and 1 day of rest. The self-discharge of PTMA at rest shows an immediate drop to the redox potential of PTMA after charging, which is followed by a slow decrease in potential. This indicates a slow loss in capacity over the whole rest time. After 24 h, the loss in capacity results to 13 % of the initial stored charge.

1.5 Publication 1: A Critical Analysis about the Underestimated Role of the Electrolyte in Batteries Based on Organic Materials

1.5.1 The Importance of the Electrolyte for Organic Materials

The electrolyte is a key component in all EES devices, since its core task, which is to ensure the movement of ions between the electrodes and at the same time prevent the transport of electrons within the cell, is needed in all systems. During the charge/discharge process the two electrodes are connected via an external circuit, which allows the electron exchange between them and therewith the exploitation of electrical work/energy. In this process, the electrolyte provides the diffusion of counter ions to the electrodes in order to allow charge compensation and therewith closes the inner circuit of the cell. Thus, it can be stated that the electrodes determine how much energy an electrochemical cell can provide, while the electrolyte among other factors heavily influences how fast this energy can be delivered due to its transport properties. At the end of the day, this also affects the power of the considered system [4].

The state-of-the-art electrolytes for batteries consist of a conductive salt dissolved in a liquid organic solvent. Nevertheless, also other electrolyte types like solid electrolytes, polymer electrolytes, ionic liquids (ILs) or solvent in salt mixtures, have been proposed. Independent from the nature of the used electrolyte, they all should meet similar principal properties for the application in electrochemical storage devices (see Table 7) [4,116].

Table 7: Desired properties for electrolytes for modern EES.

Desired Electrolyte Properties

- 1) High ionic conductivity
 - 2) Electronic insulator
 - 3) Wide electrochemical stability window
 - 4) Mechanical, thermal, and chemical stability
 - 5) Wide operative temperature window
 - 6) Environmentally friendly
-

In order to provide these general requirements on electrolytes the utilized solvents and ions should display very distinct features (see Table 8) [116].

Table 8: Desired properties for solvents and ions to form efficient electrolytes.

| Solvents | Ions |
|--------------------------|---|
| High dielectric constant | Complete dissociation |
| Low viscosity | High conductivity/ ion mobility |
| Inert | Inert |
| Wide temperature range | Stable towards oxidative or reductive decomposition |
| Nontoxic | Nontoxic |

These requirements are of course also given for the utilization of ROMPs in all cell configurations introduced in 1.3.2.

On the other hand, due to the variety of ROMPs and their very different storage mechanisms presented in 1.3.3, it is evident that a careful examination of the electrolyte is necessary for every ROMP. In practical this means that an electrolyte optimized for carbonyl compounds, does not necessarily be beneficial for the use in combination with organic stable radicals. This is true for every different organic active material.

In contrast to that for a long time, the main research effort targeting ROMP-based devices was dedicated to the development of new redox active materials. Compared to that only minor work has been done towards the improvement of the electrolyte for OBs [19,117]. Only in the last decade researchers began to understand that due to the different storage mechanisms and properties of ROMPs the electrolyte affects the performance of new developed organic materials in a major way [19]. Therefore, there is no universal electrolyte for organic materials like often proposed for the standard LIBs [116,118,119]. With this enlightenment the number of studies in this direction increased rapidly beginning from 2010 (see Figure 7).

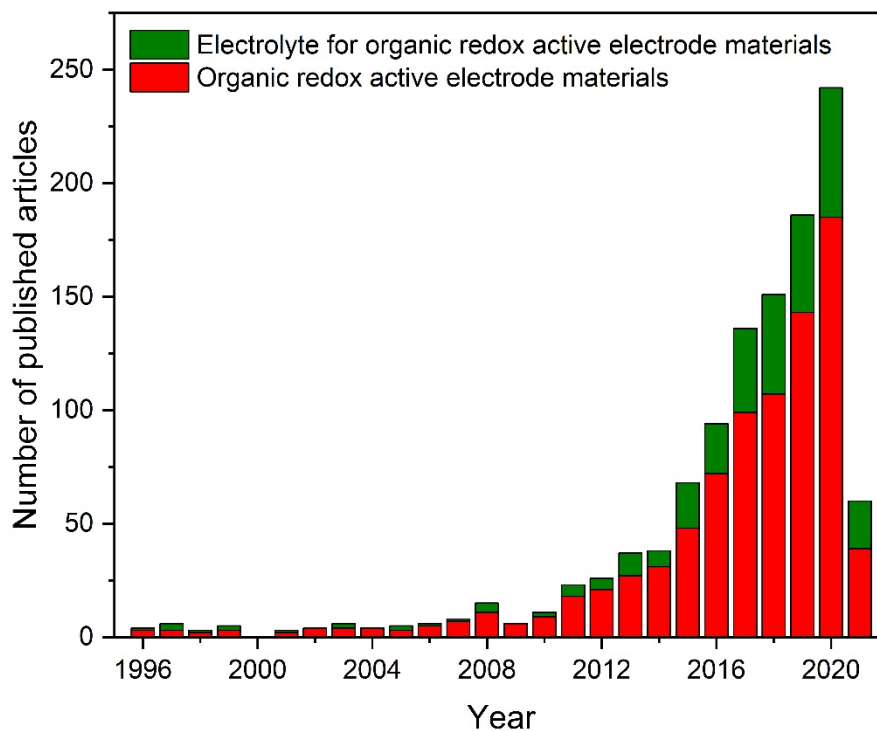


Figure 7: Number of published articles with the topic: “organic redox active electrode materials” and “electrolyte for organic redox active electrode materials” per year (derived from web of knowledge 18.03.2021).

Section 1.5.2 provides an introduction to the state-of-the-art electrolytes for ROMPs and highlights innovative electrolyte approaches, which aim to improve the performance of ROMPs.

1.5.2 Electrolytes used in Organic Batteries

1.5.2.1 State-of-the-Art Organic Electrolytes

The majority of research on ROMPs has been done considering organic electrodes as part of LIB technology (in smaller numbers also sodium-ion battery (SIB) and other metals) [11–13,15,25]. Therefore, in most cases ROMP-based electrodes have been used in combination with some kind of LIB or SIB electrodes and the optimized electrolytes used for these systems have been adopted for OBs.

Electrolytes for LIBs frequently used in literature utilize Li-salts like lithium hexafluorophosphate (LiPF_6), lithium perchlorate (LiClO_4), lithium tetrafluoroborate (LiBF_4) or lithium bis(trifluoromethylsulfonyl)imide (LiTFSI) [116]. Among those salts LiPF_6 is the most common representative, as it provides a very good mix of ion mobility, ion dissociation and SEI forming ability [4,116,119].

Regarding the organic solvent the most common used representatives are mixtures of linear and cyclic carbonates like ethyl methyl carbonate (EMC), dimethyl carbonate (DMC), propylene carbonate (PC) and especially ethylene carbonate (EC) [3,4,118,119]. The state-of-the-art mixture is a combination of EC and DMC in the ratio 1:1. In this mix, EC provides a high dielectric constant of 85.1 in order to sufficiently dissolve the conducting salt (LiPF_6). Unfortunately, at room temperature EC is still solid and displays an only moderate viscosity of 1.9 mPa s even at elevated temperature of 40°C [4,19]. Therefore, DMC with a low viscosity of 0.59 mPa s is used to lower the viscosity of the electrolyte. DMC cannot be used alone, since with a polarity of 3.1 is not suitable for efficient dissociation of the conducting salts.

With these considerations, 1M LiPF_6 in EC/DMC (1:1) (LP30) is the state-of-the-art electrolyte for commercial LIBs and can, at this time, also be regarded as the standard for ROMP-based EES devices. At 25°C LP30 displays a conductivity of 10.7 mS cm^{-1} and a viscosity of 5.1 mPa s [120].

For these reasons also works targeting all-organic devices often use these-state-of-the-art electrolytes, although in these systems there is no distinct need for metal-ions. Researchers working on the development and optimization of ROMPs are often tempted to do so, since electrolytes like 1M LiPF_6 in EC/DMC are established and the obtained

results for ROMPS are comparable to literature values, which used the same electrolyte [64,121–123].

1.5.2.2 The Need for Innovative Electrolytes

Although the described standard organic electrolytes allow high performance for ROMP systems in terms of specific capacity, there are associated to serious risk in safety due to toxicity and flammability of their components (solvent and salt) [11].

Furthermore, since these state-of-the-art electrolyte systems are mainly designed for the needs of inorganic LIB electrodes, they do not meet the special requirements of ROMPs. For instance, in these systems major aims are the maximization of the Li^+ movement during charge/discharge as well as the formation of a solid electrolyte interface (SEI) in the first cycles. Both aspects, however, are not needed in all-organic devices.

Additionally, there is the problem of dissolution of small organic molecules in the state-of-the-art electrolytes, which causes serious limitations regarding cycling stability and life time of ROMP devices [19]. Furthermore, dissolved active groups can promote self-discharge in the affected devices. Ways to address these issues are polymerization, crosslinking or the introduction of ionic groups to the active materials [12,13,15,19,124]. However, these attempts reduce the energy density of the ROMPs by increasing the molar mass of the active material.

Therefore, there is the need for innovative, tailor-made electrolytes, which address the specific limitations (like cycling stability or self-discharge) of specific organic active materials. As already discussed above, this aspect of OB development has been underestimated for a long time and in current literature there is a lack of such thoughtful electrolyte selections for ROMP-based systems. However, a few works in this regard exist of which a short introduction is given below.

Alternative organic Electrolytes

One way to prevent the dissolution of organic active material is the use of alternative organic electrolytes. This includes the application of organic solvents with opposite polarities compared to polarity of the used organic active material. Therewith the solubility of the active ROMP can be reduced significantly [125–127]. This was exploited in the case of the high polarity carboxylate DPD in combination with 1M LiTFSI in DMC as solvent, which displays a low polarity of 3.1 [127]. With this approach a stable cycling behavior was obtained for this active material [73].

Another valid approach for innovative organic electrolytes is the use of highly viscous electrolytes. Here the aim is to use an electrolyte with reduced mobility in order to suppress dissolution of electrode material and therewith increase the cycling stability [128–130]. A good example for the is 1M LiTFSI in tetraethylene glycol dimethyl ether (TEGDME), which improved the cycling stability of a DLT electrode by more than 20 % in comparison to the standard LP30 [129].

Following the same concept is the utilization of highly concentrated organic electrolytes. With the saturation of the electrolyte solution the further dissolution of other materials, which includes the ROMP of the electrodes, is reduced. Therewith, the cycling stability of ROMP systems can be increased in a major way [131–134]. Thus, with 7M LiClO₄ in EC/PC as electrolyte increased cycle life was found for a cuprous tetracyano quinodimethane (CuTCNQ) cathode compared to lower concentrations of 1, 3 and 5M with the same components [133].

Another point worth mentioning for ROMPs in combination with organic electrolytes is the possible operation at extreme temperatures. For example, there are reports of ROMP-based systems in combination with organic electrolytes reaching sufficient energy storage behavior operating at temperatures as low as - 80°C [135,136]. In this regard, Zhan et. al. presented an all-organic device utilizing polyimide (PI) and polytriphenylamine (PTPA) as active materials in combination with 1M 1-ethyl-3-methylimidazolium bis(trifluoromethylsulfonyl)imide (EMIMTFSI) in a mixture of acetonitrile (ACN) and methyl acetate (ratio 1:1). This system was able to deliver more than 80 mAh g⁻¹ at -80°C, while for PI and PTPA in 1M LiPF₆ in EC/DMC only 25 mAh g⁻¹ have been obtained

at -20°C [136]. Such a performance at low temperatures is hardly imaginable for other electrolyte concepts.

Aqueous Electrolytes

Next to the usage of organic electrolytes is the application of water-based electrolytes as environmentally friendly and safe alternative. However, these systems of course suffer from the reduced electrochemical stability window of 1.23 V. To overcome this drawback the so-called water-in-salt approach is used, which expands the electrochemical stability window to a feasible range as shown in a 2 V all-organic device utilizing PTPA and 1,4,5,8-naphthalenetetracarboxylic dianhydride-derived polyimide (PNTCDA) in 21M LiTFSI in water [137]. Due to the increased salt concentration again the solubility of ROMPs in the electrolyte can be suppressed [137,138].

Furthermore, aqueous electrolytes offer the opportunity to optimize the pH value of the electrolyte by using acids or bases in the solution. Tuning the pH value of an electrolyte allows to implement ROMPs together with different active materials in aqueous media, which are in need of certain pH values to work such as PbO_2 , LiMn_2O_4 or $\text{Ni}(\text{OH})_2$ [139].

Ionic Liquid Electrolytes

The last class of liquid electrolytes worth mentioning in this brief overview is the one of ionic liquids (ILs), which can be seen as the subsequent conclusion of the use of highly concentrated electrolytes. Ionic liquids are salts with a melting point below 100°C [140,141]. ROMPs used with ILs display increased cycling stability due to the high viscosity and high concentration of ions in the electrolyte due to the hindered dissolution of the active material [142–146]. With this approach it was possible to reach cycle numbers as high as 5000 cycles for a PI/PTPA metal-free device in pure EMIMTFSI [143]. However, the improvement in cycling stability often comes with a decrease in specific capacity due to the lower conductivity of ILs compared to classic salt and solvent mixtures.

Solid State Electrolytes

The most straight forward attempt towards reducing the solubility of ROMPs are solid state electrolytes like oxides, sulfides, spinels or polymers [147]. With the use of solid-state electrolytes for ROMPs high cycling stability and improvement in safety can be

achieved [148–151]. An interesting approach in this direction is the use of plastic crystallizers like succinonitrile (SCN), which can work as a Na⁺ conductor. In a 2.4 V all-organic cell with PAn and PAQS as active materials a stable cycling even at elevated current was achieved [151]. For the sake of higher performance in rate capability and specific capacity also a compromise between all-solid-state and liquid electrolytes has been done. This approach is referred to as quasi-solid-state electrolytes or in the case of polymers gel polymer electrolytes [152–154].

As shown here, researchers began to emphasize the use of innovative electrolytes to improve the behavior of ROMPs in EES application and even surpass the performance of conventional energy storage systems. However, it is also evident that this research of the last decade is done in small steps as often still LIB-based salts or solvents are used even in novel concepts. In the future a bigger leap towards ROMP tailored electrolytes is necessary.

This paragraph only gave an introduction for alternative electrolytes used for ROMPs. More specific details on electrolyte concepts and examples are given in publication 1.

1.5.3 Electrolytes used for PTMA

As already mentioned above, the standard electrolyte for ROMPs is 1M LiPF₆ in EC/DMC. This is also true for PTMA, especially considering the early works on the material [95,97,98,100,101]. More seldom also a mixture of EC/DEC is used with the same conducting salt [20,99]. However in more recent works (the last decade), also other electrolytes like tetraethylammonium tetrafluoroborate (Et₄NBF₄) in ACN are utilized [96,102,103]. Especially also the application of IL-based electrolytes has to be mentioned for PTMA although most of these attempts have still been made with Li⁺ salts like lithium bis(trifluoromethylsulfonyl)imide (LiTFSI) in 1-butyl-1-methylpyrrolidinium bis(trifluoromethylsulfonyl)imide (Pyr₁₄TFSI) [142,144]. Furthermore, also polymer electrolytes were used in minor numbers [155]. Thus, it can be stated that at the current point the research regarding the electrolyte for PTMA is rather one-sided. Li-salts with carbonates in the concentration of 1M represent the majority of the literature. With this in mind it is clear that there is a lack of other directions to go in terms of the electrolyte

for PTMA. Only with this approach statements on influence of the cation, anion, concentration, solvent, conductivity, viscosity and other characteristics of the electrolyte on the electrochemical behavior and performance of PTMA are possible.

A Critical Analysis about the Underestimated Role of the Electrolyte in Batteries Based on Organic Materials

Patrick Gerlach and Andrea Balducci^{*,[a]}

Electrochemical energy storage devices based on organic materials such as polymers and organic molecules (PORMs) are nowadays regarded with increasing attention. The interest on these systems is related to their promising electrochemical performance, their low cost and their high sustainability. In the last years, several works focused on the development of active materials suitable for these systems, while much less studies

have been dedicated to the electrolytes. The aim of this short review is to critically analyze these latter results, and to identify the main aspects that should be addressed in the future. Since the electrolyte is a key component of any energy storage devices, this analysis appears of particular importance for the realization of the next generation of PORM-based devices.

1. Introduction

The use of efficient and environmentally friendly energy storage devices appears nowadays indispensable for the establishment of an energetic sustainable society, which is relying in renewable resources like wind, biomass, solar, geothermal, hydro-power and tidal.^[1] Currently lithium-ion batteries (LIBs), due to their high energy and power density, are the most used electrical energy storage systems.^[2] The state-of-the-art LIB consists of an anode based on graphite, which is coupled with a cathode containing a lithium metal oxide. As electrolytes lithium salts like lithium hexafluorophosphate (LiPF₆) dissolved in mixtures of organic solvents, e.g. ethylene carbonate/dimethyl carbonate (EC/DMC), are used.^[2,3] Although these materials allow the realization of high performance devices, their use is also associated to significant drawbacks. On the one hand, the most used cathode materials like lithium nickel manganese cobalt oxide (NMC) or lithium cobalt oxide (LCO) are under resource constraint, especially because of the low abundance of cobalt.^[4–6] On the other hand, the used electrolytes cause serious safety risks, as they are volatile as well as highly flammable.^[7] Taking these points into account, the development of alternative and more sustainable energy storage systems appears of great importance.

In the last years the development of storage systems containing polymers and organic molecules as active materials, which can be generally defined as organic energy storage devices, attracted an increasing attention. The interest on these systems is related to their promising electrochemical performance, their low cost and their high sustainability.^[7]

This review is dedicated to the recent advances which have been made on the development of electrolytes for batteries based on organic materials. It is worth mentioning that very recently a review paper dedicated to electrolytes for organic materials based energy stored devices has been published.^[8] The present work differs from this latter review, as it considers and analyses in more detail the electrolytes especially developed for batteries containing organic active electrode. The aim of this work is to supply a critical analysis about the underestimated role of the electrolyte in organic batteries. Initially, the most investigated redox active compounds and their charging processes are considered. At the same time, the role and the importance of the electrolyte on the storage process, which takes place in these materials, is highlighted. Afterwards, the classes of electrolytes utilized so far in these devices are considered in detail, with the aim to understand the advantages and limitations related to their use. The review is concluded by an outlook on the most important aspects which will need to be addressed in the future.

2. Organic Molecules and Polymeric Materials in Energy Storage Devices: a Brief History

The use of polymeric materials and organic molecules (PORMs) in energy storage devices has a rather long history. (Figure 1

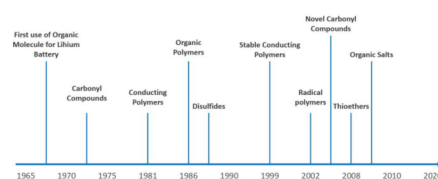


Figure 1. Development History of redox active organic molecules and polymers for energy storage application.

[a] P. Gerlach, Prof. Dr. A. Balducci
Institute for Technical Chemistry and Environmental Chemistry
Center for Energy and Environmental Chemistry Jena (CEEC Jena)
Friedrich-Schiller-Universität Jena, 07743 Jena, Germany
E-mail: andrea.balducci@uni-jena.de

© 2020 The Authors. Published by Wiley-VCH Verlag GmbH & Co. KGaA. This is an open access article under the terms of the Creative Commons Attribution License, which permits use, distribution and reproduction in any medium, provided the original work is properly cited.

shows a visual timeline evolution of these materials). The idea of using organic compounds as active materials for energy storage devices already arose in 1969, when dichloroisocyanuric acid (DCA) was used in combination with lithium in order to build a high energy density primary battery.^[9] After this first proof of concept,

a large variety of PORMs has been proposed in the '70s and early '80s. Examples of these materials are small carbonyl compounds like quinone derivatives,^[10] conducting polymers like polyacetylene, polyaniline and polypyrrole^[11] and dimeric^[12] as well as polymeric disulfides,^[13] e.g. tetraethylthiuram disulfide (TEDT) and poly(2,5-dimercapto-1,3,4-thiadiazole) (PDMCT). In 1986 a polymer (poly(quinone)) was proposed for the first time as cathodic material for lithium batteries by Foos et al.^[14] Poly(3,4-ethylenedioxythiophene) (PEDOT), one of the most utilized conducting polymers was proposed after more than 10 years later (1999).^[15,16] In 2002, Nakahara et al. were the first to propose the use of a stable radical polymer, poly(2,2,6,6-tetramethylpiperidinyloxy methacrylate) (PTMA), as active material for lithium batteries.^[16] After this pioneering work, a large number of new active materials, e.g. poly(2-phenyl-1,3-dithiolane) (PPDT) or poly(1,4-di(1,3-dithiolan-2-yl)benzene) (PDDB) in combination with lithium anodes have been proposed, in order to create high energy density cathode materials.^[15,17–24] In the recent years, Chen and Armand proposed the use of lithium or sodium salts of carbonyl molecules such as tetrahydroxybenzoquinone ($\text{Li}_4\text{C}_6\text{O}_6$).^[25,26] These salts, which are attracting an increasing interest, are often referred to as organic salts.

Depending on the type of the charge process taking place in PORMs, these materials can be divided into 3 main types: N-type, P-type and B-type. During the charge/discharge process of N-type compounds the material moves between the electro-neutral state (N) and the negative state (N^-). In P-types, the active material changes from the neutral (P) to the positive state (P^+). In the B-type the material can be either reduced or oxidized to both negative (B^-) or positive (B^+) state (Figure 2).^[15,27]

Table 1 is reporting an overview about the redox reactions taking place in some of the PORMs mentioned above. As shown, conducting polymers store charge within their polymer scaffold by a doping process and not via a redox reaction of a certain redox group.^[15] During the charging process either reduction or oxidation of the polymer leads to a gradual growing positive or negative state of the active material. In both cases, the generated charge is compensated by ions of

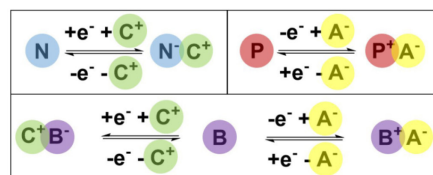


Figure 2. Redox principle of N-type, P-type and B-type organic redox active compounds.

opposite charge from the electrolyte. This process is referred to as doping.^[28,29] The intrinsic disadvantages of these materials is their sloping charge-discharge voltage and their instability.^[15,29] The group of carbonyls is an example of small organic molecules utilized in electrochemical energy storage devices.^[30,31] During the charge/discharge process, the carbonyl moieties are reduced to the oxide. The generated negative charge has to be compensated by a cation while the reduction is taking place. These materials are N-type compounds^[27] and they are usually used as anodic materials,^[32,33] except for in combination with metallic electrodes, e.g. lithium or sodium.^[27] Organic stable radical polymers exert a fast one electron exchange reaction while charging.^[34] The radical electron group can be either reduced to the corresponding anion (N-type) or oxidized to the cation (P-type). These materials are therefore belonging the B-type materials^[40] In practice, however, the reduction process is often irreversible^[35] and only a small number of N-type radicals have been successfully proposed.^[36] Therefore, organic stable radicals are mostly used as cathode materials in which, during the charge process, anions are taken from the electrolyte in order to equalize the generated charge.

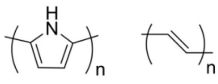
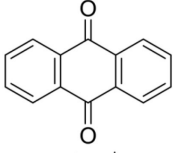
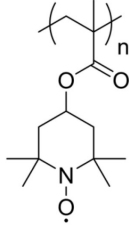
It has to be noted that although the above discussed materials have been widely investigated over more than 20 years, and they can be produced in large amount, PORM-based batteries are still not produced in large scale. The low cell voltage of organic batteries, their limited stability, caused by dissolution of the active material into the electrolyte, and their relatively high self-discharge are main reasons presently hindering their massive production. These drawbacks are originated by interplay of electrode-electrolyte within these systems, and it is therefore evident that to overcome them the electrolyte needs to be carefully considered and developed.



Patrick Gerlach is member of the research group of Prof. Dr. Andrea Balducci at the Institute for Technical Chemistry and Environmental Chemistry and at the Center for Energy and Environmental Chemistry Jena (CEEC Jena) of the Friedrich-Schiller University Jena, Germany. He is working in innovative electrolytes for organic radical active materials as well as redox active ionic liquids.



Andrea Balducci is Professor for Applied Electrochemistry at the Institute for Technical Chemistry and Environmental Chemistry and at the Center for Energy and Environmental Chemistry Jena (CEEC Jena) of the Friedrich-Schiller University Jena, Germany. He is working on the development and characterization of novel electrolytes and active/inactive materials suitable for the realization of safe and high performance electrical capacitors, metal ion batteries and polymeric batteries.

| Table 1. Used redox reactions of discussed organic active materials. | | | |
|--|---|---|---------|
| Group | Example Structure | Redox Reaction | Type |
| Conducting Polymers |  | $\left(\text{R}^{\text{C}^+ \text{y}^-} \text{R}'\right)_n \xrightarrow{+y \text{e}^- + \text{C}^+} \left(\text{R} \text{R}'\right)_n \xrightarrow{-x \text{e}^- + \text{A}^-} \left(\text{R}^{\text{A}^- \text{x}^+} \text{R}'\right)_n$ | B, N, P |
| Carbonyls |  | $\text{R}^{\text{O}} \text{R} \xrightarrow{+\text{e}^- + \text{C}^+} \text{R}^{\text{C}^+ \text{O}^-} \text{R}$ | N |
| Stable Radicals |  | $\text{R}^{\text{N}^{\cdot} \text{R}} \xrightarrow{+\text{e}^- + \text{C}^+} \text{R}^{\text{N}^+ \text{R}} \xrightarrow{-\text{e}^- + \text{A}^-} \text{R}^{\text{A}^- \text{N}^+ \text{R}}$ | (B), P |

3. The Role of the Electrolyte in Organic Storage Devices

The electrolyte is a key component of every electrochemical storage device and, without its presence, it is not possible to store energy in those systems. Electrolytes are chemical compounds (e.g., ionic liquids) or mixtures of different chemical compounds, e.g., solvent and salt, that are able to assure the movement of ions between the electrodes. Depending on the devices in which they are used, the electrolyte can act as medium for the transport of the ions involved in the storage process, e.g. lithium ions in LIBs, or act directly as active material, as in the case of electrochemical capacitors in which the charge is physically stored at the interface of electrode-electrolyte.^[37]

In order to allow an efficient storage process, the electrolytes used in electrochemical storage devices need to display several features: (i) good transport properties in order to guarantee a fast transport of ions during the charge-discharge process; (ii) large chemical, electrochemical and thermal stability in order to guarantee the realization of stable systems with high operative voltage and large temperature range of use and (iii) very low toxicity, environmental friendliness and low cost.^[3,38]

In the case of liquid electrolytes containing a salt dissolved in a solvent, these two components need to be carefully selected as the abovementioned properties are depending on both of them.

It is very important to underline that each energy storage system has its own characteristics and, thus, it is difficult to talk about an overall "ideal" electrolyte that can be universally used

in any type of electrochemical storage device. In this context, it is more appropriate to talk about designed or "task-specific electrolytes", which have to be developed taking into account the requirements and the application of a certain system.

Depending on their properties, PORMs can be utilized for the realization of different types of electrochemical energy storage devices. These devices can be divided into three main families: (1) all-organic devices, (2) metal-ion organic devices and (3) organic hybrid devices (Figure 3).

In all-organic batteries, as indicated by the name, both electrodes contain PORMs as active materials. Depending on the utilized materials, 3 different types of electrode combinations (subgroups) are possible within this family: (a) N-type electrode in combination with P-type electrode; (b) N-type electrode in combination with a N-type electrode operating at a different voltage and (c) P-type electrode in combination with a P-type electrode operating at a different voltage. In the case of the first subgroup, the electrolyte works as an ion reservoir and supplies the positive and negative ions necessary for the charge process in the two electrodes. In the case of the second and third subgroups, the electrolyte transports the ions involved in the charge process (cation in second subgroup and anion in the third subgroup). In this family, any type of ion can be used for the realization of the electrolyte.

In metal-ion organic batteries, a metallic electrode, e.g. lithium or sodium, is coupled with an N-type or a P-type electrode. In the first case, the electrolyte is acting as the media for the transport of the positive ions (the metal ions) involved on the storage process. In the second case, the electrolyte is acting as electrolyte reservoir, and it is supplying the ions necessary to the charge of the two electrodes. In this family, the

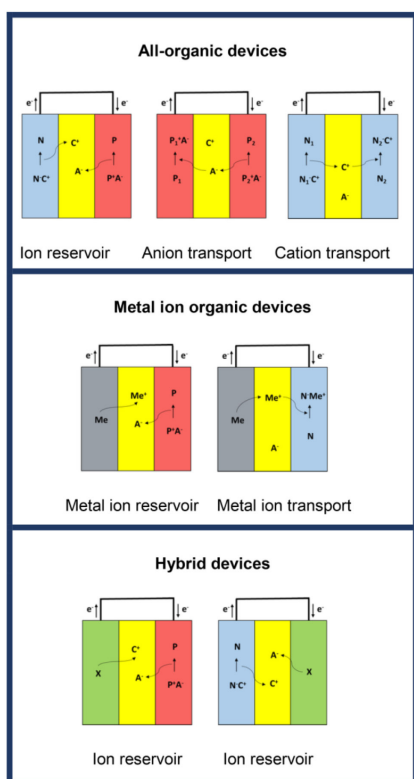


Figure 3. Possible electrode combinations for the described POM types. All-organic devices combine N- and P-type, Metal-ion-organic device: Metal-electrode and N- or P-type organic, Hybrid devices combine N- or P-types with X, which refers to battery or supercapacitor electrodes. The electrolyte has a key task in all displayed setups. All setups are shown in the discharge process.

presence of metal ions is necessary for the charge process, as they are needed for the intercalation/insertion.

In organic hybrid devices a battery material, anodic (e.g. graphite) or cathodic (e.g. NMC), or a supercapacitor material, capacitive (e.g. activated carbon) or pseudocapacitive (e.g. MnO₂), is coupled with an N-type or a P-type organic electrode. In the first case, it is also possible to address the devices as metal-ion batteries, while in the second one as supercapacitors. In both cases, the electrolyte is acting as ion reservoir. However, when POM-based electrodes are combined with a battery material the presence of metal ions in the electrolyte is necessary for the storage process. When they are used in combination with a supercapacitor electrode any type of ions can be utilized for the realization of the electrolyte.

Considering these points, it is evident that the electrolyte is dramatically influencing the charge process of devices containing POMs. Therefore, the design of electrolytes optimized for these devices need to be carefully considered and, depending of the type device, the composition of these electrolytes can differ significantly.

It is important to remark that in spite of the importance of the electrolyte, only few studies have been dedicated to this key component of all-organic batteries, metal-ion organic batteries and organic hybrid devices (Figure 4). The aim of this review is to analyze critically the results obtained so far and to identify the point that should be addressed on the future investigations.

4. Electrolytes for Organic Electrode-Based Devices

4.1 Liquid Aqueous, Organic, and Ionic Liquids-Based Electrolytes

So far, POM-based electrodes have been mostly investigated in combination with electrolytes developed for LIBs or sodium ion batteries (SIBs).^[7,15,27,39–41] As mentioned in the introduction, these electrolytes consist of mixtures of cyclic and linear carbonates, e.g. ethyl methyl carbonate (EMC), dimethyl carbonate (DMC), propylene carbonate (PC) and ethylene carbonate (EC). As salt, lithium or sodium ions in combination with hexafluorophosphate (PF₆⁻), perchlorate (ClO₄⁻), tetrafluoroborate (BF₄⁻), hexafluoroarsenate (AsF₆⁻) and bis(trifluoromethanesulfonyl)imide (TFSI⁻) anions are mostly used.

The state-of-the-art LIB electrolyte is a mixture of EC and DMC in a ratio of 1 : 1 containing 1 M LiPF₆. In this mixture, EC provides a high dielectric constant while DMC assures a low viscosity of the electrolytic solution.^[2,3,7,38,39,42,43]

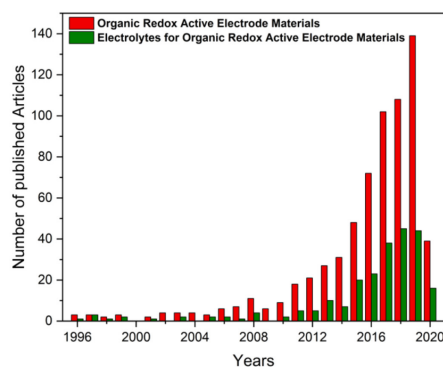


Figure 4. Number of published articles with the topic “organic battery” and “electrolytes for organic batteries” per year (from web of knowledge, 02.04.2020).

1 M LiPF₆ in EC/DMC 1:1 can be also considered the state-of-the-art electrolyte for POM-based systems. Electrodes based on the (2,2,6,6-tetramethylpiperidin-1-yl)oxyl (TEMPO), which is among the most utilized polymers for POM-based batteries^[44] are able to deliver in this electrolyte a high specific capacity (110 mAh g⁻¹) and a good capacity retention at high current density. In the same electrolyte, carbonyl based electrodes reached specific capacities of 200 mAh g⁻¹ (see Figure 5).^[25] Therefore, this electrolyte assures also high performance in POM-based batteries. However, it is important to notice that besides the safety and toxicity concerns mentioned above, its application appears problematic since it often causes the dissolution of the organic electrode active material. As a matter of fact, organic solvents like DMC and PC are able to dissolve many of the organic active groups, especially when small molecules like carbonyls are exploited as energy storage materials.^[42,45] This leads to reduced cycle life as well as elevated self-discharge.

To overcome this problem and to reduce the dissolution of the active materials, several strategies, e.g. crosslinking,^[46] addition of side groups which change the polarity of the active material^[42] and polymerization,^[47] have been proposed. Unfortunately, although they are improving the electrode stability, these strategies lead to an increase of the molar mass of active materials, which reduces their specific capacity.

The dissolution of organic redox active materials in LIB electrolytes is due to the ability of organic solvents to dissolve materials with similar polarity.^[42,48] Therefore, one way to overcome the dissolution of POM-based electrodes without decreasing their specific capacity is the use of high polar active materials, e.g. organic salts. These materials, which bear a high amount of ionic groups in their structure, display high polarity and a good stability in organic solvents.^[31] To guarantee high stability during their charge/discharge the electrolyte composition appears of great importance, and the use of solvents with low dielectric constants appears as an interesting strategy. Kim

et al. investigated the influence of the electrolyte on the electrochemical behavior of dilithium terephthalate (Li₂C₈H₄O₄).^[49] They compared the conventional 1 M LiPF₆ in EC/DMC mixture with 1 M LiTFSI in tetraethylene glycol dimethyl ether (TEGDME). TEGDME displays a viscosity not too different compared to that of organic solvents used in LIB electrolytes (3.26 mPas⁻¹ vs. 0.59 mPas⁻¹ for TEGDME and DMC, respectively).^[3,48] However, the permittivity (ϵ) of these electrolytes is significantly different. EC is a polar medium with a permittivity of 89.8, while DMC has a ϵ of 3.1. Consequently, a 1:1 mixture of EC/DMC is still rather polar and therewith able to dissolve the polar compounds. To the contrary, TEGDME display a low permittivity (7.7). It has been shown that a polar active material such as dilithium terephthalate experienced a capacity loss of 61% in the electrolyte 1 M LiPF₆ in EC/DMC after 50 cycles carried out at a current density of 1 C. The stability of the same electrodes improved by 20% in the apolar 1 M LiTFSI in TEGDME electrolyte.^[49] A similar behavior was observed for electrodes based on pyromellitic diimide dilithium salt cycled in 1 M LiTFSI in neat DMC.^[31] In this case, it was possible to show a good cycling stability for the lithiated pyromellitic diimide in the low polar solvent, while the hydrogenated reference material, which has a different dielectric constant compared to the salt, displayed very poor cycling stability.

The use of low polarity solvents appears also effective for electrodes containing carbonyls as the active material. Cao et al. compared the impact of a large number of different electrolytes based on mixtures of EC/PC/DMC on the electrochemical performance of electrodes based on polyanthraquinone sulfide (PAQS).^[48] They showed that small amounts of high permittivity solvents support the dissolution of active material into the electrolyte. When the electrolyte composition suppresses dissolution processes, it is possible to realize systems displaying high coulombic efficiency (99.5%) and high cycling stability.

Considering these results, the use of low polar solvents appears advantageous for high polar POM-based systems. However, it should be noted that since the polarity of POMs might change dramatically during the charge/discharge process, a direct correlation between the polarity of active material/electrolyte and the overall cycling stability cannot be directly established. Furthermore, to the best of our knowledge no example of a low polar active material with a high polar organic solvent has been proposed and/or investigated in literature. This latter approach could be helpful to gain a better understanding about the relation between electrode and electrolyte polarity on the electrochemical behavior of POM-based systems.

An interesting aspect which has been investigated recently is the influence of the electrolyte on the operative temperature of POM-based devices.^[50] Xia et al. presented an all-organic system containing polytriphenylamine (PTPA)- and 1,4,5,8-naphthalenetetracarboxylic dianhydride-derived polyimide (PNTCDA) as cathodic and anodic material, respectively, cycled in combination with the electrolyte 2 M LiTFSI in ethyl acetate (EA).^[50] This electrolyte provides a conductivity of 0.2 mS cm⁻¹ at -70 °C. Therewith this organic system delivers 69 mAh g⁻¹_{PTPA}

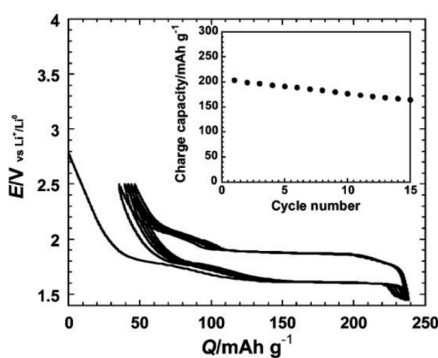


Figure 5. Voltage profile and cycling stability of Li₂C₈H₄O₄ in 1 M LiPF₆ in EC/DMC (reproduced with permission from Ref. [25], Copyright (2009) ACS Publications).

at a current density of 0.05 A g^{-1} at -70°C , which is 70% of the value obtained at room temperature (Figure 6). Furthermore, at a higher current density of 0.5 A g^{-1} the organic full cell shows a broad working window from $+55^\circ\text{C}$ to -70°C .

In a work of 2019, Zahn et al. investigated a system containing the same active materials (PTPAn and PNTCDA) utilized by Xia et al.^[51], but in combination with an electrolyte based on 1 M EMIMTFSI (ionic liquid) methyl acetate (MA) and acetonitrile (ACN) in a ratio of 1:2. This latter electrolyte shows good conductivity even at low temperatures. Using this electrodes/electrolyte combination it was possible to realize a device able to deliver 85 mAh g^{-1} at -80°C , which is 77% of the value at 20°C . Furthermore, it was also possible to cycle this all-organic cell for 2000 cycles at 1 C and -60°C with a high coulombic efficiency of 99% and a specific capacity near the theoretic value of 111 mAh/g . These results represent a clear indication about the influence of the electrolyte composition on the overall performance of PORM-based batteries. It is also important to notice that these results are indicating that through a careful design of the electrolyte it is possible to realize organic based systems which are able to work in extreme temperature conditions, which are not accessible, for kinetic reason, to metal-ion batteries.

In parallel to the work on organic electrolytes, also water-based electrolytes have been considered in the past years. Water is a cheap, safe and environmentally friendly polar solvent. Due to these properties it is a very appealing candidate for the realization of sustainable energy storage devices. The main drawback of water-based electrolytes is their limited electrochemical stability (overall 1.23 V), which is significantly limiting the operative voltage of the devices in which they are used. In the last years, however, it has been shown that the use of highly concentrated electrolytes, the so-called "water-in-salt" enable a significant enlargement of the electrochemical stability of these electrolytes and of the devices in which they are used. For this reason, "water-in-salt" solutions have been intensively investigated as electrolytes for LIBs as well as supercapacitors.^[52,53]

Wang et al. investigated the use of "water-in-salt" electrolytes in organic batteries.^[54] They considered an all-organic battery containing a cathode based on PTPAn and an anode based on PNTCDA. As electrolyte, they utilized several water solutions containing different concentrations of the salt LiTFSI. They showed that the use of relatively low concentrated

electrolytes (1 and 2 M) was not suitable due to the formation of O_2 at the cathode. However, when the salt concentration was increased to 21 m, the high amount of salt in the electrolyte was able to "trap" the free water molecules and thereby inhibits the adsorption of H_2O on the cathode surface and thus the generation of O_2 . Utilizing this "water-in-salt" electrolyte the battery was able to deliver reversible specific capacity of 105 mAh g^{-1} , a coulombic efficiency near 100% and a capacity retention of 85% after 700 cycles (see Figure 7).^[54] Another approach utilized for the implementation of aqueous electrolytes has been the tuning of the electrolyte pH value. Yao et al. were able to show that the pH value of the electrolyte is heavily influencing the cycling behavior of quinone based anodes.^[55] Among others, they presented the performance of a pyrene-4,5,9,10-tetraone (PTO) electrode together with PbO in an aqueous electrolyte. In neutral solution, PTO displays a very fast capacity decay of 80% after only 2 charge and discharge cycles. In contrast, in a very acidic electrolyte ($\text{pH} = -1$), which corresponds to a concentration of 4.4 M of sulfuric acid in H_2O , PTO could be successfully charged/discharged. At 2 C the material displayed an initial specific capacity of 395 mAh g^{-1} and after 1500 cycles the electrode was able to retain 96% of its initial capacity. The average coulombic efficiency during the cycling process was 99.6%.^[55]

Following an approach similar to that of water-in salt, also highly concentrated organic electrolytes have been proposed and investigated in the last years. As in the case of water based electrolytes, varying the salt concentration allows to tune the viscosity of these electrolytes and, also, to reduce the kinetics of the dissolution process occurring within them.^[42] Chen et al. investigated the impact of triethylene glycol dimethyl ether (TEGDME) based electrolytes containing different concentrations (1,2,3 and 4 M) of sodium trifluoromethane sulfonate (NaTFS) on the behavior of electrodes based on anthraquinone (a metallic sodium was used as anode).^[56,57] They showed that the specific capacity, cycling stability as well as coulombic efficiency of the anthraquinone electrodes in the highly concentrated electrolyte was superior towards the less concentrated systems. When the electrolyte containing a salt concen-

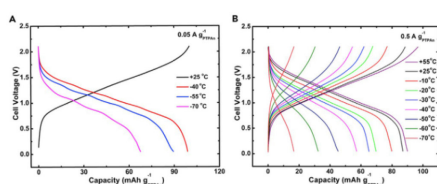


Figure 6. Capacity retention of an organic full cell using PTPAn and PNTCDA in 2 M LiTFSI in EA at low temperatures (reproduced with permission from Ref. [50], Copyright (2018) The Authors).

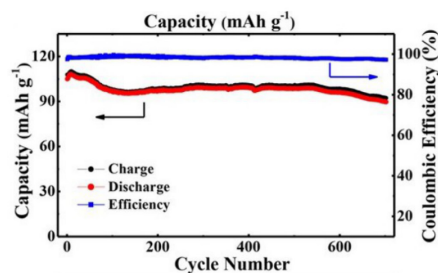


Figure 7. Cycling stability of an all-organic device with PTPAn as cathode and PNTCDA as anode material in combination with a 21 m LiTFSI aqueous electrolyte at a current density of 0.5 A g^{-1} (reproduced with permission from Ref. [54], Copyright (2017) Wiley-VCH).

tration equal to 4 M was used, the electrodes could be charged/discharged with efficiency close to 100% (while it was below 90% in the 1 M electrolyte), and thereby delivered a specific capacity of 208 mAh g^{-1} at a current density of 0.2 C (vs. ca. 160 mAh g^{-1} in 1 M). Furthermore, the use of concentrated electrolytes was also improving the electrode cycling stability (see Figure 8).^[56] Also when tannic acid (TA) is used as active anodic material in metal-ion organic batteries the use of highly concentrated electrolytes appears favorable^[58]. It is known that TA dissolves easily in LIB electrolytes, and for this reason its cycling stability in this type of electrolytes is typically low. It has been reported that the use of high concentrated electrolytes, e.g. 1, 3 and 5 M LiTFSI in EC/DEC mixtures, is suppressing the occurrence of the dissolution process of the active material.^[58] In this case, however, the increase of the salt concentration leads to a decrease in specific capacity.

As mentioned above, the self-discharge is seen as one of the main drawbacks of PORM-based electrodes and, for this reason, many efforts have been made to minimize this process, which can be caused by a shuttle-effect of dissolved redox active moieties in the electrolyte.^[34] In a recent work, the impact of the salt concentration on the self-discharge of PTMA-based electrodes has been investigated.^[59] It has been shown, that in

electrolytes containing PC and 1-butyl-1-methylpyrrolidinium tetrafluoroborate ($\text{Pyr}_{14}\text{BF}_4$) the salt concentration heavily influences the self-discharge of this active material. In fact, an electrolyte containing 3 M $\text{Pyr}_{14}\text{BF}_4$ in PC displays significantly lower self-discharge (more than the half) compared to those with a salt concentration equal to 1 M (see Figure 9). Such a reduction can be explained by a decreased dissolution of organic redox groups in the electrolyte,^[59] which reduces capacity loss during cycling as well as the self-discharge by the proposed shuttle effect. However, PTMA also displays a reduced specific capacity in combination with high concentrated systems. This is caused by the reduced ion mobility and the accompanying decreased conductivity and inhibited wetting of the electrodes.^[60]

The above discussed works clearly highlight the beneficial effect of high concentrated electrolytes (of both water and organic based electrolytes) on the cycling stability and self-discharge behavior of PORM-based electrodes. Nevertheless, it has to be noticed that in practical systems the use of this electrolytes might be difficult due to their (often) limited conductivity. Due to this reason, the use of electrolytes displaying medium-high salt concentration could be a good choice to guarantee at the same time high cycling stability, high specific capacity and low self-discharge.

Ionic liquids (ILs) are salts with melting points below 100°C and display high ion concentration, high viscosity and high polarity, when used as neat electrolytes. Due to these favorable properties, in the last decade they have been considered as electrolytes for a large variety of energy storage devices, including PORM-based systems. The use of neat ILs in these latter systems can be somehow considered as a consequent progression of the use of highly concentrated electrolytes.

The impact of IL-based electrolytes on the electrochemical behavior of organic based systems has been investigated by several authors. Recently, the influence of neat 1-butyl-1-methylpyrrolidinium bis(trifluoromethyl-sulfonyl)imide ($\text{Pyr}_{14}\text{TFSI}$) (IL) and a solution containing 1 M $\text{Pyr}_{14}\text{TFSI}$ in PC on the electrochemical behavior of PTMA-based electrodes has been considered. It has been shown that these electrodes display higher capacity in 1 M $\text{Pyr}_{14}\text{TFSI}$ in PC than in neat IL (100 mAh g^{-1} vs. 60 mAh g^{-1} , respectively). However, the use of neat $\text{Pyr}_{14}\text{TFSI}$ allows a better cycling stability compared to the mixture of IL and PC. In the same work, it has been reported that an organic hybrid device containing a PTMA positive electrode and an activated carbon negative electrode displays in neat $\text{Pyr}_{14}\text{TFSI}$ a remarkable capacity retention of almost 90% after 10,000 cycles at 10 C (Figure 10). The capacity retention of the same device in combination with 1 M $\text{Pyr}_{14}\text{TFSI}$ in PC was only 30%. This result indicates that the high viscosity, polarity and ion saturation of the IL is preventing the dissolution of the active material, and it is improving the cycling stability of the devices in which they are used. The use of neat ILs is also reducing the self-discharge of PTMA-based electrodes.^[60] In 1 M $\text{Pyr}_{14}\text{TFSI}$ in PC ca. 30% of the initial charge are lost after 3 days of self-discharge, while in the neat IL, 90% of the charge are kept in the electrode.

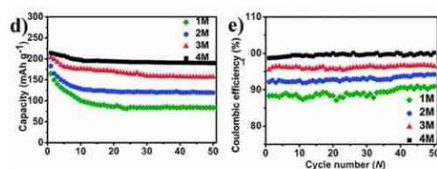


Figure 8. Cycling performance of AQ in 1, 2, 3 and 4 M NaTFS in TEGDME at 0.2 C (reproduced with permission from Ref. [56], Copyright (2015) RCS Publishing).

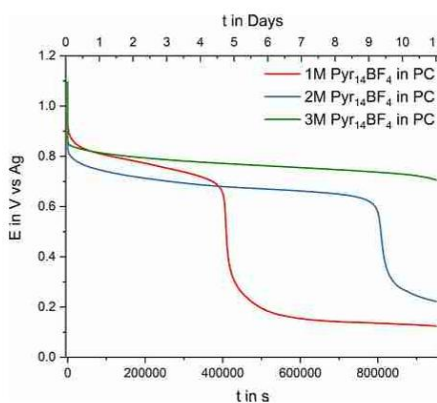


Figure 9. Self-discharge performance of PTMA in 1, 2 and 3 M $\text{Pyr}_{14}\text{BF}_4$ in PC (reproduced with permission from Ref. [59], Copyright (2019) Elsevier).

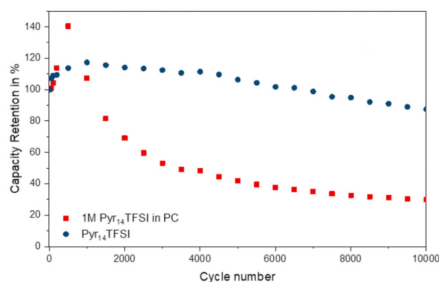


Figure 10. Cycling stability of PTMA based electrodes in 1 M Pyr₁₄TFSI in PC and neat Pyr₁₄TFSI as electrolyte with a current density of 10 C (reproduced with permission from Ref. [60], Copyright (2018) Elsevier).

Chen et al. compared the performance of 6 different ILs (3 TFSI⁻ and 3 FSI⁻ based ones) and 1,2-dimethoxyethane (DME) as electrolyte solvents for calix[4]quinone (C4Q) based organic electrodes.^[61] They showed the advantages related to the use of TFSI-based ILs over organic solvents in terms of cycling stability, proving that C4Q-based electrodes lost nearly no capacity after 300 cycles at 0.29 C in Pyr₁₃TFSI, while in DME nearly all capacity is lost after 110 cycles. They also investigated the solubility of the active material in the various ILs and in DME via UV/vis experiments. They showed that C4Q displays much higher solubility in FSI-based ILs than in TFSI-based ones. As Figure 11 shows, FSI-based electrolytes dissolve C4Q even better than the organic solvent DME, which is explainable by the lower polarity of the FSI-salts.^[61]

Considering the results discussed above, the viscosity of the electrolyte seems to play a crucial role on the behavior of PORM-based batteries, and the use of highly viscose electrolytes seems to be advantageous to suppress the kinetics of degradation processes, e.g. associate to dissolution processes, in these kind of storage devices. A work of Izgorodina et al.

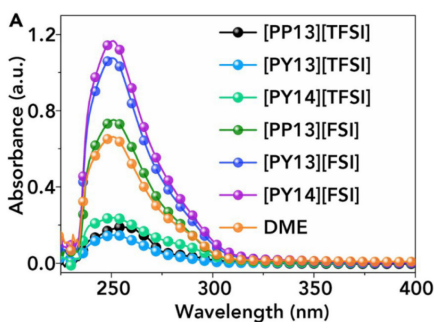


Figure 11. UV/vis spectra of C4Q in DME and 6 different FSI and TFSI based ILs (reproduced with permission from Ref. [61], Copyright (2019) The Authors).

from 2019, investigated this important aspect combining computational and spectroscopic methods.^[62] In their study the authors investigated the influence of ILs on the stability of redox active radical groups (TEMPO). In literature the positive effect of ILs on the stability of stable radicals is mostly attributed to the steric hindrance, caused by their high viscosity. Utilizing density functional calculations, the occurrence of high interaction energies between the stable radicals and (mainly) the anions of the ILs (up to 85.6 kJ mol⁻¹) were observed. The main contribution to these energies was found to be dispersion force. These theoretic results have been verified by electron paramagnetic resonance (EPR) experiments, in which the rotational diffusion coefficients τ_R were determined. For all investigated ILs, the τ_R was found to be relatively high compared that of organic solvents like DCM ($\tau_R = 1.92 \times 10^{-11}$ s), indicating that the radicals display a slower rotational diffusion in ionic liquids than in organic solvents. Among the investigated ILs, the highest value was found for 1-ethyl-3-methyl-imidazolium triflate [C₂mim][CF₃SO₃] with $\tau_R = 8.27 \times 10^{-10}$ s. In order to exclude the contribution of steric hindrance the authors carried out experiments also with paraffin oil and at different temperatures. The results of this interesting investigation indicated that nitroxide radicals are stabilized mainly by intermolecular interactions with the anions of ILs by dispersion forces, and not by steric hindrance resulting from the high viscosity.

4.2 Solid and Gel-Polymer Electrolytes

Another strategy to prevent the dissolution of organic electrode materials into the electrolyte is to move from very viscous or concentrated solvents to solid electrolytes, e.g. solid polymer electrolytes. He et al. proposed poly(2-chloro-3,5,6-trisulfide-1,4-benzoquinone) (PCTB) as organic electrode material, showing that this polymer display a reversible specific capacity of ca. 140 mAh/g.^[63] Nevertheless, when used in combination with the conventional 1 M LiPF₆ in EC/DME PCTB-based electrodes displayed a capacity retention of only 63% after 100 cycles of charge/discharge. To overcome this limitation caused by the dissolution of PCTB into the liquid organic electrolyte, the same group prepared an all-solid-state electrolyte based on poly(ethylene glycol) (PEO). In order to increase the ionic conductivity of the PEO-based electrolyte, 10% of the filler Li_{0.3}La_{0.56}TiO₃ (LLTO) were added to the polymer.^[64] Utilizing this composite electrolyte, PCTB electrode could retain 90% of their initial capacity after 300 cycles at 70 °C.

Xia et al. investigated the interfacial and charge transfer resistance of anthraquinone-based cathodes via impedance spectroscopy.^[65] They showed that due to the interaction of the active material and electrolyte at the cathode surface, anthraquinone-based cathodes display a strong increase in interfacial as well as charge transfer resistance when cycled in combination with an organic electrolyte (1 M LiTFSI in DOL/DME) at 65 °C. To the contrary, when these electrodes are cycled in combination with PEO based polymer electrolytes only a small rise in resistance is observed. This latter behavior was attributed to the ability of the solid electrolyte to inhibit the dissolution of

active material (see Figure 12). Nevertheless, in order to exploit the advantages related to the use of solid electrolytes high operative temperatures are needed.

To overcome this limitation and realize systems able to operate at room temperature, gel polymer electrolytes (GPE), in which a polymer backbone soaked with a liquid electrolyte, has been utilized. Chen et al. proposed the use of a mixture of poly(ethylene glycol) (PEG) and poly(methacrylate) (PMA) loaded with LiClO_4 in dimethyl sulfoxide (DMSO) as electrolyte for an organic metal battery containing calix[4]quinone (C4Q) as cathode material.^[66] The proposed GPE displayed at room temperature a conductivity of 0.57 mS cm^{-1} , when a salt concentration of 0.7 M is used. In conventional liquid electrolytes, C4Q-based electrodes display a specific capacity of 431 mAh g^{-1} at 0.2 C. However, they lose 77% of their initial capacity after five cycles of charge/discharge. To the contrary, when PMA/PEG-based GPE are utilized, C4Q can retain ca. 90% of their initial capacity after 100 cycles. However, although the use of the GPE does not reduce the electrode capacity at low C-rate, the low conductivity of these electrolytes -compared to liquid electrolytes- is limiting the rate performance of the devices in which they are used. In their work, Chen et al. were also able to transfer this successful strategy to 2,2'-bi(1,4-naphthoquinone) (BNQ).

These works highlight the applicability of the GPE concept for several organic active materials. It is important to notice that GPEs do not exclusively have to be loaded with liquid organic electrolytes, but also ILs can be used for their realization. In this latter case, it is possible to address these electrolytes as ionic liquid polymer electrolyte (ILPE). Kim et al. showed that the use of IL based electrolytes inhibit the dissolution of PTMA compared to conventional liquid electrolytes^[67]. Furthermore, they also showed that the use ILPEs improve even further the performance of these systems. Specifically, they compared the self-discharge of PTMA based electrodes in the liquid 1 M LiTFSI in Pyr14TFSI and in the nano-fibrous poly(vinylidene fluoride-co-hexafluoropropylene) (PVdF-HFP) polymer matrix soaked with

1 M LiTFSI in Pyr₁₄TFSI. They showed that after 15 days of self-discharge the voltage of PTMA-based electrodes in the IL electrolyte dropped from 3.6 V vs. Li/Li^+ to 2.5 V vs. Li/Li^+ , while PTMA used in combination with the ILPE stabilized at ca. 3.5 V vs. Li/Li^+ (see Figure 13), as the ions immobilization realized by the GPE stops the dissolution of the active material.

Considering the results discussed above, it is possible to draw some general considerations about the status of investigation dedicated to the electrolytes for PORM-based devices. Presently, the state-of-the-art electrolytes of LIBs can be considered also as the state-of-the-art electrolytes of PORM-based devices. These electrolytes have been used because they are largely available and guarantee good conductivities. However, their application on these organic devices can neither be considered satisfactory, nor desirable for many reasons. PORM-based systems aim to be green, sustainable and safe alternatives to LIBs and the use of these flammable and dangerous electrolytes appears to be an obstacle to achieve these goals. Furthermore, these electrolytes are not "task-specific". They contain metal ions, which are generally not needed for PORM-based devices, and they have been designed to maximize the lithium ion mobility. As illustrated above, in all-organic and hybrid organic devices positive and negative ions should display comparable mobilities to allow and optimize the charge-discharge process (Dual-ion-battery). Finally, they are not able to reduce neither the dissolution of the organic active material within the electrolytic solution, nor the self-discharge, which is typical for PORM-based electrodes. Due to these limitations, in the last years an increasing number of studies has been dedicated to alternative electrolytes. These investigations showed that the nature of the solvent and the salt has a dramatic impact on the behavior of PORM-based systems. Highly concentrated electrolytes (both water and organic based) appear presently as one of the most interesting classes of electrolytes for these devices as they allow sufficient and stable capacities and, at the same time, they are very effective

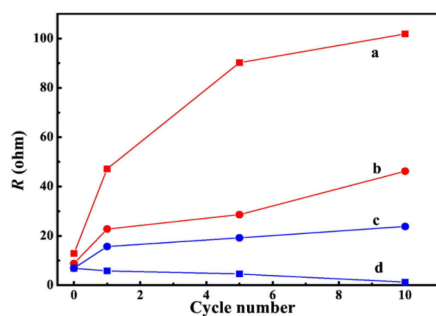


Figure 12. a) Interfacial resistance, b) charge transfer resistance of a cell (AQ cathode and Li anode) in a liquid electrolyte and c) interfacial resistance, d) charge transfer resistance of a cell (AQ cathode and Li anode) in a PEO based solid electrolyte (reproduced with permission from Ref. [65], Copyright (2017) Elsevier).

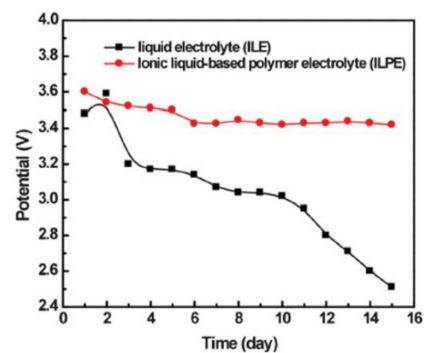


Figure 13. Self-discharge performance of PTMA liquid 1 M LiTFSI in Pyr14TFSI and in polymer matrix soaked with 1 M LiTFSI in Pyr14TFSI (reproduced with permission from Ref. [67], Copyright (2012) RSC Publishing).

in reducing the electrode self-discharge. In the future, it will be important to identify the most suitable concentrations, which can be utilized to reach at the same time high performance at high current densities as well as low self-discharge. Ionic liquid-based electrolytes appear also as interesting alternatives. Although their use is limiting the performance at high current density of PORM-based systems (as in the case of LIBs and supercapacitors), this kind of electrolytes are able to reduce the electrode self-discharge. In the future it will be necessary to investigate the influence of the temperature on IL-based devices and the impact of protic and, eventually, redox active ILs on the electrochemical behavior of PORM-based systems. Solid electrolytes and gel polymer electrolytes can also be regarded as promising alternatives. As in the case of the electrolytes discussed above, their use is reducing the self-discharge of the PORM-based systems. However, their conductivity at room temperature should be increased, as it is presently too low. Furthermore, also their chemistry should be reconsidered. As in the case of the LIB electrolytes discussed above, most of these solid electrolytes have been designed with the aim to optimize the lithium ion mobility. For this reason, these electrolytes appear well suited for metal-ion devices, but their implementation in all-organic and hybrid organic devices will require novel design. Table 2 is giving a visual comparison of the categories considered in this review.

5. Future Directions

Although in the last years interesting results have been obtained, it is evident that further efforts are needed to realize advanced electrolytes for PORM-based batteries. It is important to remark once more that PORMs can be subject to different type of redox reactions, and that they can be combined in several ways with other classes of battery and supercapacitor materials for the realization of different types of electrochemical energy storage devices. In each of these devices the electrolyte fulfills a specific task and needs to be specifically designed in

order to allow the realization of stable and high performance PORM-based systems. Therefore, the development of "task-designed" electrolytes appears of crucial importance for the future of these type of storage devices.

For the realization of "task-specific" electrolytes a profound knowledge of the electrode-electrolyte interface is mandatory. In a recent work, the Dominko's group investigated (among other materials) the storage mechanism of PAQS together with Li^+ as well as Mg^{2+} ions via in operando attenuated total reflectance infrared spectroscopy (ATR-IR).^[68] Figure 14a shows the assumed storage mechanism of PAQS with a lithium anode and a LIB electrolyte. Utilizing a specific cell setup, the authors were able to detect structural changes of the organic active material during the cycling (via ATR-IR). They found that during the discharge process a decrease of the C=O band and an increase of the C-O⁻ signal were occurring (and vice versa in the charge), confirming the storage mechanism for PAQS with lithium ions (Figure 14). This analysis was then extended to other PORMs, e.g. AQ, PAQ and PANI. Furthermore, they also exchanged lithium by magnesium observing important differences between the two systems.^[68] This work is a very good example of how the combination of electrochemical and in-situ techniques can supply novel and extremely valuable information about the electrode-electrolyte interface. This kind of combined investigations, however, are still not very common in the field of PORM batteries. It is therefore evident that their use should be strongly intensified in the future for the realization of task designed electrolytes.

Another aspect that should be investigated in the future is the realization of task-designed electrolytes for innovative PORM-based devices. As discussed above, a large number of investigations dedicated to these systems has been carried out coupling a PORM-based electrode with a metallic lithium and utilizing a LIB electrolyte. Nevertheless, as illustrated in Figure 3, there is a large number of devices which could be realized with PORMs. Currently there is great and increasing interest on battery systems based on metals such as sodium, potassium, magnesium or aluminum, which are much more abundant than

Table 2. Qualitative comparison of performance of PORM-based systems in the different presented electrolyte classes.

| | State-of-the-Art Organic | Aqueous Highly conc. | Organic Highly conc. | Ionic Liquid | Solid |
|-----------------------|--------------------------|----------------------|----------------------|--------------|-------|
| Specific Capacity | ++ | + | + | 0 | 0 |
| Cycle Life | - | 0 | + | ++ | ++ |
| Self-Discharge | - | 0 | + | + | ++ |
| Operative Temperature | 0 | 0 | 0 | + | - |
| Safety | - | + | 0 | + | ++ |

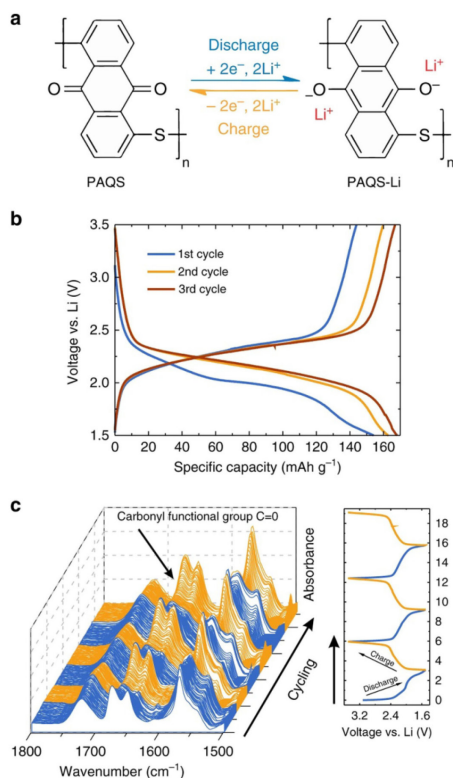


Figure 14. a) Storage Mechanism of PAQS with a Lithium anode, b) voltage profile c) in-operando ATR-IR spectra (reproduced with permission from Ref. [68], Copyright (2018) The Authors).

lithium. The use of PORMs in these systems has been only marginally considered. Recently, a proof of concept system containing an aluminum metal anode, an AQ cathode and $\text{AlCl}_3/\text{EMIMCl}$ (1.5/1) as electrolyte has been presented.^[69] Therewith a full cell with a cell potential of 1.1 V, a specific capacity of 183 mAh g^{-1} (78% of theoretic capacity) and a good coulombic efficiency near 99% was realized. Unfortunately, this setup lacked in cycling stability. However, this issue was circumvented using polymerized AQ (PAQS) and multi-walled-carbon nano tubes (MWCNT) in the cathode. In order to complete the understanding of processes of this new cell combination the authors applied in-operando ATR-IR spectroscopy, ex-situ X-Ray photoelectron spectroscopy (XPS), and scanning electron microscopy (SEM) coupled with energy dispersive spectrometry (EDS). By this analysis it was possible to determine that in the discharged state, the carbonyl groups of AQ are not coupled to Al^{3+} species but AlCl_2^+ from the electrolyte, delivering remarkable insight to this cell setup. This

study is an interesting example of how PORMs can be introduced in novel battery concepts and, at the same time, of how the electrolyte is affecting the performance of these novel systems. For this reason, the development of "task-specific" electrolytes for these novel systems appears of great interest and will represent a new and important challenge for the future of PORM-based devices.

6. Conclusions

The development of advanced PORM-based batteries is an actual research topic, which is attracting an increasing attention within the scientific and, also, industrial communities. In order to develop innovative systems, which can be commercialized, the development of novel electrolytes appears essential. In this review we showed that the use of LIB electrolytes, which are nowadays the state-of-the-art electrolyte in PORM-based devices is limiting the performance, especially the stability, and the safety of these devices. In the future it will be therefore necessary to develop a new generation of "task-specific" electrolytes, able to guarantee high stability for the electrode materials, low self-discharge and a very broad temperature range of use. Highly concentrated electrolytes (both aqueous and organic) and ionic liquids appears at the moment as interesting candidates, but it will be necessary to improve their transport properties. Also, the use of solid electrolytes is interesting but, as for other devices, the conductivity of these electrolytes at room temperature needs to be improved. In the future, it will be necessary also to acquire a deeper understanding of the processes taking place at the interface of electrode-electrolytes in these devices, as this is one of the keys to achieve high stability. Furthermore, it will be essential to design electrolytes suitable for emerging battery technologies containing PORM-based electrodes.

Acknowledgements

The authors wish to thank the Deutsche Forschungsgemeinschaft (DFG) within the project "Redox-active ionic liquids in redox-flow-batteries" for the financial support.

Conflict of Interest

The authors declare no conflict of interest.

Keywords: electrolyte · organic redox active materials · polymer · energy storage

- [1] D. Larcher, J.-M. Tarascon, *Nat. Chem.* **2015**, *7*, 19–29.
- [2] G. Zubri, R. Dufo-López, M. Carvalho, G. Pasaoglu, *Renewable Sustainable Energy Rev.* **2018**, *89*, 292–308.
- [3] K. Xu, *Chem. Rev.* **2004**, *104*, 4303–4418.
- [4] E. A. Olivetti, G. Ceder, G. G. Gaustad, X. Fu, *Joule* **2017**, *1*, 229–243.
- [5] P. C. K. Vesborg, T. F. Jaramillo, *RSC Adv.* **2012**, *2*, 7933.

- [6] C. Wadia, P. Albertus, V. Srinivasan, *J. Power Sources* **2011**, *196*, 1593–1598.
- [7] Y. Liang, Y. Yao, *Joule* **2018**, *2*, 1690–1706.
- [8] R. Chen, D. Bresser, M. Saraf, P. Gerlach, A. Balducci, S. Kunz, D. Schröder, S. Passerini, J. Chen, *ChemSusChem* **2020**.
- [9] D. I. Williams, J. J. Byrne, J. S. Driscoll, *J. Electrochem. Soc.* **1969**, *116*, 2–4.
- [10] H. Alt, H. Binder, A. Köhling, G. Sanstede, *Electrochim. Acta* **1972**, *17*, 873–887.
- [11] P. J. Nigrey, D. MacInnes Jr., D. P. Nairns, A. G. MacDiarmid, A. J. Heeger, *J. Electrochem. Soc.* **1981**, *128*, 1651–1654.
- [12] S. J. Visco, L. C. DeJonghe, *J. Electrochem. Soc.* **1988**, *135*, 2905–2909.
- [13] N. Oyama, T. Tatsuma, T. Sato, T. Sotomura, *Nature* **1995**, *373*, 598–600.
- [14] J. S. Foos, S. M. Erker, L. M. Rembetsy, *J. Electrochem. Soc.* **1986**, *133*, 836–841.
- [15] Z. Song, H. Zhou, *Energy Environ. Sci.* **2013**, *6*, 2280.
- [16] Y. O. Kudoh, K. Akami, Y. Matsuya, *Synth. Met.* **1999**, 973–974.
- [17] A. J. Wain, G. G. Wildgoose, C. G. R. Heald, L. Jiang, T. G. J. Jones, R. G. Compton, *J. Phys. Chem. B* **2005**, *109*, 3971–3978.
- [18] X. Han, C. Chang, L. Yuan, T. Sun, J. Sun, *Adv. Mater.* **2007**, *19*, 1616–1621.
- [19] R. Gracia, D. Mecerreyes, *Polym. Chem.* **2013**, *4*, 2206.
- [20] J. Bigot, B. Charleux, G. Cooke, F. Delattre, D. Fournier, J. Lyskawa, F. Stoffelbach, P. Woisel, *Macromolecules* **2010**, *43*, 82–90.
- [21] S. Inagi, K. Naka, Y. Chujo, *J. Mater. Chem.* **2007**, *17*, 4122.
- [22] L. Zhan, Z. Song, J. Zhang, J. Tang, H. Zhan, Y. Zhou, C. Zhan, *Electrochim. Acta* **2008**, *53*, 8319–8323.
- [23] J. Y. Zhang, L. B. Kong, L. Z. Zhan, J. Tang, H. Zhan, Y. H. Zhou, C. M. Zhan, *J. Power Sources* **2007**, *168*, 278–281.
- [24] J. Tang, Z.-P. Song, N. Shan, L.-Z. Zhan, J.-Y. Zhang, H. Zhan, Y.-H. Zhou, C.-M. Zhan, *J. Power Sources* **2008**, *185*, 1434–1438.
- [25] H. Chen, M. Armand, M. Courty, M. Jiang, C. P. Grey, F. Dolhem, J.-M. Tarascon, P. Poizot, *J. Am. Chem. Soc.* **2009**, *131*, 8984–8988.
- [26] H. Chen, M. Armand, G. Demailly, F. Dolhem, P. Poizot, J.-M. Tarascon, *ChemSusChem* **2008**, *1*, 348–355.
- [27] B. Häupler, A. Wild, U. S. Schubert, *Adv. Energy Mater.* **2015**, *5*, 1402034.
- [28] J. Caja, *J. Electrochem. Soc.* **1984**, *131*, 2744.
- [29] P. Novák, K. Müller, K. S. V. Santhanam, O. Haas.
- [30] D. J. Kim, S. H. Je, S. Sampath, J. W. Choi, A. Coskun, *RSC Adv.* **2012**, *2*, 7968.
- [31] S. Renault, J. Geng, F. Dolhem, P. Poizot, *Chem. Commun.* **2011**, *47*, 2414–2416.
- [32] A. Choi, Y. K. Kim, T. K. Kim, M.-S. Kwon, K. T. Lee, H. R. Moon, *J. Mater. Chem. A* **2014**, *2*, 14986–14993.
- [33] Z. Zhu, H. Li, J. Liang, Z. Tao, J. Chen, *Chem. Commun.* **2015**, *51*, 1446–1448.
- [34] K. Nakahara, J. Iriyama, S. Iwasa, M. Suguro, M. Satoh, E. J. Cairns, *J. Power Sources* **2007**, *165*, 398–402.
- [35] C. Friebe, U. S. Schubert, *Top. Curr. Chem.* **2017**, *375*, 19.
- [36] T. Janoschka, M. D. Hager, U. S. Schubert, *Adv. Mater.* **2012**, *24*, 6397–6409.
- [37] F. Béguin, V. Presser, A. Balducci, E. Frackowiak, *Adv. Mater.* **2014**, *26*, 2219–51, 2283.
- [38] V. Aravindan, J. Gnanaraj, S. Madhavi, H.-K. Liu, *Chem. Eur. J.* **2011**, *17*, 14326–14346.
- [39] S. Muench, A. Wild, C. Friebe, B. Häupler, T. Janoschka, U. S. Schubert, *Chem. Rev.* **2016**, *116*, 9438–9484.
- [40] Y. Liang, Z. Tao, J. Chen, *Adv. Energy Mater.* **2012**, *2*, 742–769.
- [41] P. K. Nayak, L. Yang, W. Brehm, P. Adelhelm, *Angew. Chem. Int. Ed.* **2018**, *57*, 102–120; *Angew. Chem.* **2018**, *130*, 106–126.
- [42] Y. Liang, Y. Yan, *Gen. Chem.* **2017**, *3*, 207–212.
- [43] K. Xu, *Chem. Rev.* **2014**, *114*, 11503–11618.
- [44] J.-K. Kim, J.-H. Ahn, G. Cheruvally, G. S. Chauhan, J.-W. Choi, D.-S. Kim, H.-J. Ahn, S. H. Lee, C. E. Song, *Met. Mater. Int.* **2009**, *15*, 77–82.
- [45] Q. Zhao, C. Guo, Y. Lu, L. Liu, J. Liang, J. Chen, *Ind. Eng. Chem. Res.* **2016**, *55*, 5795–5804.
- [46] T. Suga, H. Konishi, H. Nishide, *Chem. Commun.* **2007**, 1730–1732.
- [47] S. Lee, G. Kwon, K. Ku, K. Yoon, S.-K. Jung, H.-D. Lim, K. Kang, *Adv. Mater.* **2018**, *30*, e1704682.
- [48] S. Phadke, M. Cao, M. Anouti, *ChemSusChem* **2018**, *11*, 965–974.
- [49] J.-E. Lim, J.-K. Kim, *Korean J. Chem. Eng.* **2018**, *35*, 2464–2467.
- [50] X. Dong, Z. Guo, Z. Guo, Y. Wang, Y. Xia, *Joule* **2018**, *2*, 902–913.
- [51] J. Qin, Q. Lan, N. Liu, Y. Zhao, Z. Song, H. Zhan, *Energy Storage Mater.* **2020**, *26*, 585–592.
- [52] L. Suo, O. Borodin, T. Gao, M. Olguin, J. Ho, X. Fan, C. Luo, C. Wang, K. Xu, *Science* **2015**, *350*, 938–943.
- [53] P. Lannelongue, R. Bouchal, E. Mourad, C. Bodin, M. Olarte, S. le Vot, F. Favier, O. Fontaine, *J. Electrochem. Soc.* **2018**, *165*, 657–663.
- [54] X. Dong, H. Yu, Y. Ma, J. L. Bao, D. G. Truhlar, Y. Wang, Y. Xia, *Chem. Eur. J.* **2017**, *23*, 2560–2565.
- [55] Y. Liang, Y. Jing, S. Gheyhani, K.-Y. Lee, P. Liu, A. Facchetti, Y. Yao, *Nat. Mater.* **2017**, *16*, 841–848.
- [56] C. Guo, K. Zhang, Q. Zhao, L. Pei, J. Chen, *Chem. Commun.* **2015**, *51*, 10244–10247.
- [57] L. Suo, Y.-S. Hu, H. Li, M. Armand, L. Chen, *Nat. Commun.* **2013**, *4*, 1481.
- [58] Z. Xu, H. Ye, H. Li, Y. Xu, C. Wang, J. Yin, H. Zhu, *ACS Omega* **2017**, *2*, 1273–1278.
- [59] P. Gerlach, R. Burges, A. Lex-Balducci, U. S. Schubert, A. Balducci, *Electrochim. Acta* **2019**, *306*, 610–616.
- [60] P. Gerlach, R. Burges, A. Lex-Balducci, U. S. Schubert, A. Balducci, *J. Power Sources* **2018**, *405*, 142–149.
- [61] X. Wang, Z. Shang, A. Yang, Q. Zhang, F. Cheng, D. Jia, J. Chen, *Chem* **2019**, *5*, 364–375.
- [62] L. Wylie, Z. L. Seeger, A. N. Hancock, E. I. Izgorodina, *Phys. Chem. Chem. Phys.* **2019**, *21*, 2882–2888.
- [63] W. Wei, L. Li, L. Zhang, J. Hong, G. He, *Mater. Lett.* **2018**, *213*, 126–130.
- [64] W. Wei, L. Li, L. Zhang, J. Hong, G. He, *Electrochem. Commun.* **2018**, *90*, 21–25.
- [65] W. Li, L. Chen, Y. Sun, C. Wang, Y. Wang, Y. Xia, *Solid State Ionics* **2017**, *300*, 114–119.
- [66] W. Huang, Z. Zhu, L. Wang, S. Wang, H. Li, Z. Tao, J. Shi, L. Guan, J. Chen, *Angew. Chem. Int. Ed.* **2013**, *52*, 9162–9166; *Angew. Chem.* **2013**, *125*, 9332–9336.
- [67] J.-K. Kim, A. Matic, J.-H. Ahn, P. Jacobsson, *RSC Adv.* **2012**, *2*, 9795.
- [68] A. Vizintin, J. Bitenc, A. Kopač Lautar, K. Pirnat, J. Grdadolnik, J. Stare, A. Randon-Vitanova, R. Dominko, *Nat. Commun.* **2018**, *9*, 661.
- [69] J. Bitenc, N. Lindahl, A. Vizintin, M. E. Abdelhamid, R. Dominko, P. Johansson, *Energy Storage Mater.* **2020**, *24*, 379–383.

Manuscript received: January 31, 2020
 Revised manuscript received: April 2, 2020
 Accepted manuscript online: April 6, 2020

MINIREVIEWS

The importance of the electrolyte: Redox active organic materials are currently considered as very interesting candidates for the realization of sustainable energy storage devices. This review aims to supply a critical overview about the work carried out so far on the development of electrolytes suitable for these materials.



*P. Gerlach, Prof. Dr. A. Balducci**

1 – 13

A Critical Analysis about the Underestimated Role of the Electrolyte in Batteries Based on Organic Materials

1.6 Aim of the Work

In section 1.1 it has been highlighted that a sustainable energy supply for human society calls for innovative energy storage devices meeting the requirements for our future energy handling.

Section 1.3 presented several redox active organic molecules and polymers, which could fit to those requirements. A lot of those materials have already been investigated intensively and optimized from a material design point of view.

However, coming from section 1.5, it is obvious that not only novel materials have to be found, but also innovative electrolytes, which act as an active component in organic energy storage devices and tremendously affect the performance of ROMPs. Not many of these studies have been considered so far compared to the number of works targeting the material point of view. Therewith there is a lack of information about the interactions of ROMPs and different task specific electrolytes used for those systems.

The aim of this work is to address exactly this topic. The redox active radical polymer PTMA, which was studied extensively since 2002, has been tested in combination with several different electrolytes. In doing so, each work targets a different aspect of the important interactions of electrolyte and active material. These are the influence of the electrolyte composition, the influence of the electrolyte concentration, subsequent the influence of different types of ionic liquids and finally a more specific work aiming for the interesting influence of the electrolyte on the self-discharge on PTMA at different charge/discharge conditions. Each study aims to clarify the interactions of PTMA in these different electrolyte environments and draws conclusions for the big picture of ROMPs in energy storage application.

2 Results and Discussion

2.1 Publication 2: The influence of the electrolyte composition on the electrochemical behaviour of cathodic materials for organic radical batteries

Publication 2 reports an investigation about the influence of the electrolyte composition on the electrochemical behavior of PTMA.

PTMA has been tested thoroughly with LIB electrolytes in the past. However, as explained above the energy storage mechanism of PTMA itself has no need for any specific ion in the electrolyte. Thus, the restriction to only use Li^+ as cation and corresponding anions like PF_6^- represents a limitation of choices made by current research. One goal of this work was to overcome this limitation and extend the number of tested electrolytes for PTMA. Furthermore, as the introduction part of this thesis clarified, the electrolyte has to be seen as an active component in EES devices. Therefore, significantly different performances are to be expected in electrolytes with different ions, solvents and transport properties.

To shed light on this underestimated aspect, in the first half of this work we decided to present the performance of PTMA-based electrodes with a selection of three different alternative metal free electrolytes.

The selected electrolytes are 1M 1-butyl-1-methylpyrrolidinium bis(trifluoromethylsulfonyl)imide ($\text{Pyr}_{14}\text{TFSI}$) in PC, tetraethylammonium bis(trifluoromethylsulfonyl)imide (Et_4NTFSI) in PC and neat $\text{Pyr}_{14}\text{TFSI}$, which can also be used without solvent, since it is an ionic liquid. These model electrolytes have been used in high power supercapacitors and proved feasible performance in this application [156,157]. Since the presented electrolytes display very different transport properties with viscosities of 5.1, 4.6 and 90 mPa s and conductivities of 7.3, 9.1 and 2.2 mS cm^{-1} (in the order of 1M $\text{Pyr}_{14}\text{TFSI}$ in PC, 1M Et_4NTFSI in PC and $\text{Pyr}_{14}\text{TFSI}$), PTMA displays a very different electrochemical behavior in each of them [157–159].

At first, after CV measurements, the diffusion coefficients of the PTMA half-cell systems are calculated via the Randles-Sevcik equation [160]:

$$i_p = 0.4463 nFAc \left(\frac{nFvD}{RT} \right)^{\frac{1}{2}} \quad (8)$$

Where i_p is the peak current in the CV in A, n is number of transferred electrons in the redox reaction (here 1), F is the Faraday constant (96485 C mol^{-1}), A is the area of the working electrode in cm^2 , c is the concentration in mol cm^{-3} , v is the scan rate in V s^{-1} , D is the diffusion coefficient in $\text{cm}^2 \text{ s}^{-1}$, R is the universal gas constant ($8.314 \text{ J K}^{-1} \text{ mol}^{-1}$) and T is the temperature in K. By summarizing all terms except of the scan rate v into a factor a , this equation simplifies to

$$i_p = av^b \quad (9)$$

By plotting the logarithm of i_p versus the logarithm v the b-value of a system can be determined. A b-value of 0.5 indicates a diffusion-controlled system, while a value of 1 would suggest a surface-controlled process [161]. In this study b-values of 0.66, 0.65 and 0.58 were found for 1M Pyr₁₄TFSI in PC, 1M Et₄NTFSI in PC and neat Pyr₁₄TFSI respectively, which emphasizes a diffusion-controlled process in all three systems.

Afterwards the behavior of PTMA-based electrodes during charge/discharge has been examined. At a current density of 1C, the PTMA cycled in 1M Pyr₁₄TFSI in PC displays the highest specific capacity of 100 mAh g^{-1} , followed by 1M Et₄NTFSI in PC with 75 mAh g^{-1} . The lowest capacity is displayed by PTMA in neat Pyr₁₄TFSI with 60 mAh g^{-1} . This low value can be explained by the high viscosity and low conductivity of this IL. The coulombic efficiency is near 100 % for all systems.

In rate capability tests up to 10C, PTMA in combination with the organic electrolytes is able to retain 90 % of their initial capacity displayed at 0.2C. In the neat IL only 50 % are kept at 10C.

In cycling stability tests carried out at a current density of 1C (100 cycles) PTMA displays a very stable behavior in all electrolytes. However, in float tests a different picture is observed. Floating means to hold the potential of an electrochemical cell at a certain value (1.1 V vs. Ag in this work) for a certain amount of time, in order to test the system

in stressful conditions. In this study after 80 h of floating, PTMA displays a very different behavior in all three electrolytes. The worst can be seen in 1M Et₄N TFSI where 60 % of the initial capacity is lost, which indicates an electrode decomposition at elevated potentials. After 80 h of floating in 1M Pyr₁₄TFSI in PC, PTMA is able to keep 100 % of its specific capacity. Therefore, no decomposition can be seen here. In neat Pyr₁₄TFSI the capacity even increases over time at 1.1 V vs. Ag. This behavior can be explained by an increase of accessible active sites of the PTMA electrode by the viscous electrolyte.

Another test where the beneficial effect of the IL electrolyte can be observed is the self-discharge of PTMA. After three days of self-discharge, all charge is lost when PTMA is used in 1M Et₄N TFSI in PC. In 1M Pyr₁₄TFSI in PC, 30 % of the stored charge is lost after 3 days. In the IL on the other side, PTMA is able to retain 90 % of its initial charge.

After these first evaluations in a half-cell setup, we decided to test PTMA in a hybrid device together with an activated carbon (AC) electrode in 1M Pyr₁₄TFSI in PC and Pyr₁₄TFSI. In this work, already in several paragraphs it has been mentioned that for PTMA itself the use of Li-ion-based electrolytes is not necessary. However, this is obviously not given for PTMA in combination with a LIB-based anode. Therefore, in order to emphasize the findings and statements made in publication 2 for PTMA in alternative metal-free electrolytes, an introduction of novel EES systems e.g., all-organic or hybrid devices is needed.

In this hybrid device one of the electrodes displays a faradic energy storage process (PTMA), while the other one stores energy via a non-faradic process (AC), which is the accumulation of ions on the surface of the electrode (double layer) in this case. This combination results to a device displaying characteristics between classical batteries and supercapacitors. We decided to use PTMA in combination with an AC electrode in order to exploit the high rate capability of PTMA, which marks one of the big benefits of ORPs and aligns with the characteristics of AC electrodes.

In this study both hybrid devices have been cycled at a current of 10C between 0 - 2 V. The results of the charge/discharge measurements confirm the expectations drawn from the PTMA-electrode tests. The hybrid device containing 1M Pyr₁₄TFSI in PC displays a maximum energy of 23 Wh kg⁻¹ and power of 0.37 kW kg⁻¹ after 500 cycles. The hybrid device containing Pyr₁₄TFSI needs 1300 cycles to reach its maximum at 7.5 Wh kg⁻¹ for

the specific energy and 0.4 kW kg^{-1} . This emphasizes the better transport properties in the organic electrolyte in the hybrid devices as well.

On the other hand, the IL-based electrolyte provides high stability of the PTMA electrode in comparison to organic electrolytes also in this application during long term cycling at elevated current densities. After 10000 cycles at 10C, the PTMA electrode in Pyr₁₄TFSI retains 87 % of the initial capacity, while the electrode in the organic pendants decreases to 30 %.

The findings of publication 2 emphasize the strong impact of the nature of the electrolyte on the electrochemical behavior of PTMA in half-cell configuration as well as in combination with an AC electrode in a hybrid full-cell.

On the one side, although in all electrolytes the same anion has been used, a strong influence of the utilized conducting salt was observed. With these findings it is evident that also the choice of the cation influences the performance of the P-type PTMA in this setup, which is rather counter intuitive. This aspect of publication 1 highlights that a careful investigation of electrolytes for ROMPs is needed to elucidate every aspect of material-electrolyte interaction.

On the other side a clear impact of the presence of an organic solvent was found. In organic electrolytes a general better performance in regard of specific capacity and rate capability was found, while the absence of an organic solvent in the IL-based electrolyte ensures stability at elevated potentials and low self-discharge rates. These findings highlight that even for the same OB system different electrolyte concepts should be used in order for the ROMPs to fulfill the requirements of the specific application.

One of the alternative applications is the realization of hybrid devices, which was examined in this work. The results of energy and power density here show that already with little optimization in cell design working alternative energy storage concepts can widen the possible application for PTMA and ROMPs in general enormously. This increase in application possibilities again increase the number of possible electrolytes, which calls for detailed consideration of novel electrolyte systems.



Contents lists available at ScienceDirect

Journal of Power Sources

journal homepage: www.elsevier.com/locate/jpowsour

The influence of the electrolyte composition on the electrochemical behaviour of cathodic materials for organic radical batteries

P. Gerlach^{a,b}, R. Burges^{b,c}, A. Lex-Balducci^{b,c}, U.S. Schubert^{b,c}, A. Balducci^{a,b,*}

^a Institute for Technical Chemistry and Environmental Chemistry, Friedrich Schiller University Jena, Philosophenweg 7a, 07743, Jena, Germany

^b Center for Energy and Environmental Chemistry Jena (CEEC Jena), Friedrich Schiller University Jena, Philosophenweg 7a, 07743, Jena, Germany

^c Laboratory of Organic and Macromolecular Chemistry (IOMC), Friedrich Schiller University Jena, Humboldtstr. 10, 07743, Jena, Germany



HIGHLIGHTS

- The electrolyte composition affects strongly the behaviour of PTMA electrodes.
- Neat ionic liquids are promising electrolytes for ORBs.
- PTMA electrodes retain almost 90% of their capacity after 10.000 cycles in Pyr_{1,4}TFSI.

ARTICLE INFO

Keywords:
PTMA
Electrolyte
Ionic liquids
Self-discharge

ABSTRACT

Poly(2,2,6,6-tetramethylpiperidiny-*N*-oxymethacrylate) (PTMA) is presently considered as one of the most promising cathodic materials for the realization of advanced organic radical batteries (ORBs). In this work we report an investigation about the influence of three electrolytes, namely 1 M tetraethylammoniumbis(trifluoromethylsulfonyl)imide (Et₄N⁺TFSI⁻) in propylene carbonate (PC); 1 M 1-butyl-1-methylpyrrolidiniumbis(trifluoromethylsulfonyl)imide (Pyr_{1,4}TFSI) in PC and neat Pyr_{1,4}TFSI, on the electrochemical performance of PTMA-based cathodes. The results of this study showed that the electrolyte composition has a significant effect on the performance of PTMA-based electrodes. The use of Pyr_{1,4}TFSI appears particularly promising as it allows the realization of electrodes with very good cycling stability (almost 90% of capacity retention after 10.000 cycles carried out at 10C) and very low self-discharge.

1. Introduction

The realization of cheap, flexible and environmentally friendly electrochemical storage devices is nowadays considered of key importance for the solution of the “energy issue” which our society is facing [1,2]. In this context, the use of polymeric materials appears extremely promising due to their limited costs and their large design options. In the past several types of polymers have been proposed, and in the last years an increasing interest has been directed toward the utilization of redox active polymers which are featuring a non-conjugated scaffold and a redox active centre in pendant groups of the monomeric units [3]. These redox active centres exert a distinct redox reaction and, thereby, yield to a stable cell potential while charging or discharging the cell [4]. It has been shown that thanks to these features these polymers can be successfully exploited for the realization of electrochemical storage devices such as redox flow batteries (RFB) [5,6]

and organic radical batteries (ORBs) [7,8].

Among the organic stable radicals that were proposed for battery applications [2,9–12] the 2,2,6,6-tetramethylpiperidiny-*N*-oxyl (TEMPO)-group has been most investigated [10,13] as it displays good electrochemical properties and is able to keep the radical moieties for more than a year in aprotic solution [7,12]. Nakahara et al. were the first who investigated the use of these kind of redox active polymers in battery systems, and in their pioneering work they used poly(2,2,6,6-tetramethylpiperidiny-*N*-oxymethacrylate) (PTMA) as cathodic active material [14]. In the following years PTMA became one of the most used cathodic material for ORBs. In large part of these investigations, composite PTMA-based electrodes have been tested in combination with lithium-ion battery (LIB) electrolytes, e.g. mixtures of ethylene carbonate (EC)/diethyl carbonate (DEC) containing lithium hexafluorophosphate (LiPF₆) as conductive salt [9,14–18]. It has been shown that in these electrolytes PTMA-based cathodes are able to

* Corresponding author. Institute for Technical Chemistry and Environmental Chemistry, Friedrich Schiller University Jena, Philosophenweg 7a, 07743, Jena, Germany.

E-mail address: andrea.balducci@uni-jena.de (A. Balducci).

<https://doi.org/10.1016/j.jpowsour.2018.09.099>

Received 22 April 2018; Received in revised form 28 September 2018; Accepted 29 September 2018

Available online 29 October 2018

0378-7753/ © 2018 Elsevier B.V. All rights reserved.

deliver capacities close to their theoretical value, which is 111 mAh g⁻¹, good cycling stability as well as good rate performance [9,14,16–18]. One drawback associated to the use of PTMA-based electrodes in combination with these electrolytes appears to be the self-discharge [17]. This process, which is caused by the dissolution of the active material into the electrolyte, can be nevertheless limited by cross-linking of the polymer [19]. Furthermore, it has to be mentioned that the electrodes can regain their full capacity after recharging [17].

It is important to notice that, in contrast to metal-ion batteries such as LIBs, the electrolytes of ORBs do not need to contain a metal ion. As a matter of fact, in these latter battery systems the charge is stored in the redox moieties of the polymer and, therefore, there is not a “functional need” which is motivating the choice of lithium-ion battery electrolytes for ORBs. Very likely, these electrolytes have been selected because they are largely available and well characterized. Nevertheless, in view of the realization of “metal-free” devices, as ORBs could be, this choice does not appear very convenient because it introduces metal (although in form of salts) into the systems. Moreover, it is well-known that the use of the state-of-the-art LIB electrolytes poses serious safety risks and, at the same time, is limiting the temperature range of use of the devices in which they are utilized [20]. For these reasons, the use of other types of electrolytes would be more favourable for the realization of advanced and safer ORBs. In spite of this, however, only a limited number of studies has been dedicated to this subject in the past [10,21–26].

In this work, we report on an investigation about the influence of the electrolyte composition on the electrochemical performance of PTMA-based cathodes. We utilized three different electrolytes: 1 M tetraethylammoniumbis(trifluoromethylsulfon)imide (Et₄N⁺TFSI⁻) in propylene carbonate (PC); 1 M 1-butyl-1-methylpyrrolidiniumbis(trifluoro-methylsulfon)imide (Pyr_{1,4}⁺TFSI⁻) in PC and neat Pyr_{1,4}TFSI. The first two electrolytes have been selected with the aim to acquire information about the influence of the cation nature of “not-metallic” salts on the performance of PTMA-based cathodes. The third electrolyte, which is a neat ionic liquid (IL), has been selected to study the influence of the solvent on the behaviour of this type of electrode materials. In the first part of the manuscript the influence of these electrolytes on the capacity, capacity retention and self-discharge of PTMA-based cathodes have been investigated in detail. Based on these results, a device containing a PTMA-based positive electrode, an activated carbon-based negative electrode and neat Pyr_{1,4}TFSI as electrolyte has been assembled and tested. The behaviour of these devices is described in the second part of the work.

2. Experimental

For the synthesis of cross-linked PTMA the monomer 2,2,6,6-tetramethylpiperidine-4-yl methacrylate (TEMPMA, TCI) and triethylene glycol dimethacrylate (TEGDMA, Sigma Aldrich) as a crosslinker were polymerized via a free radical polymerization in MeOH/H₂O 1/3 using 5 mol% 4,4'-azobis(4-cyanovaleric acid (ACVA, Sigma Aldrich)). The molar ratio of the monomer/cross-linker was 96/4. To convert the secondary amine into the nitroxyl radical the cross-linked prepolymer was oxidized according to a modified method from literature [27]. In a first step the prepolymer was oxidized with H₂O₂ (Carl Roth) and Na₂WO₄ × 2H₂O (Acros Organics) and in a second step with H₂O₂ and MgSO₄ (VWR) to result in PTMA with a radical content of 90%, determined with electron spin resonance (ESR, Bruker).

PTMA-based electrodes were prepared by mixing 60% active material (crosslinked PTMA), 5% binder (polyvinylidene fluoride (PVdF), Sigma Aldrich) and 35% carbon black (SuperP⁺, Alfa Aesar) in *N*-methyl-2-pyrrolidone (NMP, TCI) with a dissolver (Dispermat⁺, VMA-GETZMANN). The NMP slurry was casted with a doctor blade (250 μm wet film thickness) on an aluminium current collector and dried in a drying oven with air circulation overnight at 80 °C. The electrode mass loading was on average 0.66 mg cm⁻², while the electrode area was equal to 1.13 cm².

Activated carbon-based electrodes were prepared according to the procedure described in Ref. [28]. The mass ratio of active material (AC, DLC Super 30, Norit), conductive agent (Super C65, Imerys) and binder (CMC, Walocel CRT 2000 PPA 12 from Dow Wolff Cellulosis) was 90:5:5. The electrode area was 1.13 cm², while the electrode mass loading varied from 0.63 to 1.09 mg cm⁻². Oversized free-standing activated carbon-based electrodes were also prepared and used as counter electrodes [29]. In case of these latter electrodes, the mass ratio between activated carbon, (AC, DLC Super 30, Norit), conductive agent (Super C65, Imerys) and binder (polytetrafluoroethylene (PTFE), Sigma Aldrich) was 85:10:5. The electrodes displayed an average mass loading of 40 mg cm⁻² and an area of 1.13 cm².

The electrolytes utilized in this investigation were prepared by dissolving 1 M of Et₄N⁺TFSI or Pyr_{1,4}⁺TFSI (both from Iolitec, Germany) in dry PC. In case of neat Pyr_{1,4}TFSI the IL was used as received, and no further purifications were carried out. The water content of all electrolytes was lower than 20 ppm, as measured with Karl Fischer titration. The electrolytes were prepared and stored in a glove box (LabMaster, MBRAUN GmbH) under argon atmosphere with a water and oxygen content below 0.1 ppm.

The electrochemical tests reported in the following have been all carried out utilizing a Swagelok-cell type with a three electrodes configuration. In the first part of the manuscript the PTMA electrodes were used as working electrodes (W), the oversized electrodes as counter electrodes (C) and a Ag wire as a quasi-reference. In the second part of the work the oversized electrodes were replaced by AC-based electrodes. In all tests glass fibre sheets (Whatmann) were used as separator and were drenched with 160 μL of electrolyte.

All electrochemical measurements were carried out using a VMP multichannel potentiostatic-galvanostatic workstation (Biologic Science Instruments, VMP 3) at room temperature. Before starting the actual measurements, 3 h of open circuit voltage (OCV) were recorded in order to set the systems into an equilibrium.

Cyclic voltammetry (CV) was performed using scan rates ranging from 0.1 mV s⁻¹ to 50 mV s⁻¹. The Randles-Sevcik equation (1) was used to calculate the diffusion coefficient in every electrolyte.

$$i_p = 0.4463 nFAc \left(\frac{nFvD}{RT} \right)^{\frac{1}{2}} \quad (1)$$

where i_p is the peak current of the measured CV, n is the number of transferred electrons, F is the Faraday constant, A is the electrode area, c is the concentration of the electrolyte, v is the applied scan rate, D is the diffusion coefficient, R is the universal gas constant and T is the temperature. In order to determine the b -value of the system equation (1) can be simplified to

$$i = av^b \quad (2)$$

In that way by plotting the logarithm of the current i versus the scan rate the b -value is the resulting slope [33].

Galvanostatic charge-discharge cycling (CC) was carried out between 0.3 V and 1.1 V vs. Ag/Ag⁺ using current densities ranging from 0.2C to 10C for half-cells (PTMA vs. oversized AC electrodes). The theoretical capacity of PTMA, 111 mAh g⁻¹, has been utilized to define 1C. The self-discharge of PTMA-based electrodes was recorded by fully charging (at 1.1 V vs. Ag) the electrodes at 1C and afterward monitoring the residual stored charge of the active material by galvanostatic discharge for three days. Float tests were performed by charging the PTMA-based electrodes to 1.1 V vs. Ag and keeping this voltage for a total of 80 h. In order to monitor the changes over the time of the experiment, every 10 h charge/discharge cycles and impedance spectra were carried out [30].

Devices containing PTMA-based positive electrode and AC-based negative electrodes were cycled between 0 and 2 V at 10C (this latter value has been defined on the basis of the theoretical capacity of PTMA). During the test, the behaviour of the positive and negative

electrode has been constantly monitored. The values of coulombic efficiency (η), average specific energy (E) and average specific power (P) of these device have been calculated using equations (3)–(5) in which m is the mass of active material of both electrodes, V is the voltage of the device, A is the area of the electrode and t_c and t_d are the charge and discharge time. The integral in equation (4) refers to the area under the discharge curve.

$$\eta = \frac{t_d}{t_c} \cdot 100 \% \quad (3)$$

$$E_{\text{average}} = I \int \frac{V}{m \cdot 3.6} dt_d \quad (4)$$

$$P_{\text{average}} = \frac{E_{\text{average}} \cdot 3.6}{t_d} \quad (5)$$

3. Results and discussion

The electrolytes 1 M Et₄N⁺TFSI in PC, 1 M Pyr₁₄⁺TFSI in PC and (neat) Pyr₁₄⁺TFSI have been investigated as electrolytes for supercapacitors [31–33] but, to the best of our knowledge, they have been never used in ORBs. At 20 °C the electrolyte 1 M Et₄N⁺TFSI in PC displays a conductivity of 9.1 mS cm⁻¹ and a viscosity of 4.6 mPa s [29]. The substitution of the cation Et₄N⁺ with the cation Pyr₁₄⁺ which results in the electrolyte 1 M Pyr₁₄⁺TFSI in PC leads to a slightly decrease of the conductivity (7.3 mS cm⁻¹) and to a slightly increase of the viscosity (5.1 mPa s). Since Pyr₁₄⁺TFSI is a room temperature IL, this salt can also be used as neat electrolyte. At 20 °C, the conductivity and the viscosity of Pyr₁₄⁺TFSI are 2.6 mS cm⁻¹ and 62 mPa s, respectively. Considering these values, these electrolytic solutions appear as good “model electrolytes” to investigate the influence of this component on the electrochemical behaviour of PTMA-based electrodes.

Fig. 1 compares the CVs, carried out with a scan rate of 0.1 mV s⁻¹, of PTMA-based electrodes in the investigated electrolytes. As shown, all the electrodes displayed the characteristic voltammetric shape of this polymeric material [10,14,15,17]. Nevertheless, it is evident that the nature of the electrolyte has a strong influence on the peak potential (in both oxidation and reduction) as well as on the intensity of the peaks. In spite of the similar properties of 1 M Et₄N⁺TFSI in PC and 1 M Pyr₁₄⁺TFSI in PC, the current density observed for the PTMA-based electrodes in this latter electrolyte appears higher than that observed in the former. The cathodic peak of 1 M Pyr₁₄⁺TFSI in PC is located at 0.83 V vs. Ag, while that observed in 1 M Et₄N⁺TFSI in PC is located at 0.88 V vs. Ag.

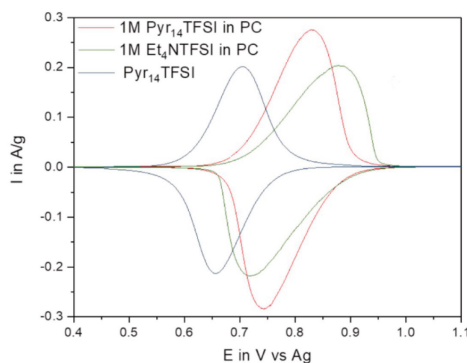


Fig. 1. CVs of PTMA-based electrodes in 1 M Pyr₁₄⁺TFSI in PC, 1 M Et₄N⁺TFSI in PC and Pyr₁₄⁺TFSI. The measurements have been carried out at room temperature utilizing a scan rate of 0.1 mV s⁻¹.

On the other hand, the anodic peaks in 1 M Pyr₁₄⁺TFSI in PC and 1 M Et₄N⁺TFSI in PC are located at 0.75 V vs. Ag and 0.72 V vs. Ag, respectively. The use of neat Pyr₁₄⁺TFSI, which is much more viscous than the other two electrolytes, does not affect significantly the intensity of the current density, but it rather leads to a shift towards negative potential of the cathodic (0.7 V vs. Ag) and anodic (0.65 V vs. Ag) peaks.

In order to investigate the influence of the electrolytes on the diffusion behaviour within the electrode, CVs were measured with an increasing scan rate, ranging from 0.1 to 50 mV s⁻¹. Fig. 2 shows a comparison of the diffusion coefficient of PTMA-based electrodes, at a scan rate of 0.1 mV s⁻¹, obtained utilizing the Randles-Sevcik equation (see experimental part). As shown in the figure, the diffusional behaviour observed in the electrodes is well in line with the chemical-physical properties of the electrolytes, and both PC-based electrolytes show much higher diffusion coefficients than that observed in the neat IL. To gain preliminary information about the nature of the redox process (diffusion controlled or surface controlled) occurring at the PTMA-based electrodes the so-called b-value [34–36] has been calculated for each system. A b-value equal to 0.5 indicates the presence of a diffusion controlled redox process [36]. The b-values resulted to be equal to 0.65 for 1 M Pyr₁₄⁺TFSI in PC, to 0.66 for 1 M Et₄N⁺TFSI in PC and to 0.58 for Pyr₁₄⁺TFSI. It is well-known that when composite electrodes (as those utilized in this study) are used, deviations from the ideal value of 0.5 are unavoidable. In spite of this, the results shown in Fig. 2 indicate that, independently of the electrolyte composition, all PTMA-based electrodes display a diffusional controlled behaviour, as expected [7].

After these tests, galvanostatic charge-discharge experiments have been carried out in the voltage range between 0.3 and 1.1 V vs. Ag, utilizing different C-rates. Fig. 3 shows the results of these tests. As shown in Fig. 3a, the capacity of the PTMA-based electrode is influenced by the electrolyte composition. When the electrodes are cycled in 1 M Pyr₁₄⁺TFSI in PC they can deliver a capacity of ca. 100 mAh g⁻¹ at 1C, which corresponds to 90% of the theoretical capacity. Taking into account the amount of PTMA in the composite electrodes utilized in this study, which is significantly higher than those of most of the PTMA-based electrodes reported in literature [9,21], this value appears very promising. In the electrolyte 1 M Et₄N⁺TFSI in PC the electrode capacity decreases to ca. 75 mAh g⁻¹. This result, which is in line with the CV results, indicates that the electrode capacity is not only determined by the transport properties of the electrolyte, but that also the ion-ion and ion-solvent interactions are influencing it. This is an interesting aspect, which has not been deeply investigated in the past and that certainly deserves additional investigations (which, however, are out of the scope of this study). In neat Pyr₁₄⁺TFSI, which displays the highest viscosity and lowest conductivity among the investigated electrolytes, the PTMA-based electrodes deliver a capacity of ca. 60 mAh g⁻¹. This value is significantly lower than that observed in 1 M Pyr₁₄⁺TFSI in PC. This behaviour has been already reported for other battery materials and, therefore, is not surprising [37,38]. Fig. 3b compares the capacity retention displayed by the PTMA-based electrodes in the three investigated electrolytes during tests carried out from 0.2C to 10C. As shown in the figure, when 1 M Pyr₁₄⁺TFSI in PC and 1 M Et₄N⁺TFSI in PC are utilized, the electrodes are able to retain at 10C ca. 90% of their initial capacity. These high values clearly indicate the good high power behaviour of PTMA-based electrodes [12,39]. When neat Pyr₁₄⁺TFSI is used the electrodes display a lower retention, and at 10C they could retain only 50% of their initial capacity. This lower capacity retention value, which was not unexpected, is comparable with that observed for other battery materials in this IL [37].

After these tests, the stability upon cycling of the PTMA-based electrodes has been investigated. These tests have been carried out at 1C. As shown in Fig. 4, the PTMA-based electrodes display good stability in all electrolytes and at the end of the cycling they could retain almost all their initial capacity. Nevertheless, it is important to notice that the coulombic efficiency of the charge-discharge process was not identical in all electrolytes. As a matter of fact, while in 1 M Pyr₁₄⁺TFSI

Results and Discussion

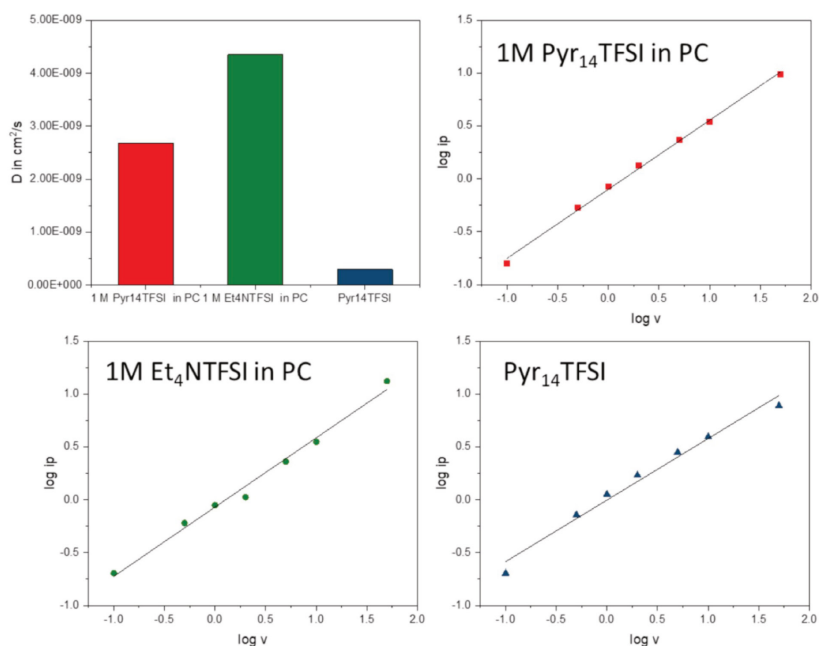


Fig. 2. Comparison of the diffusion coefficients and of the linear correlations resulting from the logarithm of the redox peaks of PTMA-based in 1 M Pyr₁₄TFSI in PC, 1 M Et₄NTFSI in PC and Pyr₁₄TFSI, as obtained during CVs carried out with scan rates ranging from 0.1 mV s⁻¹ to 100 mV s⁻¹.

in PC the efficiency was more than 99%, the efficiency of the electrode in 1 M Et₄NTFSI in PC and in Pyr₁₄TFSI were 90% and 95%, respectively. Although these lower values might be partially related to the utilization of not optimized electrodes, these results indicate that the electrolyte composition has an influence on the efficiency of the storage process.

With the aim to acquire further indication about the stability of PTMA-based electrodes in the investigated electrolytes, also float tests have been carried out. This kind of tests are commonly used in supercapacitor technology, and they are particularly helpful to investigate

the influence of the potential (or cell voltage) on the stability of an electrode (or device) [30]. In the case of our experiments, we kept the electrode potential at 1.1 V vs. Ag, which is the highest potential experienced by the electrode during the charge-discharge tests, for 80 h. As shown in Fig. 5, after this time the PTMA-based electrodes which were cycled in 1 M Pyr₁₄TFSI in PC were able to retain their entire capacity. On the other hand, the electrodes cycled in 1 M Et₄NTFSI in PC were able to retain only 60% of their initial capacity. The electrode used in combination with the neat Pyr₁₄TFSI displayed a completely different behaviour, and after 80 h their capacity increased by 10%.

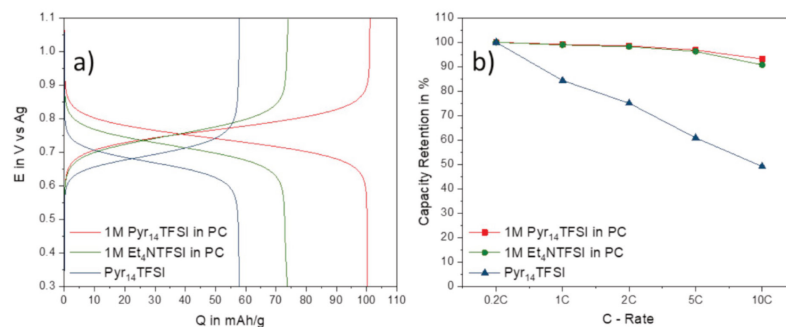


Fig. 3. a) Voltage profiles of PTMA-based electrodes in 1 M Pyr₁₄TFSI in PC, 1 M Et₄NTFSI in PC and Pyr₁₄TFSI during test carried out at 1C; b) capacity retention displayed by the same electrodes during C-rate test carried out from 0.2C to 10C.

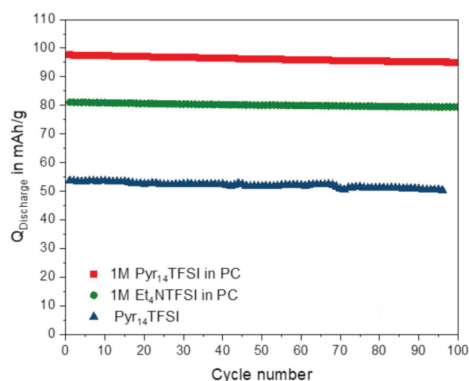


Fig. 4. Cycling stability of PTMA-based electrodes in 1 M Pyr₁₄TFSI in PC, 1 M Et₄NTFSI in PC and Pyr₁₄TFSI during test carried out at 1C.

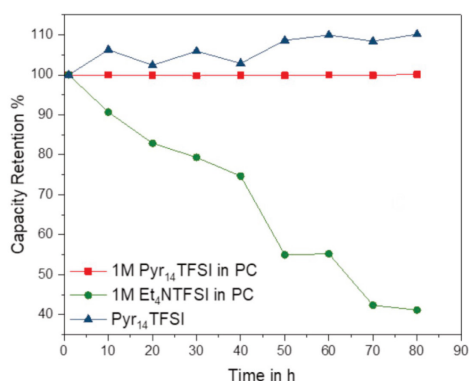


Fig. 5. Capacity retention of PTMA-based electrodes in 1 M Pyr₁₄TFSI in PC, 1 M Et₄NTFSI and Pyr₁₄TFSI during float test carried out at 1.1 V vs. Ag for 80 h.

These different capacity retention values indicate that the electrolyte composition has a strong influence on the electrode stability during this stressful test. The result obtained with the neat Pyr₁₄TFSI is very likely related to the improvement of the electrode wetting over time. In the past several works illustrated that in neat IL the electrode wetting in much slower compared to that of organic electrolytes and, as a consequence, in IL the electrode capacity can increase during the first cycles [22]. Obviously, this increase can happen only if the electrode (and the electrolyte) is stable at the investigated potential. From the results obtained with PTMA-based electrodes in the neat Pyr₁₄TFSI (which display an overall electrochemical stability higher than 5 V [38,40]) this seems to be the case. The addition of a solvent to the IL, as in 1 M Pyr₁₄TFSI in PC, does not appear to reduce this stability, as the PTMA-based electrodes are highly stable, as mentioned before. To the contrary, the use of a different cation, as in 1 M Et₄NTFSI in PC, seems to have a negative effect on the electrode stability. Nevertheless, further investigations are needed to better clarify the impact of the electrolyte on the electrode stability at high potential.

As mentioned in the introduction, the self-discharge of the PTMA-based electrode represents one of their main drawback. In order to investigate the influence of the electrolyte composition on this process,

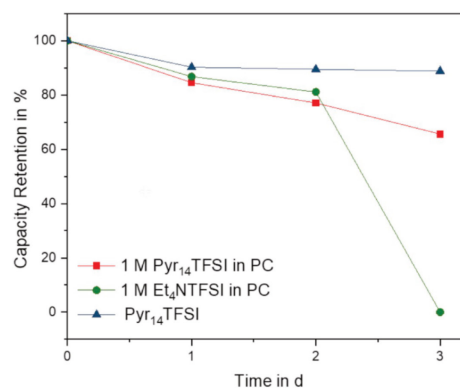


Fig. 6. Self-discharge of PTMA-based electrodes in 1 M Pyr₁₄TFSI in PC, 1 M Et₄NTFSI and Pyr₁₄TFSI over 3 days.

we charged the electrode at 1.1 V vs. Ag and monitored the self-discharge of the electrodes over three days. As shown in Fig. 6, the electrode used in combination 1 M Et₄NTFSI in PC was completely discharged after this time. The electrode cycled in 1 M Pyr₁₄TFSI in PC was able to maintain about 70% of the initial capacity. The electrode used in combination with neat Pyr₁₄TFSI was able to retain about 90% of its initial capacity after three days. To the best of our knowledge, this latter value is one of the lowest self-discharge reported so far for PTMA-based electrodes. As mentioned in the introduction, the self-discharge is caused by the dissolution of redox active polymer in the electrolyte which is functioning as a redox shuttle discharging the battery [4,17]. Considering the results reported above, it is reasonable to suppose that the different solubility of PTMA in the ILs and in organic solvents could be the reason of this different behaviour and, consequently, of the different self-discharge of cells [17]. Nevertheless, further investigations are needed to confirm this hypothesis and to accurately quantify the different solubility of PTMA on the investigated media.

The results reported above are clearly showing that the nature of the electrolytes has a dramatic influence on the electrochemical behaviour of PTMA-based electrodes. Among the electrolytes investigated above, the use of neat Pyr₁₄TFSI appears to be very interesting as it allows the achievement of decent capacity and capacity retention, high efficiency during the charge-discharge process, high stability at high potential and very low self-discharge. Taking into account these favourable properties, we decided to further investigate the use of this electrolyte. With this aim, we studied the impact of Pyr₁₄TFSI on the cycling stability of a device containing a PTMA-based positive electrode and an activated carbon (AC)-based negative electrode. The device has been tested utilizing a maximum cell voltage of 2 V, and it has been charged and discharged at 10C for 10,000 cycles. The cut-off applied during the cycling process were 1.1 V vs. Ag for the positive electrode in the charge process, and 0 V for the device in the discharge process. It is important to notice that the aim of this experiment was not to realize an optimized hybrid device. For this reason, we did not apply a higher voltage, e.g. 3 V, which could have been in theory achievable (preliminary test about this device, including the investigation about the best positive/negative electrode weight ratio, have been carried out and they are reported in the supporting information, S1, S2 and S2). The aim of this test was rather to investigate the impact of a prolonged cycling process of the PTMA-based electrode. To better evaluate the impact of this electrolyte on the electrode stability, the same test have been also carried out utilizing the electrolyte 1 M Pyr₁₄TFSI in PC. Fig. 7a shows the voltage profile of the system containing the neat Pyr₁₄TFSI after 1300 cycles. As

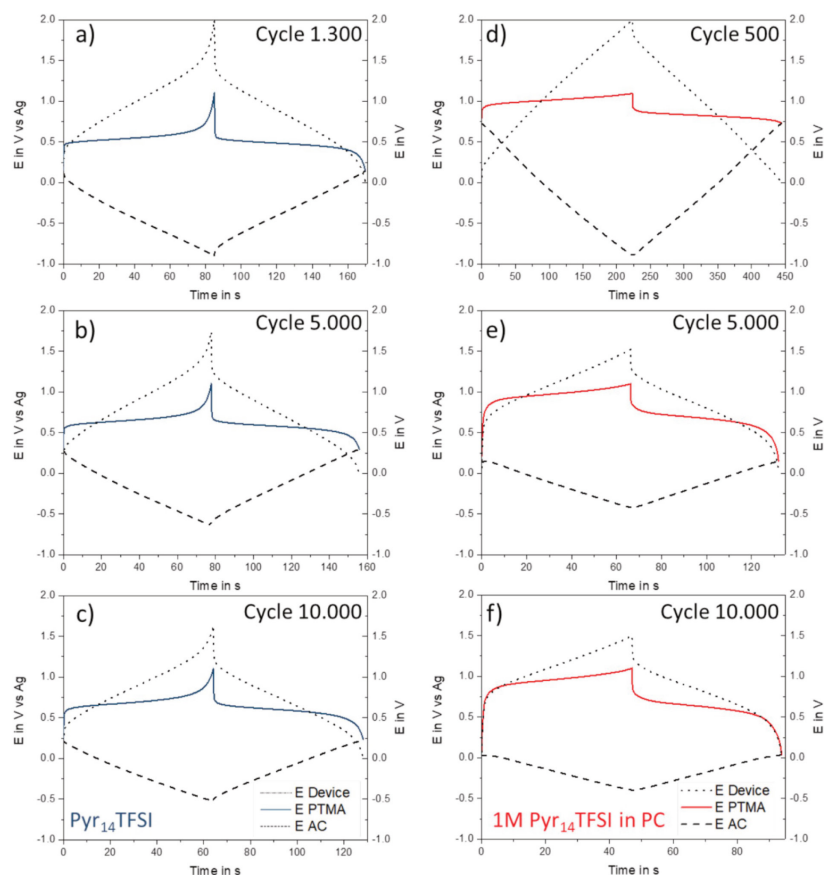


Fig. 7. Evolution of the voltage profiles of PTMA-based electrode; AC-based electrodes and (not-optimized) hybrid devices over 10,000 cycles. The test has been carried out at 10C in neat $\text{Pyr}_{14}\text{TFSI}$ (a-c) and in 1 M $\text{Pyr}_{14}\text{TFSI}$ IN PC (d-f).

shown, the PTMA-based electrode displayed a plateau of charge-discharge at about 0.5 V vs. Ag, while the AC-based electrode displayed the triangular shape characteristic for non-faradaic electrodes. These two different profiles were both influencing the voltage profile of the device, as expected [28]. The coulombic efficiencies of the charge-discharge processes of the PTMA electrode, AC electrode and resulting from this of the full cell were close to 100%, in line with results reported above. It is interesting to notice that the energy efficiency of the AC and PTMA were 77% and 88%, respectively. At the cycle number of 1300 the average energy and average power of the devices were 7.5 Wh kg^{-1} and 0.4 kW kg^{-1} , respectively. These values are not very high, but they are reasonably comparable with those reported for other non-aqueous polymer-based system working at 2 V [40]. After 5000 cycles the electrode as well as the devices profiles changed. As shown in Fig. 7b, the voltage profile of the PTMA-based electrode did not change significantly, and only a slight shift toward higher potential was observed. In addition, the voltage profile of the negative electrode did not change, and no faradaic contribution were visible on the profile of the AC-based electrode. Nevertheless, the voltage excursion of this

electrode was significantly reduced, and during the charge-discharge process it was moving only between 0 and -0.6 V vs. Ag. As a consequence, the cell voltage was reduced to 1.7 V. Although the efficiency of the charge-discharge process was always high, the decrease of the cell voltage reduced the energy and the power of the device by 20%. This behaviour was also observed on the following 10,000 cycles, although the voltage profiles of both electrodes, and consequently of the device, did not change dramatically during these cycles. The system cycled in 1 M $\text{Pyr}_{14}\text{TFSI}$ in PC (Fig. 7 d-f) displayed a different behaviour. As a matter of fact, at the beginning of the cycling, cycle 500 (Fig. 7d), the device reached its maximum capacity with an average energy of 23 Wh kg^{-1} and an average power of 0.37 kW kg^{-1} with a coulombic efficiency near 100% and an energy efficiency of 97% for the AC and 80% for the PTMA electrode. However, in the following cycles the device loses rapidly energy density. After 10,000 cycles only 4.07 Wh kg^{-1} remained, which corresponds to 17.7% of its initial specific energy. This behaviour indicates a great loss in active polymer material in the organic electrolyte during cycling, which is well visible from the variation of the voltage profiles of the electrodes, as well as of

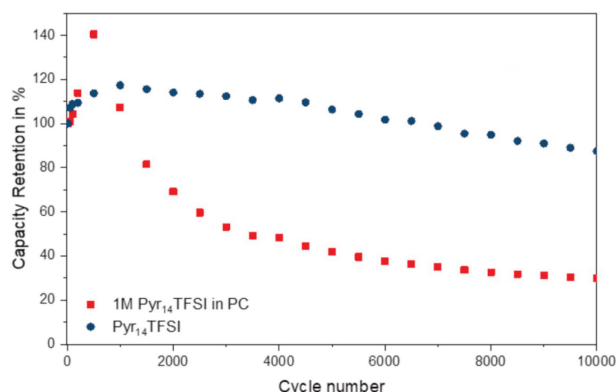


Fig. 8. Capacity retention of the PTMA-based electrodes in 1 M Pyr₁₄TFSI in PC and Pyr₁₄TFSI during test carried out at 10C.

the device during the cycling process. Also the self-discharge of the systems has been investigated, and it has been found that after 3 days, the device cycled in Pyr₁₄TFSI was able to retain ca. 20% of its initial energy, while that cycled in Pyr₁₄TFSI in PC was almost fully discharged.

Fig. 8 is plotting the capacity retention showed by the PTMA electrodes over the 10,000 cycles investigated in the test described above. As shown, the electrode in 1 M Pyr₁₄TFSI in PC displayed initially an increase of capacity reaching a maximum after the first 500 cycles. Afterward, the electrode capacity started to decrease and at the end of the cycling the electrode was able to deliver only 30% of its initial capacity. The electrode cycled in the neat Pyr₁₄TFSI displayed a different behaviour. As visible in the figure, during the initial cycles the electrode capacity of the IL device increased and reached a maximum after ca. 1,000 cycles. This increase of capacity was due to the improvement of the electrode wettability discussed above. Afterward, the electrode capacity started slowly to decrease. After 10,000 cycles the electrode retained 87% of the initial capacity. Although these results indicate the occurrence of a capacity fade, it is important to notice that the stability of the investigated device is among the highest so far reported for PTMA electrodes. Taking these results into account, it is evident that the electrolyte nature/composition has a strong influence on the stability of these polymeric electrodes and that ILs appear as very promising electrolytes for the realization of high stable systems.

4. Conclusions

PTMA is presently considered as one of the most promising redox active polymers suitable for the realization of ORBs. In the past PTMA-based electrodes have been mainly investigated in combination with LIB electrolytes. Nevertheless, there is not a “functional need” which is motivating the use of this toxic and flammable electrolytes. In this work we investigated the influence of three model electrolytes on the electrochemical behaviour of PTMA-based electrodes. We showed that the cation-anion composition as well as the presence/absence of the solvent have a strong impact on the electrode behaviour. Among the considered electrolytes, the neat Pyr₁₄TFSI appeared particularly promising. As a matter of fact, its use in combination with PTMA-based electrodes allows good capacity and capacity retention, high efficiency during the charge-discharge process, high stability at high potential and very low self-discharge. We showed that in this electrolyte PTMA-based electrodes are able to retain almost 90% of their initial capacity after 10,000 cycles carried out at 10C. To the best of our knowledge, this is

one of the highest capacity retention reported so far for this type of electrodes. Taking these results into account, it is evident that the electrolyte composition has a dramatic effect on the electrochemical performance of PTMA-based electrodes. In the future further effort should be therefore directed toward the understanding of the influence of the electrolyte composition, e.g. salt concentration, on the electrochemical behaviour of ORBs.

Acknowledgements

The authors wish to thank the Friedrich Schiller University Jena for the financial support. USS and ALB thank the TMWWDG and the TAB for financial support (RIS3 Innovationszentrum CEEC Jena).

Appendix A. Supplementary data

Supplementary data to this article can be found online at <https://doi.org/10.1016/j.jpowsour.2018.09.099>.

References

- [1] C. Friebe, U.S. Schubert, *Top. Curr. Chem.* 375 (2017) 19.
- [2] K.O.H. Nishide, *Science (New York, N.Y.)* 319 (2008) 736–737.
- [3] P. Novák, K. Müller, K.S.V. Santhanam, O. Haas, *Chem. Rev.* 97 (1997) 207–282.
- [4] T. Janoschka, M.D. Hager, U.S. Schubert, *Adv. Mater. (Deerfield Beach, Fla.)* 24 (2012) 6397–6409.
- [5] T. Janoschka, N. Martin, U. Martin, C. Friebe, S. Morgenstern, H. Hiller, M.D. Hager, U.S. Schubert, *Nature* 527 (2015) 78–81.
- [6] X. Wei, W. Xu, M. Vijayakumar, L. Cosimbescu, T. Liu, V. Sprenkle, W. Wang, *Adv. Mater.* 26 (2014) 7649–7653.
- [7] K. Nakahara, K. Oyaizu, H. Nishide, *Chem. Lett.* 40 (2011) 222–227.
- [8] K. Oyaizu, H. Nishide, *Adv. Mater.* 21 (2009) 2339–2344.
- [9] J.-K. Kim, J.-H. Ahn, G. Cheruvally, G.S. Chauhan, J.-W. Choi, D.-S. Kim, H.-J. Ahn, S.H. Lee, C.E. Song, *Met. Mater. Int.* 15 (2009) 77–82.
- [10] H. Nishide, S. Iwasa, Y.-J. Pu, T. Suga, K. Nakahara, M. Satoh, *Electrochim. Acta* 50 (2004) 827–831.
- [11] J. Qu, T. Katsumata, M. Satoh, J. Wada, J. Igarashi, K. Mizoguchi, T. Masuda, *Chemistry* 13 (2007) 7965–7973.
- [12] S. Muench, A. Wild, C. Friebe, B. Hauptler, T. Janoschka, U.S. Schubert, *Chem. Rev.* 116 (2016) 9438–9484.
- [13] M. Suguro, S. Iwasa, Y. Kusachi, Y. Morioka, K. Nakahara, *Macromol. Rapid Commun.* 28 (2007) 1929–1933.
- [14] K. Nakahara, S. Iwasa, M. Satoh, Y. Morioka, J. Iriyama, M. Suguro, E. Hasegawa, *Chem. Phys. Lett.* 359 (2002) 351–354.
- [15] J.-K. Kim, G. Cheruvally, J.-H. Ahn, Y.-G. Seo, D.S. Choi, S.-H. Lee, C.E. Song, *J. Ind. Eng. Chem.* 14 (2008) 371–376.
- [16] K. Nakahara, J. Iriyama, S. Iwasa, M. Suguro, M. Satoh, E.J. Cairns, *J. Power Sources* 163 (2007) 1110–1113.
- [17] K. Nakahara, J. Iriyama, S. Iwasa, M. Suguro, M. Satoh, E.J. Cairns, *J. Power Sources* 165 (2007) 398–402.

Results and Discussion

- [18] K. Nakahara, J. Iriyama, S. Iwasa, M. Suguro, M. Satoh, E.J. Cairns, *J. Power Sources* 165 (2007) 870–873.
- [19] L. Bugnon, C.J.H. Morton, P. Novak, J. Vetter, P. Nesvadba, *Chem. Mater.* 19 (2007) 2910–2914.
- [20] B. Scrosati, J. Garche, *J. Power Sources* 195 (2010) 2419–2430.
- [21] Y.-Y. Cheng, C.-C. Li, J.-T. Lee, *Electrochim. Acta* 66 (2012) 332–339.
- [22] Y. Dai, Y. Zhang, L. Gao, G. Xu, J. Xie, *J. Electrochem. Soc.* 158 (2011) A291.
- [23] J.K. Kim, G. Cheruvally, J.-W. Choi, J.H. Ahn, D.S. Choi, C.E. Song, *J. Electrochem. Soc.* 154 (2007) 839–843.
- [24] K. Koshika, N. Sano, K. Oyaizu, H. Nishide, *Chem. Commun. (Cambridge, England)* (2009) 836–838.
- [25] A. Vlad, N. Singh, J. Rolland, S. Melinte, P.M. Ajayan, J.-F. Gohy, *Sci. Rep.* 4 (2014) 4315.
- [26] J.-K. Kim, A. Matic, J.-H. Ahn, P. Jacobsson, *RSC Adv.* 2 (2012) 9795.
- [27] T. Janoschka, A. Teichler, A. Krieg, M.D. Hager, U.S. Schubert, *J. Polym. Sci. Polym. Chem.* 50 (2012) 1394–1407.
- [28] A. Krause, P. Kossyrev, M. Oljaca, S. Passerini, M. Winter, A. Balducci, *J. Power Sources* 196 (2011) 8836–8842.
- [29] C. Schütter, T. Husch, V. Viswanathan, S. Passerini, A. Balducci, M. Korth, *J. Power Sources* 326 (2016) 541–548.
- [30] R.-S. Kühnel, A. Balducci, *J. Power Sources* 249 (2014) 163–171.
- [31] S. Pohlmann, C. Ramirez-Castro, A. Balducci, *J. Electrochem. Soc.* 162 (2015) A5020–A5030.
- [32] S. Pohlmann, R.-S. Kühnel, T.A. Centeno, A. Balducci, *CHEMELECTROCHEM* 1 (2014) 1301–1311.
- [33] S. Pohlmann, B. Lobato, T.A. Centeno, A. Balducci, *Phys. Chem. Chem. Phys.* 15 (2013) 17287.
- [34] V. Augustyn, J. Come, M.A. Lowe, J.W. Kim, P.-L. Taberna, S.H. Tolbert, H.D. Abruña, P. Simon, B. Dunn, *Nat. Mater.* 12 (2013) 518–522.
- [35] J. Wang, J. Polleux, J. Lim, B. Dunn, *J. Phys. Chem. C* 111 (2007) 14925–14931.
- [36] R. Lin, P. Huang, J. Ségalini, C. Largeot, P.L. Taberna, J. Chmiola, Y. Gogotsi, P. Simon, *Electrochim. Acta* 54 (2009) 7025–7032.
- [37] S. Menne, R.-S. Kühnel, A. Balducci, *Electrochim. Acta* 90 (2013) 641–648.
- [38] A. Balducci, *Top. Curr. Chem.* 375 (2017) 20.
- [39] Y.-H. Wang, M.-K. Hung, C.-H. Lin, H.-C. Lin, J.-T. Lee, *Chem. Commun. (Cambridge, England)* 47 (2011) 1249–1251.
- [40] F. Béguin, V. Presser, A. Balducci, E. Frackowiak, *Adv. Mater. (Deerfield Beach, Fla.)* 26 (2014) 2219–2251 2283.

2.2 Publication 3: Influence of the salt concentration on the electrochemical performance of electrodes for polymeric batteries

From the previous investigations, it was evident that the electrolyte has a big influence on the performance of PTMA electrodes. At the same time, the results of PTMA electrodes in neat IL gave an indication that also the concentration of the electrolyte might affect the behavior of the electrode. At this point it is again worth mentioning that the consideration of different concentrations (other than 1M) in organic electrolytes is predominantly ignored by the majority of studies addressing the electrochemical performance of ROMPs and specifically PTMA. However, considering that the electrolyte is an active component in all EES devices, it is evident that this aspect should play a huge role in the device performance.

Therefore, in publication 3 it was our aim to clarify the influence of the electrolyte concentration on the electrochemical behavior of PTMA electrodes. In this regard we prepared three electrolytes dissolving 1, 2 and 3M 1-butyl-1-methylpyrrolidinium tetrafluoroborate ($\text{Pyr}_{14}\text{BF}_4$) in PC. This salt/solvent combination was chosen because of the very high solubility of $\text{Pyr}_{14}\text{BF}_4$ in PC. The utilization of these electrolytes allows the realization of a model electrolyte matrix with tuned properties. The displayed conductivities of the 1, 2 and 3M electrolyte at 20°C are very similar at 8.26, 8.84 and 8.65 mS cm^{-1} , respectively. The viscosities at 20°C on the other hand show significant differences (3.56, 6.66 and 16.33 mPa s) for 1, 2 and 3M $\text{Pyr}_{14}\text{BF}_4$ in PC, respectively.

During CVs carried out at 2 mV s^{-1} no significant impact of the electrolyte concentration was found. This was also the case for the voltage profiles at 1C at which PTMA in 1 and 2M $\text{Pyr}_{14}\text{BF}_4$ in PC present the capacities of ca. 90 mAh g^{-1} , while in 3M it is reduced to 82 mAh g^{-1} .

The biggest influence of the different transport properties of the three electrolytes on the charge/discharge performance was found in the rate capability tests. At a current of 10C the capacity retention results to 90 % for 1M, 80 % for 2M and 70 % for 3M $\text{Pyr}_{14}\text{BF}_4$ in PC. With these values the influence of the electrolyte viscosity on the cell kinetics is

visible. A higher viscosity reduces the ion mobility in the electrolyte. Therewith, at elevated charge/discharge rate, not all redox active sites of PTMA in the electrode are accessed by the ions.

In the cycling stability tests at 1C for 100 cycles PTMA shows a very stable behavior in all electrolytes. In this experiment, PTMA in 2M Pyr₁₄BF₄ in PC displays the highest specific capacity of 86 mAh g⁻¹.

In the floating stability PTMA experienced only minor degradation in all electrolytes. After 90 h at 1.1 V more than 95 % of the capacity is retained in all electrodes.

In this study we decided to perform a deep analysis of the self-discharge of PTMA in the differently concentrated electrolytes.

After fully charging the PTMA-based electrodes at 1C, a rest step of 11 days has been applied to all half-cells. Here significant differences in the electrode self-discharge have been observed for the three electrolytes.

In 1M Pyr₁₄BF₄ in PC the electrode was fully discharged after 4.5 days of rest. In the 2M electrolyte the electrode was fully discharged after 9 days. In the 3M electrolyte on the contrary, the PTMA electrode was able to retain residual charge even after 11 days (2 %). To investigate the processes leading to the self-discharge, the voltage curve of the rest step over 11 days has been examined following the model utilized by Andreas et al. and Conway et al. [162–169].

Following these works the self-discharge in an electrochemical system can be caused by:

- 1) An activation-controlled faradic process on the electrode surface

In which the voltage displays a linear behavior with respect to the logarithm of the rest time.

$$V = V_i - A \log(t + \tau) \quad (10)$$

V_i is the initial voltage after fully charging, A is the Tafel slope and τ is an integration constant.

- 2) A diffusion-controlled process

Where the voltage displays a linear behavior with respect to the square root of the rest time.

$$V = V_i - B\sqrt{t} \quad (11)$$

B represents the slope of the plot.

3) An ohmic leakage

Where the logarithm of the voltage plotted versus the rest time would give a linear behavior.

$$\ln V = \ln V_i - \frac{t}{RC} \quad (12)$$

R is the ohmic resistance and C is the double layer capacitance.

In this study we found a linear region in the plot of V vs. \sqrt{t} , which suggest a diffusion-controlled process in the half-cell. This is an indication of a shuttle process caused by the dissolution of active moieties into the electrolyte [20]. In this matter the dissolution of organic groups as well as mobility of organic groups is reduced in high concentrated electrolytes due to the saturation of the solution and the increased viscosity.

Considering these results, the self-discharge observed in PTMA electrodes in combination with the three model electrolytes is mainly connected to the transport properties of the used electrolyte. To further investigate this transport and clarify the effects of the viscosity on the self-discharge, we decided to measure the capacity loss of PTMA in 1M Pyr₁₄BF₄ in PC at 0°C and 20°C for 7 days after a full charge at 1C.

The results of these experiments confirmed that the self-discharge is a diffusion-controlled process. After 7 days at 0°C, the PTMA electrode was able to keep 81 % of its initial capacity, while the cell at 20°C was fully discharged. This is an indication for a reduced shuttling in the system (lower diffusion of dissolved species) due to higher viscosity and lowered kinetics at reduced temperature.

Afterwards, also the cell performance at reduced temperature was considered and a cycling stability test at 1C over 350 cycles has been carried out at 0°C and 20°C. In this

investigation the PTMA-based electrode at 0°C retained 98 % of the capacity, while at 20°C only 85 % was kept.

The results of publication 3 give a clear indication about the strong impact of the electrolyte concentration on the performance of PTMA. We showed that the rate capability tests as well as self-discharge tests are affected by the salt concentration in a major way. Thereby higher specific capacities are obtained with low concentrated electrolytes at elevated current densities, due to the better transport properties. For the self-discharge performance, however, a beneficial effect is found for high concentrated electrolytes. There the reduction of the transport within the electrolyte hinders the diffusion-controlled self-discharge mechanism and therewith reduced the loss of charge in the electrode.

These findings indicate that next to the careful selection of conducting salts of the electrolyte also its concentration needs to be optimized for every ROMP-based system and for each application in order to achieve task specific performance. Lower concentration benefits applications with fast charges while high concentration ensures low self-discharge at rest. An all-round system should meet a compromise of low and high concentration of conducting ions in the solvent.

In addition, the improved stability performance PTMA at reduced temperature could open a new chapter of the utilization of PTMA for low temperature applications. This direction needs to be pursued by further research.



Contents lists available at ScienceDirect

Electrochimica Acta

journal homepage: www.elsevier.com/locate/electacta

Influence of the salt concentration on the electrochemical performance of electrodes for polymeric batteries

P. Gerlach^{a, b}, R. Burges^{b, c}, A. Lex-Balducci^{b, c}, U.S. Schubert^{b, c}, A. Balducci^{a, b, *}^a Institute for Technical Chemistry and Environmental Chemistry, Friedrich Schiller University Jena, Philosophenweg 7a, 07743, Jena, Germany^b Center for Energy and Environmental Chemistry Jena (CEEC Jena), Friedrich Schiller University Jena, Philosophenweg 7a, 07743, Jena, Germany^c Laboratory of Organic and Macromolecular Chemistry (IOMC), Friedrich Schiller University Jena, Humboldtstr. 10, 07743, Jena, Germany

ARTICLE INFO

Article history:

Received 30 October 2018

Received in revised form

30 January 2019

Accepted 20 March 2019

Available online 23 March 2019

Keywords:

PTMA

Electrolyte

Salt concentration

Stability

Self-discharge

ABSTRACT

In this work we report an investigation about the influence of the salt concentration on the electrolyte 1-Butyl-1-methylpyrrolidinium tetrafluoroborate (Pyr₁₄BF₄) in propylene carbonate (PC) on the electrochemical behaviour of composite electrodes containing poly(2,2,6,6-tetramethylpiperidyl-N-oxymethacrylate) (PTMA) as the active material. The results of this study show that the salt concentration within the electrolyte has a strong influence on the behaviour of PTMA-based electrodes. The use of concentrated electrolytes displaying a good compromise between conductivities and viscosities appears very favourable for the optimization of the capacity and the reduction of the self-discharge of PTMA electrodes.

© 2019 Elsevier Ltd. All rights reserved.

1. Introduction

Polymeric materials can be cheap, flexible, non-toxic, environmental friendly and they can be made from sustainable resources [1]. Thanks to these features their use for the realization of sustainable energy storage devices able to replace metal-based storage systems, e.g. lithium-ion batteries (LIBs), is nowadays considered with increasing interest by the scientific and industrial communities. Among the various classes of polymeric materials, organic stable radical polymers (ORPs) have been one of the most investigated for the use in battery applications [2–6]. ORPs are cheap, provide a favourable redox chemistry and favourable kinetics for energy storage and they can be used for the fabrication of flexible devices [2]. They bear an unpaired electron at pendant groups of the polymer scaffold, which exerts a one-electron transfer reaction during charge and discharge. These characteristics are favourable for the realization of devices with relatively high power and good cycling stability [7].

In 2002 the group of Nakahara et al. presented for the first time a

battery system using poly(2,2,6,6-tetramethylpiperidyl-N-oxymethacrylate) (PTMA) as cathode active material [8]. PTMA, which is bearing a TEMPO-group ((2,2,6,6-Tetramethylpiperidin-1-yl)oxyl) in every repeating unit, is nowadays one of the most investigated polymeric cathodic materials for battery application, as it displays promising performance during tests at high current density as well as good cycling stability [3,4,8–11]. During the charge process the TEMPO radical of PTMA is oxidized to the oxoammonium cation generating a positive charge inside the polymer, which has to be compensated by the anions of the electrolyte. During the discharge process, the reduction of the TEMPO cation to the radical and the release of the anion from the polymer backbone are taking place.

The large majority of the work dedicated to PTMA-based systems have been carried out using conventional LIB electrolytes [3,8–12]. These electrolytes consist of mixtures of organic solvent, e.g. ethylene carbonate (EC) and dimethyl ethyl carbonate (DEC), in which a lithium salt, e.g. lithium hexafluorophosphate (LiPF₆) is dissolved. These electrolytes are largely available, and they display good conductivities and viscosities. Nevertheless, they display serious limitations in term of safety and flammability. Furthermore, considering the abovementioned mechanism, it is evident that the presence of metallic ions is not mandatory for the use of PTMA-based electrodes in electrochemical storage devices. Thus, also metal-free electrolytes can be used. Another crucial aspect to be

* Corresponding author. Institute for Technical Chemistry and Environmental Chemistry, Friedrich Schiller University Jena, Philosophenweg 7a, 07743, Jena, Germany.

E-mail address: andrea.balducci@uni-jena.de (A. Balducci).

<https://doi.org/10.1016/j.electacta.2019.03.147>

0013-4686/© 2019 Elsevier Ltd. All rights reserved.

highlighted is that the chemical composition, mobility and concentration of the anions present on the electrolyte are playing a key role on the storage process of PTMA-based devices [13]. Taking this point into account, it is evident that the electrolyte composition and concentration cannot be neglected while designing PTMA-based devices. In spite of this, however, until now only few works have been dedicated to the influence of the anion concentration on the behaviour of storage systems containing this polymer [4,13–18].

It has been shown that one of the major drawbacks of PTMA is the self-discharge. Already in a work of 2007 Nakahara et al. reported for PTMA electrodes a self-discharge rate of 38% after seven days of rest in combination with the electrolyte LiPF_6 in EC/DEC [10]. This tremendous loss in charge was explained by the dissolution of active polymer moieties in the electrolyte, which can work as redox shuttles in the self-discharge process [10]. Nonetheless, in the following years the influence of the electrolyte composition on the self-discharge of PTMA-based electrodes has been considered only marginally.

In this work, we report an investigation about the influence of the salt concentration on the electrochemical performance of PTMA-based cathodes. We utilized propylene carbonate (PC)-based electrolytes containing 1 M, 2 M and 3 M of the salt 1-Butyl-1-methylpyrrolidinium tetrafluoroborate ($\text{Pyr}_{14}\text{BF}_4$). Previous studies showed that this salt/solvent mixture allows the realization of electrolytes with good transport properties, which can be used for the realization of stable storage devices [19]. Herein, the influence of these electrolytes on the capacity, capacity retention at different current densities, cycling stability and especially self-discharge of PTMA electrodes are considered in detail.

2. Experimental

The synthesis of PTMA has been carried out as described in Ref. [20], leading to a polymer with a radical content of 90%, as determined with electron spin resonance (ESR, Bruker).

PTMA-based electrodes were prepared by mixing 60% of active material (crosslinked PTMA) with 35% of conducting agent (SuperP[®], Alfa Aesar) and 5% of binder (polyvinylidene fluoride (PVdF, Sigma Aldrich) in *N*-methyl-2-pyrrolidone (NMP, TCI) with a dissolver (Dispermat[®], VMA-GETZMANN). The slurry was casted with a doctor blade (250 μm wet film thickness) on an aluminium current collector and dried in a drying oven with air circulation overnight at 80 °C. The electrode area was equal to 1.13 cm^2 and the mass loading was on average 0.66 mg/cm^2 . As counter electrodes, oversized free-standing activated carbon-based electrodes have been prepared using a procedure identical to that reported in Ref. [21]. The mass ratio between activated material (Activated carbon, DLC Super 30, Norit), conductive agent (Super C65, Imerys) and binder (polytetraethylene PTFE, sigma Aldrich) was 85:10:5. The average mass loading of these electrodes was 40 mg/cm^2 , while their area was 1.13 cm^2 .

The electrolytes utilized in this investigation were prepared by dissolving 1 M, 2 M and 3 M $\text{Pyr}_{14}\text{BF}_4$ (Iolitec, Germany) in dry PC. The water content of all electrolytes was lower than 20 ppm, as measured by Karl Fischer titration. The electrolytes were prepared and stored in a glove box (LabMaster, MBRAUN GmbH) under argon atmosphere with a water and oxygen content below 0.1 ppm. The viscosity of the electrolytes was measured with a rheometer (Anton Paar, MCR 102) using a shear rate of 1000 1/s, while their conductivity was determined by impedance spectroscopy using a ModuLab XM ECS Electrochemical Test System (AMETEK Scientific Instruments). Both investigation have been carried out at 20 °C.

All the electrochemical tests reported in this study have been carried out utilizing a Swagelok-cell type with a three electrodes

configuration, in which an Ag wire was used as a quasi-reference and a glass fibre sheets (Whatmann), drenched with 160 μL of electrolyte, was used as separator.

Cyclic voltammetry (CV) was performed using a scan rate of 0.1 mV/s. Galvanostatic charge-discharge cycling (CC) was carried out between 0.3 V and 1.4 V vs Ag using current densities ranging from 0.2C to 10C (1C has been defined considering the theoretical capacity of PTMA, 111 mAh/g). The self-discharge of PTMA-based electrodes was recorded by fully charging (at 1.1 V vs Ag) the electrodes at 1 C and afterwards monitoring the residual stored charge of the active material by galvanostatic discharge for eleven days at room temperature and for 7 days at 0 °C. Float tests were performed by charging the PTMA-based electrodes to 1.1 V vs Ag and keeping this voltage for a total of 90 h. In order to monitor the changes over the time of the experiment, every 10 h charge/discharge cycles were carried out [22]. All electrochemical measurements were carried out using a VMP multichannel potentiostatic-galvanostatic workstation (Biologic Science Instruments, VMP 3) at room temperature (if not indicated otherwise). Before starting the actual measurements, 3 h of open circuit voltage (OCV) were recorded in order to set the systems into an equilibrium.

3. Results and discussion

Fig. 1 displays the conductivity and viscosity of the electrolytes 1 M, 2 M and 3 M $\text{Pyr}_{14}\text{BF}_4$ in PC from -30 °C to 80 °C. As expected at low temperatures (-30-10 °C) the higher concentrated electrolytes show lower conductivity than the 1 M mixture, as the ion mobility decreases with a high amount of ions. This trend inverts at higher temperatures, because the mobility of the ions increases and the electrolytes benefit from a high number of charge carriers. 20 °C is the intersection point of conductivity as all electrolytes display comparable values of about 8.5 mS/cm at this point. In Fig. 1b higher viscosities are observed for high concentrated mixtures especially at low temperatures. With higher temperatures (30–80 °C), the curves approximate and similar values are reached for all electrolytes. Table 1 compares the viscosities and the conductivities of the electrolytes 1 M, 2 M and 3 M $\text{Pyr}_{14}\text{BF}_4$ in PC at 20 °C. As shown, and already mentioned above, at this temperature the salt concentration does not have a dramatic impact on the conductivity of the investigated electrolytes. To the contrary, the salt concentration appears to have a significant influence on the viscosity of these electrolytes. At 20 °C 2 M $\text{Pyr}_{14}\text{BF}_4$ in PC displays a viscosity which is almost the double than that of 1 M $\text{Pyr}_{14}\text{BF}_4$ in PC (6.66 mPas vs. 3.56 mPas). In the case of 3 M $\text{Pyr}_{14}\text{BF}_4$ in PC this difference becomes even more significant, and this highly concentrated electrolyte is almost five times more viscous (16.33 mPas) than 1 M $\text{Pyr}_{14}\text{BF}_4$ in PC. In summary, the considered electrolytes display identical chemical composition and similar conductivity, but significantly different viscosities. Considering these results, they appear as suitable for the investigation of the influence of the ion concentration and viscosity on the electrochemical behaviour of PTMA-based electrodes.

Fig. 2 compares the CVs (carried out at a scan rate of 0.1 mV/s) of PTMA-based electrodes in the investigated electrolytes. As shown, the electrodes display the typical redox peak of PTMA [4,8,10,12] in each electrolyte. In 1 M $\text{Pyr}_{14}\text{BF}_4$ in PC the electrode displays an oxidation peak at 0.83 V vs. Ag and a reduction peak at 0.76 V vs. Ag (which corresponds to 3.83 V and 3.76 V vs Li/Li^+). In 2 M $\text{Pyr}_{14}\text{BF}_4$ in PC a shift toward higher potentials is taking place, and the oxidation peak of the electrode is located at 0.87 V vs. Ag, while the reduction peak at 0.77 V vs. Ag. To the contrary, in 3 M $\text{Pyr}_{14}\text{BF}_4$ in PC a shifting toward lower potentials, with respect the 1 M electrolyte, is taking place and the oxidation peak is located at 0.81 V vs.

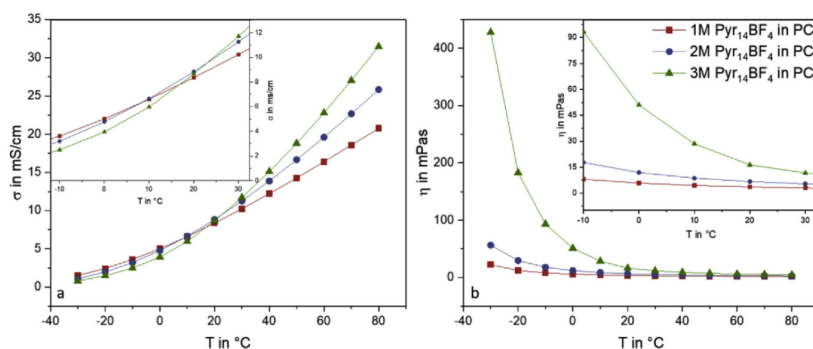


Fig. 1. Conductivity (a) and viscosity (b) of 1 M, 2 M and 3 M $\text{Pyr}_{14}\text{BF}_4$ in PC from -30 – 80 °C.

Table 1

Viscosity and Conductivity of 1 M $\text{Pyr}_{14}\text{BF}_4$, 2 M $\text{Pyr}_{14}\text{BF}_4$ and 3 M $\text{Pyr}_{14}\text{BF}_4$ in PC measured at 20 °C.

| Electrolyte | Conductivity in mS/cm at 20 °C | Viscosity in mPas at 20 °C |
|----------------------------------|----------------------------------|------------------------------|
| 1 M $\text{Pyr}_{14}\text{BF}_4$ | 8.36 | 3.56 |
| 2 M $\text{Pyr}_{14}\text{BF}_4$ | 8.84 | 6.66 |
| 3 M $\text{Pyr}_{14}\text{BF}_4$ | 8.65 | 16.33 |

Ag and the reduction at 0.75 V vs. Ag. Taking these results into account, it appears that at the considered scan rate the salt concentration within the electrolyte has a very limited impact on the shape and location of the oxidation and reduction peaks of PTMA

electrodes.

Fig. 3 displays the voltage profile of PTMA electrodes in all investigated electrolytes as obtained during tests carried out at 0.2C . As shown, the plateau associated to the charge-discharge process of PTMA is located around 0.8 V vs. Ag, independently on the used electrolytes. This potential value is in good agreement with the CV measurements as well as with the findings of previous works dedicated to this polymeric cathodic material [3]. The coulombic efficiency of the charge-discharge was close to 100% in all investigated systems. It is important to observe, however, that the capacity delivered by the PTMA-based electrode was not the same in all electrolytes. In 1 M $\text{Pyr}_{14}\text{BF}_4$ in PC and 2 M $\text{Pyr}_{14}\text{BF}_4$ in PC the electrodes display almost identical discharge capacities (89

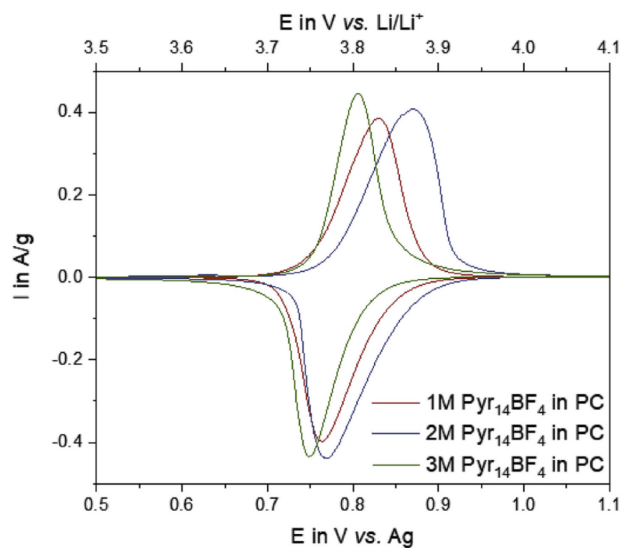


Fig. 2. CVs of PTMA-based electrodes in 1 M, 2 M and 3 M $\text{Pyr}_{14}\text{BF}_4$ in PC. The measurements have been carried out at room temperature utilizing a scan rate of 0.1 mV/s

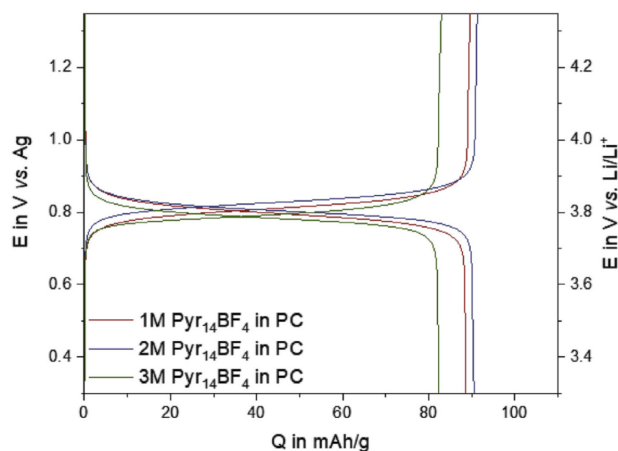


Fig. 3. Voltage profile of PTMA-based electrodes in 1 M, 2 M and 3 M $\text{Pyr}_{14}\text{BF}_4$ in PC. The measurements have been carried out at room temperature utilizing a C-rate of 0.2C.

mAh/g in the former and 90 mAh/g in the latter electrolyte). In 3 M $\text{Pyr}_{14}\text{BF}_4$ in PC the PTMA electrode displayed a lower discharge capacity, equal to 82 mAh/g. The lower capacity observed in this highly concentrated electrolyte is most likely associated to its higher viscosity with respect to the other two investigated electrolytes [15].

The results reported above showed that when low scan rate and C-rates are used, the different conductivities and viscosities of the investigated electrolytes have a limited impact on the electrochemical behaviour of PTMA electrodes. Fig. 4 is comparing the capacity retention toward higher C-rate displayed by PTMA electrodes. As shown in Fig. 4, when high current densities are applied, the properties of the electrolytes are influencing the electrode behaviour. At 1C, the electrode cycled in combination with 1 M $\text{Pyr}_{14}\text{BF}_4$ in PC was able to retain all its capacity, while those cycled in 2 M $\text{Pyr}_{14}\text{BF}_4$ in PC and 3 M $\text{Pyr}_{14}\text{BF}_4$ in PC retained 98% and 90%,

respectively, of their initial values. At 10C the differences in term of capacity retention become more pronounced and the electrodes were able to retain 90%, 80% and 70% of their initial capacity in 1 M $\text{Pyr}_{14}\text{BF}_4$ in PC, 2 M $\text{Pyr}_{14}\text{BF}_4$ in PC and 3 M $\text{Pyr}_{14}\text{BF}_4$ in PC, respectively. These retention values are perfectly in line with the different viscosities of the investigated electrolytes, and they are indicating the strong influence of this property on the electrochemical behaviour of PTMA-based electrodes.

Afterwards, also the stability of PTMA electrodes in the three different electrolytes has been investigated with the aim to understand if the salt concentration could have an effect on this important parameter. Fig. 5 shows the evolution of the PTMA electrodes capacity over 100 charge-discharge cycles carried out at 1C. The initial capacity delivered by the PTMA electrode in 1 M $\text{Pyr}_{14}\text{BF}_4$ in PC was 81 mAh g^{-1} . In 2 M $\text{Pyr}_{14}\text{BF}_4$ in PC the capacity

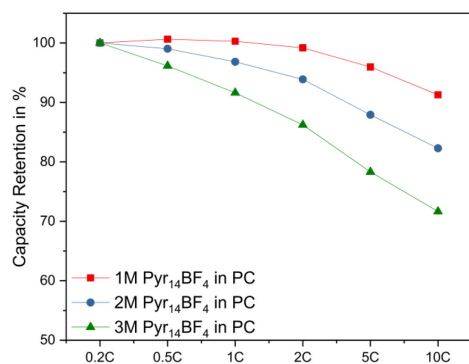


Fig. 4. Rate capability of PTMA-based electrodes in 1 M $\text{Pyr}_{14}\text{BF}_4$ in PC, 2 M $\text{Pyr}_{14}\text{BF}_4$ in PC and 3 M $\text{Pyr}_{14}\text{BF}_4$ in PC. The measurements have been carried out at room temperature utilizing C-rates from 0.2C to 10C.

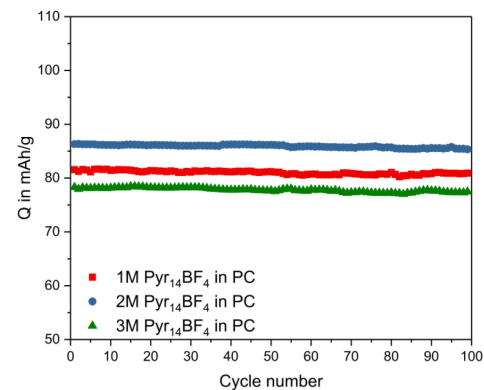


Fig. 5. Cycling stability of PTMA-based electrodes in 1 M, 2 M and 3 M $\text{Pyr}_{14}\text{BF}_4$ in PC. The measurements have been carried out at room temperature utilizing a C-rate of 1C.

was 86 mAh g^{-1} , while in $3 \text{ M Pyr}_{14}\text{BF}_4$ in PC it was 78 mAh g^{-1} . The higher capacity observed in $2 \text{ M Pyr}_{14}\text{BF}_4$ in PC can be justified taking into account the conductivity of this electrolyte and the good retention of this devices at 1C (see above). Among the investigated electrolytes, $2 \text{ M Pyr}_{14}\text{BF}_4$ in PC is the one displaying the best compromise between conductivity and viscosity, which is able to provide good mobility to most charge carriers. As shown in Fig. 5, during the cycling process all the electrodes displayed a very good stability, and they were all able to keep their initial capacity after 100 cycles.

As already mentioned above, previous works showed that one of the drawbacks of PTMA electrodes is their self-discharge, which is associated to the dissolution of active material (PTMA moieties) into the electrolyte [10]. In order to understand if the salt concentration has an impact on this process, the self-discharge of the PTMA electrodes has been investigated over 11 days and the results of this investigation are reported in Fig. 6. As shown, during this period all electrodes displayed a rather significant self-discharge. The PTMA electrodes used in combination with $1 \text{ M Pyr}_{14}\text{BF}_4$ in PC experienced a voltage drop of ca. 980 mV , the electrode used in combination with $2 \text{ M Pyr}_{14}\text{BF}_4$ in PC displayed a voltage drop of ca. 880 mV , and that used in combination with $3 \text{ M Pyr}_{14}\text{BF}_4$ in PC showed a voltage drop of ca. 390 mV (Fig. 6a). These voltage drops are causing a loss of capacity for the PTMA electrodes. After 11 days the electrode used in combination with $3 \text{ M Pyr}_{14}\text{BF}_4$ in PC was the only one able to deliver some residual capacity (2.16% of initial charge, more details are available in Table 1 of the supplementary information). It is important to notice that the self-discharge of the electrodes was not constant over the time, and that the fastest and largest (in percent) charge loss occurred during the first 100 s of the experiments (see inset Fig. 6a). During this short time, the potential drop of the electrodes cycles in 1 M , 2 M and $3 \text{ M Pyr}_{14}\text{BF}_4$ in PC was 150 mV , 240 mV and 210 mV , respectively. After 100 s, the behaviour of the electrodes changes significantly, and the salt concentration within the electrolyte seems to have a strong impact on the self-discharge dynamics of the PTMA electrodes. This is very well visible when the slope of the self-discharge curves is compared. Fig. 6b reports the variation of the electrode potential against the logarithm of the time. As reported by Andreas et al., this type of plot is helpful to identify the presence of activation controlled processes as well as charge redistribution processes, which can be associated to the linear region (if present) of these curves [23,24]. As shown, a linear behaviour can be observed only in the very first second of the experiment. Afterwards, no clear linear behaviour was observable in the systems indicating that activation driven processes are not a main driving force for the self-discharge of the investigated electrodes. Fig. 6c is plotting the voltage excursion vs. the square root of the time for the three investigated systems. As shown in Fig. 6c, in all curves it is possible to identify a linear region, which is starting after 100 s. In this type of plots the presence of a linear region indicates the occurrence of a diffusion controlled process [23]. The slope of the curves, however, is different in each electrolyte. The linear region of the self-discharge process in $1 \text{ M Pyr}_{14}\text{BF}_4$ in PC displays the largest slope of -2.66 , followed by the 2 M system with a slope of -1.8 . PTMA in $3 \text{ M Pyr}_{14}\text{BF}_4$ in PC shows the smallest slope of -1.2 . The results of this investigation, which are in line with those reported in previous work [10,25], suggest that the self-discharge of the PTMA electrodes is caused by the occurrence of a diffusion-controlled process. The dissolution of redox shuttle polymer moieties appears as the most plausible process driving to the electrode self-discharge. As visible in Fig. 6, the (diffusion controlled) electrode self-discharge is depending on the salt concentration and on the viscosity of the electrolyte, and highly concentrated electrolytes with relatively high viscosity are those displaying the lowest self-discharge.

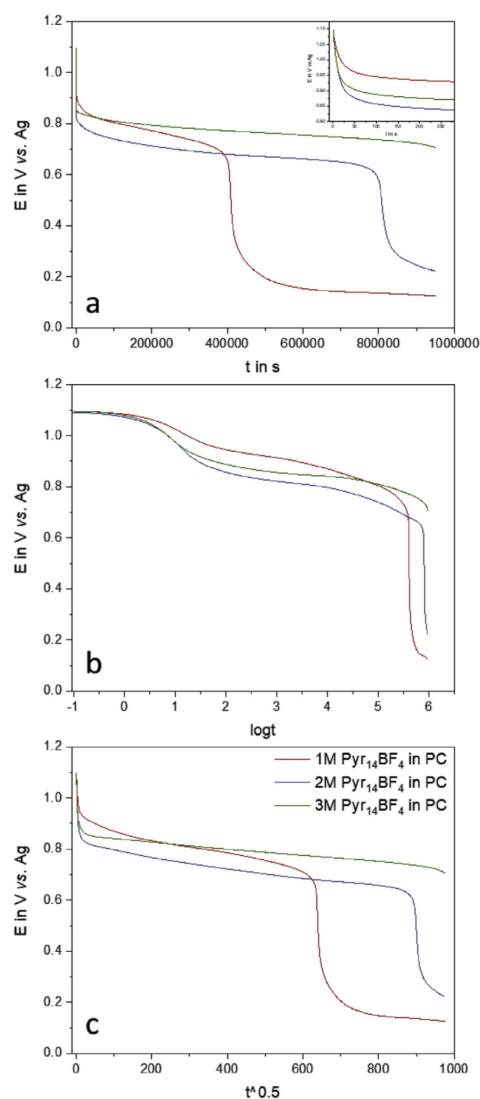


Fig. 6. Self-Discharge of PTMA-based electrodes in 1 M , 2 M and $3 \text{ M Pyr}_{14}\text{BF}_4$ in PC after 11 days: a) Voltage excursion vs. time, b) Voltage excursion vs. $\log t$ and c) Voltage excursion vs. $t^{1/2}$. The measurements have been carried out at room temperature.

After the self-discharge experiments, the stability of the electrode at 1.1 V vs. Ag , which is the maximum potential experienced by the electrodes during the charge-discharge process, has been investigated. More precisely, the electrodes have been held at this potential for 90 h and their capacity retention over this time has

been monitored. As shown in Fig. 7, after 90 h all the electrodes displayed a good capacity retention. The PTMA electrodes used in combination with 1 M Pyr₁₄BF₄ in PC lost 4% of its initial capacity. The electrode used in combination with 2 M Pyr₁₄BF₄ in PC lost 2%, while the one used in combination with 3 M Pyr₁₄BF₄ in PC lost 1% of its initial capacity. These results indicated that in the investigated time all the electrolytes are allowing a good stability and that a high viscosity is beneficial for the electrode stability.

In order to gain further information about the behaviour of the PTMA-electrodes, we also considered the impact of the operative temperature. Specifically, we monitored the self-discharge of the PTMA electrodes in 1 M Pyr₁₄BF₄ in PC, which was the electrolyte leading to the highest self-discharge in the previous experiment, at room temperature as well as 0 °C for seven days. The results are displayed in Fig. 8. As shown, the impact of the temperature on the self-discharge is significant. At room temperature the voltage excursion of the charged PTMA remains the same as previously observed, and the electrode discharges completely within 5 days (Fig. 8a). At 0 °C, to the contrary, a nearly perfect voltage plateau is reached after the initial potential drop in the first seconds, indicating that at low temperature the self-discharge process is strongly inhibited. Fig. 8b is showing the variation of the electrode potential against the logarithm of the time. As observed in the previous set of experiment, also in this case no linear region was visible, suggesting the absence of an activation-controlled process. On the other hand, when the voltage excursion vs. the square root of the time is plotted (Fig. 8c), both cells display a linear behaviour, indicating the occurrence of a diffusion controlled self-discharge process (in agreements with previous findings). After 7 days the PTMA electrode used in combination with 1 M Pyr₁₄BF₄ in PC at 0 °C was able to retain 81% of its initial capacity. After the same time, the electrode working at room temperature was fully discharged (more details are given in Fig. 1 of the Supplementary information). The results of these tests are particular interesting for two reasons. The first one is that they are showing, for the first time, the positive impact of low temperature on the self-discharge of PTMA electrodes. The second one is that they are supplying indirect, but very helpful, information about the factors influencing the self-discharge, indicating that the transport properties of the electrolyte are affecting this process more than the ion concentration of

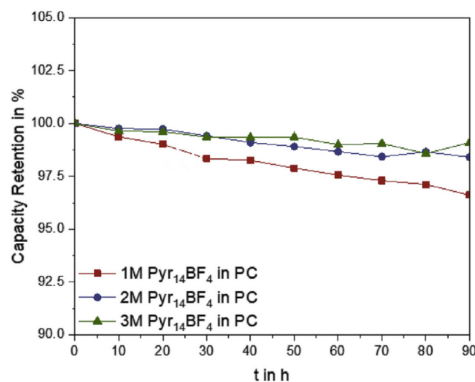


Fig. 7. Capacity retention of PTMA-based electrodes in 1 M, 2 M and 3 M Pyr₁₄BF₄ in PC during float test carried out at 1.1 V vs. Ag. The electrode capacity has been determined at room temperature utilizing a discharge current density equivalent to 5C in interval of 10 h.

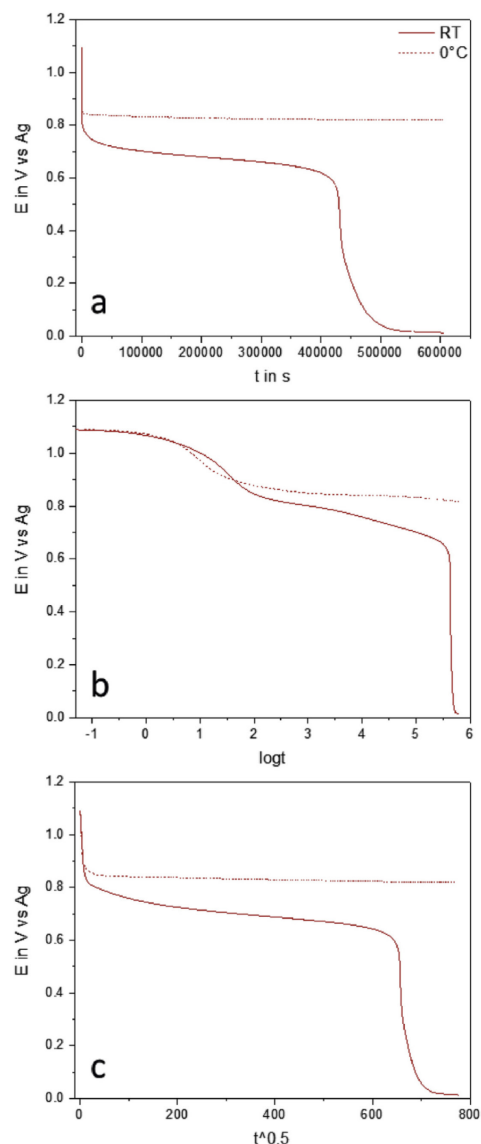


Fig. 8. Self-Discharge of PTMA-based electrodes in 1 M Pyr₁₄BF₄ in PC after 7 days at room temperature as well as 0 °C: a) Voltage excursion vs. time, b) Voltage excursion vs. log t and c) Voltage excursion vs. $t^{1/2}$.

the electrolytes. This is evident considering the values of conductivity and viscosity of Fig. 1.

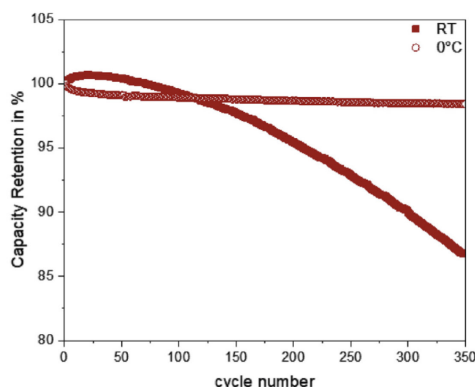


Fig. 9. Cycling stability of PTMA-based electrodes in 1 M Pyr₁₄BF₄ in PC after self-discharge experiments at room temperature as well as 0 °C utilizing a C-rate of 1C.

Finally, also the influence of the temperature on the cycling stability of the PTMA electrodes has been investigated. Fig. 9 shows the capacity retention displayed by the PTMA electrode in 1 M Pyr₁₄BF₄ in PC during charge–discharge tests carried out at 1C at room temperature and 0 °C. As shown, after 350 cycles the PTMA electrode cycled at room temperature was able to retain more than 85% of its initial capacity. At 0 °C, after the same number of cycles, the PTMA electrode kept 98% of its initial capacity. This remarkable difference is clearly indicated the strong influence of the temperature on the electrochemical behaviour of PTMA electrode and the high performance of the investigated system at low temperature.

4. Conclusion

The understanding of the influence of the electrolyte on the electrochemical behaviour of PTMA-based electrode is a topic of great importance in view of the realization of advanced organic batteries.

In this work we investigated the use of three model electrolytes, displaying comparable conductivities but different viscosities (1 M, 2 M and 3 M Pyr₁₄BF₄ in PC), in combination with PTMA-based electrodes. We showed that when slow scan rates and/or current densities are applied, the electrolyte composition does not affect significantly the electrochemical behaviour of the PTMA electrodes. To the contrary, when high current densities are applied the transport properties of the electrolytes are strongly influencing the performance of these polymeric electrodes. The transport properties of the used electrolyte have also a strong impact on the entity of the self-discharge of PTMA electrodes, and the use of highly concentrated and highly viscose electrolytes appears favourable for the buffering of this process. Furthermore, we showed that the

operative temperature has a strong effect on the self-discharge as well as cycling behaviour of PTMA based electrodes, and that at 0 °C these electrodes can display a low self-discharge and high cycling stability.

In summary, the electrolyte design appears of critical importance for the optimization of the performance of PTMA electrodes. Taking into account the results of this work, the use of highly concentrated and relatively high viscose electrolyte, e.g. 2 M Pyr₁₄BF₄ in PC, appears as the most suitable choice for the realization of high performance PTMA-based systems.

Acknowledgements

The authors wish to thank the Friedrich Schiller University Jena for the financial support. USS and ALB thank the TMWWWDG and TAB for financial support (RIS3 Innovationszentrum CEEC Jena).

Appendix A. Supplementary data

Supplementary data to this article can be found online at <https://doi.org/10.1016/j.electacta.2019.03.147>.

References

- [1] C. Friebe, U.S. Schubert, *Top. Curr. Chem.* 375 (2017) 19.
- [2] S. Muench, A. Wild, C. Friebe, B. Hauptler, T. Janoschka, U.S. Schubert, *Chem. Rev.* 116 (2016) 9438–9484.
- [3] J.-K. Kim, J.-H. Ahn, G. Cheruvally, G.S. Chauhan, J.-W. Choi, D.-S. Kim, H.-J. Ahn, S.H. Lee, C.E. Song, *Met. Mater. Int.* 15 (2009) 77–82.
- [4] H. Nishide, S. Iwasa, Y.-J. Pu, T. Suga, K. Nakahara, M. Satoh, *Electrochim. Acta* 50 (2004) 827–831.
- [5] K.O.H. Nishide, *Science* 319 (2008) 736–737.
- [6] J. Qu, T. Katsumata, M. Satoh, J. Wada, J. Igarashi, K. Mizoguchi, T. Masuda, *Chemistry* 13 (2007) 7965–7973.
- [7] T. Janoschka, M.D. Hager, U.S. Schubert, *Adv. Mater.* 24 (2012) 6397–6409.
- [8] K. Nakahara, S. Iwasa, M. Satoh, Y. Morioka, J. Iriyama, M. Suguro, E. Hasegawa, *Chem. Phys. Lett.* 359 (2002) 351–354.
- [9] K. Nakahara, J. Iriyama, S. Iwasa, M. Suguro, M. Satoh, E.J. Cairns, *J. Power Sources* 163 (2007) 1110–1113.
- [10] K. Nakahara, J. Iriyama, S. Iwasa, M. Suguro, M. Satoh, E.J. Cairns, *J. Power Sources* 165 (2007) 398–402.
- [11] K. Nakahara, J. Iriyama, S. Iwasa, M. Suguro, M. Satoh, E.J. Cairns, *J. Power Sources* 165 (2007) 870–873.
- [12] J.-K. Kim, G. Cheruvally, J.-H. Ahn, Y.-G. Seo, D.S. Choi, S.-H. Lee, C.E. Song, *J. Ind. Eng. Chem.* 14 (2008) 371–376.
- [13] K. Nakahara, K. Oyaizu, H. Nishide, *J. Mater. Chem.* 22 (2012) 13669.
- [14] Y.-Y. Cheng, C.-C. Li, J.-T. Lee, *Electrochim. Acta* 66 (2012) 332–339.
- [15] Y. Dai, Y. Zhang, L. Gao, G. Xu, J. Xie, *J. Electrochem. Soc.* 158 (2011) A291.
- [16] J.-K. Kim, G. Cheruvally, J.-W. Choi, J.-H. Ahn, D.S. Choi, C.E. Song, *J. Electrochem. Soc.* 154 (2007) 839–843.
- [17] K. Koshika, N. Sano, K. Oyaizu, H. Nishide, *Chem. Commun.* (2009) 836–838.
- [18] A. Vlad, N. Singh, J. Rolland, S. Melinte, P.M. Ajayan, J.-F. Gohy, *Sci. Rep.* 4 (2014) 4315.
- [19] S. Pohlmann, C. Ramirez-Castro, A. Balducci, *J. Electrochem. Soc.* 162 (2015) A5020–A5030.
- [20] T. Janoschka, A. Teichler, A. Krieg, M.D. Hager, U.S. Schubert, *J. Polym. Sci. A Polym. Chem.* 50 (2012) 1394–1407.
- [21] C. Schütter, T. Husch, V. Viswanathan, S. Passerini, A. Balducci, M. Korth, *J. Power Sources* 326 (2016) 541–548.
- [22] R.-S. Kühnel, A. Balducci, *J. Power Sources* 249 (2014) 163–171.
- [23] A.M. Oickle, H.A. Andreas, *J. Phys. Chem. C* 115 (2011) 4283–4288.
- [24] J. Black, H.A. Andreas, *Electrochim. Acta* 54 (2009) 3568–3574.
- [25] P. Gerlach, R. Burges, A. Lex-Balducci, U.S. Schubert, A. Balducci, *J. Power Sources* 405 (2018) 142–149.

2.3 Publication 4: Aprotic and Protic Ionic Liquids as Electrolytes for Organic Radical Polymers

The previous sections showed that the use of ILs and highly concentrated electrolytes has a beneficial effect towards stability and self-discharge of PTMA-based electrodes. Therefore, after the investigation dedicated to the influence of the salt concentration on the electrochemical behavior of PTMA-based electrodes, the use of neat ionic liquid electrolytes has been carried out. The use of ILs as electrolyte media has already been considered in a small number of investigations dedicated to PTMA and other ROMPs. However, there the use of binary mixtures of Li-salts and ILs was mainly considered. Furthermore, the influence of protic ionic liquids has not been investigated so far. As observed in publication 2, the nature of the cations might change the performance of PTMA-based electrodes drastically.

For these reasons, we investigated the impact of the aprotic ILs (AILs) Pyr₁₄TFSI and 1-butyl-1-methylpyrrolidinium bis(fluorosulfonyl)imide (Pyr₁₄FSI) and the two protic ILs (PILs) 1-butyl-pyrrolidinium bis(trifluoromethylsulfonyl)imide (Pyr_{H4}TFSI) and 1-butyl-pyrrolidinium bis(fluorosulfonyl)imide (Pyr_{H4}FSI) on the electrochemical behavior of PTMA. Therewith, the influence of the combination of two different anions and cations on the performance can be investigated.

All considered ILs have already been successfully utilized in supercapacitors and/or LIBs [159,170,171]. In these works, the chemical physical transport properties have been identified. There it was found that the nature of the anion seems to have a strong impact on the electrolyte properties at room temperature. Pyr₁₄TFSI and Pyr_{H4}TFSI display the highest viscosities of 90 and 60 mPa s (measured at 40°C for Pyr_{H4}TFSI). The conductivities were found at 2.2 mS cm⁻¹ for Pyr₁₄TFSI and 2.7 mS cm⁻¹ for Pyr_{H4}TFSI (at 40°C). In the meantime, the FSI-based ILs show lower values in viscosity of 58 and 35 mPa s for Pyr₁₄FSI and Pyr_{H4}FSI, respectively. The conductivities of the FSI-based ILs are very comparable (5.32 and 5.30 mS cm⁻¹ for Pyr₁₄FSI and Pyr_{H4}FSI, respectively). With these values a general better performance for PTMA in combination with FSI-based ILs is to be expected.

This suggestion is found to be valid in the case of the tested AILs. In the CV and voltage profile the redox potentials of the PTMA reaction are located at 0.6 - 0.8 V vs. Ag. While both systems show a high coulombic efficiency close to 100 %, a big difference in the specific capacity is observed. In Pyr₁₄TFSI 58 mAh g⁻¹ are measured at 1C. At the same time, PTMA electrodes deliver 74 mAh g⁻¹ when used in combination with Pyr₁₄FSI.

In the rate capability tests the influence of the relatively high viscosity is evident, since a decrease in capacity is visible for PTMA in both electrolytes with every increase in current density. However, PTMA in Pyr₁₄FSI still delivers 29 % of the initially capacity at a very high rate of 100C. At the same current no charge is accessible in Pyr₁₄TFSI.

When the cycling stability at 1C and the self-discharge performance of the electrodes are considered, the beneficial effect of the highly viscous, high concentrated electrolytes can be seen. PTMA displays only minor degradation during charge/discharge over 100 cycles and loses only 30 % of the initial charge after 7 days of self-discharge in both AILs.

On the other hand, a big difference is obtained in the long-term floating behavior at 1.1 V vs. Ag. After 8 days, a complete decomposition of the electrode material is observed for PTMA in Pyr₁₄TFSI. To the contrary, PTMA in Pyr₁₄FSI shows an increase of the specific capacity from 32 to 50 mAh g⁻¹, which indicates an increase in accessible active sites in the electrode. Afterwards, a stable behavior is measured for 50 additional days.

After the investigation of PTMA in combination with AILs, also the electrochemical performance of PTMA-based electrodes with PILs as electrolytes was tested for the first time. To start with it can be stated that PTMA works in principle with both PILs as electrolyte. However, while PTMA in combination with AILs displays high stability, especially in the case of Pyr₁₄FSI, the same cannot be said for the use of PILs.

At first a reduction in the average redox potential of 0.2 V as well as a decrease in specific capacity is noticeable. In Pyr_{H4}TFSI only 34 mAh g⁻¹ of specific capacity are accessible for the PTMA electrode, while in Pyr_{H4}FSI 54 mAh g⁻¹ are found. Furthermore, already at 20C no capacity is obtained in both electrolytes, although PTMA with the FSI⁻-based IL again displays the higher rate capability.

During the cycling stability tests at 1C a strong degradation was found for both PILs, which indicates an interaction of the active electrode material with the proton of these electrolytes.

This instability of the electrodes in PILs was also observed during the self-discharge tests. After 1 day of rest after an initial full charge at 1C, no charge was left in PTMA in combination with Pyr_{H4}TFSI. In Pyr_{H4}FSI only 20 % of leftover charge is obtained after 1 day.


In the floating test a very interesting behavior is observed. While PTMA in Pyr_{H4}TFSI does not show significant capacity after the first 10 h of stable potential, which indicated a complete decomposition, a significant increase in capacity to 44 mAh g⁻¹ is displayed in Pyr_{H4}FSI during the first four days. However, after pauses in the experiment a decrease in capacity is visible within each break, which is reversible over time with the further application of stable potential. This behavior highlights the very complex interaction of PTMA and the present protons of the PILs. Considering the results from the self-discharge and floating experiments a loss of accessible active sites of PTMA in the PILs at rest can be assumed. However, in the case of PTMA in Pyr_{H4}FSI this loss is reversible with the application of a stable potential.

In this work, a systematic study of four neat ILs as electrolytes for PTMA-based electrodes has been carried out. Therewith a very stable performance was found for aprotic ILs, especially for PTMA in Pyr₁₄FSI. Also, for the first time a proof of concept for the use of protic IL electrolytes for PTMA was reported. However, the stability performance of PTMA in these electrolytes needs further investigation and improvement. These results highlight a strong impact of the cation as well as anion of the IL electrolytes on the electrochemical behavior of PTMA-based electrodes. On the one side the change from TFSI to FSI⁻-based ILs is accompanied by an improvement in all tested performance criteria. On the other side, the use of protic cations instead of their aprotic counterparts increases the PTMA electrode degradation in this study.

Therefore, aprotic FSI⁻-based ILs should be considered as high concentration electrolytes for ROMPs, which enable high cycling stability with feasible capacity performance. In the meantime, protic ILs should be the object of further research on the interaction of PTMA with the protons in the electrolytes. With the understanding on these occurring degradation processes the general stability of PTMA electrode could be improved.



Aprotic and Protic Ionic Liquids as Electrolytes for Organic Radical Polymers

P. Gerlach,^{1,2} R. Burges,^{2,3} A. Lex-Balducci,^{2,3} U. S. Schubert,^{2,3} and A. Balducci^{1,2,*} 

¹Institute for Technical Chemistry and Environmental Chemistry, Friedrich Schiller University Jena, 07743 Jena, Germany

²Center for Energy and Environmental Chemistry Jena (CEEC Jena), Friedrich Schiller University Jena, 07743 Jena, Germany

³Laboratory of Organic and Macromolecular Chemistry (IOMC), Friedrich Schiller University Jena, 07743 Jena, Germany

In this study we systematically investigated the impact of aprotic and protic ionic liquids on the electrochemical behavior of poly(2,2,6,6-tetramethylpiperidinyloxy methacrylate) (PTMA) based electrodes. We showed that the use of aprotic ILs based on the FSI⁻ anion enables the realization of electrodes able to display high capacity, good capacity retention at high current density (42% at 50 C), low self-discharge and high stability during float tests. We also reported, for the first time, that it is possible to successfully use PTMA-based electrodes in combination with PILs. We showed that the PTMA electrodes display good capacity but a limited cycling stability in these ionic liquids. This investigation confirms that ionic liquids are very interesting candidates for the realization of high performance PTMA-based electrodes. A deeper understanding of the interactions taking place between ionic liquids and organic active materials will be required to finely tune the properties of these promising electrolytes for an application in organic radical polymer-based energy storage systems.

© 2020 The Electrochemical Society ("ECS"). Published on behalf of ECS by IOP Publishing Limited. [DOI: [10.1149/1945-7111/abb382](https://doi.org/10.1149/1945-7111/abb382)]

Manuscript submitted June 5, 2020; revised manuscript received August 25, 2020. Published September 9, 2020.

Supplementary material for this article is available [online](#)

In the last years, the interest on the use of organic radical polymers (ORPs) in electrochemical storage devices increased constantly. ORPs hold a stable radical in their redox active centers, which provides a fast electron exchange reaction with fast kinetics and high power densities.^{1–4} The first and most investigated ORP for the application in energy storage is poly(2,2,6,6-tetramethylpiperidinyloxy methacrylate) (PTMA) introduced by Nakahara et al. in 2002.⁵ PTMA bears a (2,2,6,6-tetramethylpiperidin-1-oxyl)-(TEMPO-) group attached to the polymer chain. During the charging process, this redox active TEMPO-moiety alters from the electronneutral state (free stable radical) to the positive state (oxoammonium cation).¹ Therewith PTMA belongs to the p-type polymers, and during the charging process anions need to be inserted in its structure in order to compensate the generated charge.⁶ Taking this point into account, it is evident that the nature of the salt present in the electrolyte, and in particular of the anion, is significantly affecting the dynamics of the charge process and, consequently, the electrochemical behavior of these materials.⁷

To date, PTMA-based electrodes have been mostly investigated in combination with electrolytes for lithium-ion batteries (LIBs) and the state-of-the-art electrolyte of these devices, 1 M lithium hexafluorophosphate in ethylene carbonate/dimethyl carbonate (1 M LiPF₆ in EC/DMC), can also be considered the state-of-the-art electrolyte for PTMA-based systems. It has been shown that the use of these electrolytes allows the realization of PTMA-based electrodes displaying a stable voltage plateau (3.5 V vs Li/Li⁺), a specific capacity close the theoretic value (111 mAh g⁻¹) and high rate capability.^{8–14} However, LIB electrolytes are not designed for the specific needs of organic radical materials, and their use is causing some serious drawbacks like high self-discharge^{12,15,16} and dissolution of the active material into the electrolyte, which are negatively affecting the cycling stability of these materials.^{17,18} In order to overcome these limitations, "alternative" electrolytes for organic active materials,^{19,20} e.g. high concentrated organic electrolytes,^{21–23} water-in-salt electrolytes,^{24–26} highly viscous electrolytes,^{27,28} ionic liquids (ILs),²⁹ polymer electrolytes^{30–36} or solid state electrolytes,^{37,38} have been proposed in the last years. These studies indicate that the use of highly viscous electrolytes might improve the cycling stability^{32,39,40} and reduces the self-discharge⁴¹ of PTMA-based electrodes. Recently, it has been also shown that ILs,

due to the occurrence of dispersion force, are stabilizing the free electron of TEMPO.⁴²

Considering these points, ILs can therefore be considered as promising electrolytes for PTMA, but more in general for ORP-based systems. Nonetheless, it is important to notice that a systematic investigation about the influence of the nature of the cation, anion (and their combination) of ILs of the electrochemical behavior of PTMA-based electrodes has not been carried out so far. Furthermore, to the best of our knowledge, until now only aprotic ILs (AILs) have been considered, while no studies have been dedicated to the use of protic ILs (PILs) in combination with PTMA-based electrodes. PIL-based electrolytes display transport and thermal properties similar to those of AILs but, due to the presence of an additional proton in their cation structure, have markedly different ion-ion interactions compared to the latter.⁴³ In the last years it has been shown that PILs are interesting electrolytes for supercapacitors and LIBs.^{44–51} For this reason, the investigation of PIL-based electrolytes in combination with PTMA-based electrodes appears important in order to understand whether this class of ILs can also be introduced in organic batteries.

In this work we present an investigation about the impact of four different ILs, namely 1-butyl-1-methylpyrrolidinium bis(trifluoromethanesulfonyl)imide (Py₁₄TFSI, AIL), 1-butyl-1-methylpyrrolidinium bis(fluorosulfonyl)imide (Py₁₄FSI, AIL), 1-butyl-pyrrolidinium bis(trifluoromethane-sulfonyl)imide (Py_{TH4}TFSI, PIL) and 1-butyl-pyrrolidinium bis(fluorosulfonyl)imide (Py_{TH4}FSI, PIL), on the electrochemical behavior of PTMA-based electrodes. These ILs have been selected because their use enables a systematic investigation of the influence of the anion and cation nature on the electrochemical behavior of PTMA. At the same time, a direct comparison of the impact of AILs and PILs on the performance of PTMA-based electrodes is possible.

Experimental

The synthesis of PTMA has been carried out as described in Ref. 52, leading to a polymer with a radical content of 90%, as determined with electron spin resonance (ESR, Bruker). The electrode composition resulted to 60% of active material (crosslinked PTMA) with 35% of conducting agent (SuperP®, Alfa Aesar) and 5% of binder (polyvinylidene fluoride (PVdF, Sigma Aldrich). All components were mixed in *N*-methyl-2-pyrrolidone (NMP, TCI) with a dissolver (Dispermat®, VMA-GETZMANN). The slurry was casted with a doctor blade (250 μm wet film thickness) on an aluminum current

*Electrochemical Society Member.

[†]E-mail: andrea.balducci@uni-jena.de

collector and dried in a drying oven with air circulation overnight at 80 °C. The electrode area was equal to 1.13 cm² and the mass loading was on average 0.7 mg cm⁻². As counter electrodes, oversized free-standing activated carbon-based electrodes have been prepared using a procedure identical to that reported in Ref. 53. The aprotic ionic liquids utilized in this investigation were purchased from IoLiTec (Ionic Liquids Technology, Germany). Protic ILs were synthesized similar as described in Ref. 49. All ILs were used neat. The water content of all ionic liquids was lower than 20 ppm, as measured by Karl Fischer titration. The ILs were stored in a glove box (LabMaster, MBRAUN GmbH) under argon atmosphere with a water and oxygen content below 0.1 ppm. The viscosity of the electrolytes was measured with a rheometer (Anton Paar, MCR 102) using a shear rate of 1000 1/s, while their conductivity was determined by impedance spectroscopy using a Modu-Lab XM ECS Electrochemical Test System (AMETEK Scientific Instruments). Both investigations have been carried out at 20 °C. All electrochemical tests reported in this study have been carried out utilizing a Swagelok-cell type with a three electrodes configuration, in which an Ag wire was used as a quasi-reference and a glass fiber sheet (Whatmann), drenched with 160 μ l of electrolyte, was used as separator. Cyclic voltammetry (CV) was performed using a scan rate of 2 mV s⁻¹. Galvanostatic charge-discharge cycling (CC) was carried out between 0.3 V and 1.4 V vs Ag (which corresponds to 3.3 V and 4.4 V vs Li/Li⁺) using current densities ranging from 0.2 C to 100 C (1 C has been defined considering the theoretical capacity of PTMA, 111 mAh g⁻¹). The self-discharge of PTMA-based electrodes was recorded by fully charging (to 1.4 V vs Ag) the electrodes at 1 C and afterwards monitoring the residual stored charge of the active material by galvanostatic discharge for seven days at room temperature. Float tests were performed by charging the PTMA-based electrodes to 1.1 V vs Ag and keeping this voltage for a total of 70 d. In order to monitor the changes over the time of the experiment, every 10 h charge/discharge cycles with a current density of 5 C were carried out.

All electrochemical measurements were carried out using a VMP multichannel potentiostatic-galvanostatic workstation (Biologic Science Instruments, VMP 3) or an Arbin potentiostat-galvanostat workstation (Arbin instruments, LBT21084) at room temperature (if not indicated otherwise). Before starting the actual measurements, 3 h of open circuit voltage (OCV) were recorded to set the systems into an equilibrium.

Results and Discussion

Figure 1 compares the viscosity and the conductivity of the 4 ILs investigated in this work: The aprotic ILs Pyr₁₄TFSI and Pyr₁₄FSI and the protic ILs Pyr_{H4}TFSI and Pyr_{H4}FSI. In the past years these ILs have been utilized as electrolytes for supercapacitors and LIBs.^{24,47,49,51,54-57} However, to the best of our knowledge, Pyr₁₄TFSI is the only one that

until now has been used in combination with organic redox active materials.^{29,32,40} The values reported in Fig. 1 are given for 20 °C, except for Pyr_{H4}TFSI, which is solid at room temperature. For this reason, the values relative to this PIL are referring to 40 °C. This latter temperature has been also utilized for all electrochemical tests carried out with this PIL. As shown, Pyr₁₄TFSI displays the highest viscosity and the lowest conductivities of all investigated ionic liquids (90 mPa s and 2.2 mS cm⁻¹, respectively, at 20 °C).⁴⁷ The substitution of the TFSI⁻ anion with the FSI⁻ is considerably decreasing the viscosity (58 mPa s) and increasing the conductivity (5.32 mS cm⁻¹), making Pyr₁₄FSI an IL with promising transport properties.⁴⁷ The trend observed in the AILs is also observed in the PILs. At 40 °C Pyr_{H4}TFSI displays a viscosity of 60 mPa s and a conductivity of 2.7 mS cm⁻¹.⁵¹ On the other hand, Pyr_{H4}FSI displays at 20 °C a viscosity of 35 mPa s and a conductivity of 5.3 mS cm⁻¹.⁴⁹ Taking these values into account, it appears that the viscosity and the conductivities of the investigated ILs are mainly determined by the nature of the anion, which is in good agreement with literature.⁵⁸⁻⁶⁰ Furthermore, the use of FSI⁻ enables the realization of ILs with improved transport properties compared to TFSI⁻. In the meantime, the use of the cations Pyr₁₄⁺ and Pyr_{H4}⁺ is leading to ILs with very comparable properties. The overall electrochemical stability windows of the aprotic ILs are more than 5 V, while the windows for the protic ones are ca. 3 V.^{44,47,51} (the ESW of Pyr_{H4}FSI is reported in the Supplementary Information S1 is available online at stacks.iop.org/JES/167/120546/mmedia). Due the presence of the proton, the cathodic stability of the investigated PIL is lower compared to their aprotic counterparts (ca. -1 V vs Ag for the PIL). Nevertheless, all ILs show comparable anodic stability (up to 2.5 V vs Ag). In the presented study, all experiments have been carried out at a potential of maximum 1.5 V vs Ag, which is within the stability of all ILs.

Figure 2 shows the electrochemical behavior of PTMA-based electrodes used in combination with Pyr₁₄TFSI and Pyr₁₄FSI. Figure 2a compares the CVs (scan rate 2 mV s⁻¹) of PTMA-based electrodes in these two AILs. As shown, in both of them the electrodes reveal a reversible single step redox peak. However, the nature of the used AIL strongly affects the potential at which the storage process is occurring as well as its according peak intensity. In Pyr₁₄TFSI the cathodic peak is located at 0.75 V vs Ag, while the anodic peak can be found at a potential of 0.51 V vs Ag. This broad peak shift for oxidation and reduction is typical for highly viscous electrolytes. When Pyr₁₄FSI is used, the cathodic and anodic peaks associated to the storage process are much closer (0.89 V vs Ag and 0.7 V vs Ag, respectively). Furthermore, the intensity of the peak is significantly increased, almost doubling. These latter results are clearly related to the low viscosity and higher conductivity of Pyr₁₄FSI compared to that of Pyr₁₄TFSI. It must be noted, nonetheless, that the use of both AILs guarantees a high coulombic efficiency. Figure 2b reports the voltage profile of

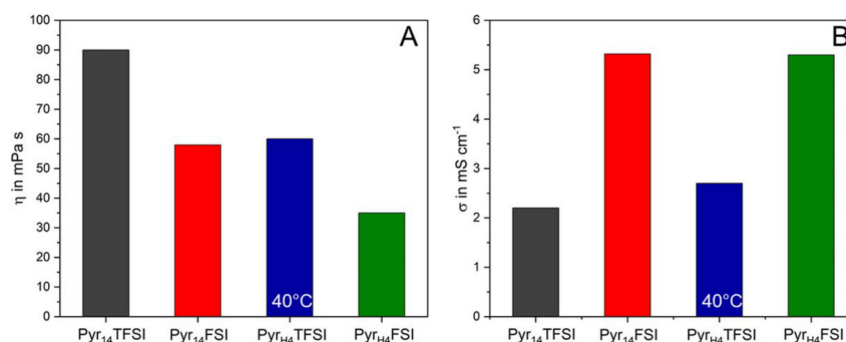


Figure 1. (a) viscosity and (b) conductivity of Pyr₁₄TFSI, Pyr₁₄FSI, Pyr_{H4}TFSI (40 °C), Pyr_{H4}FSI at 20 °C.

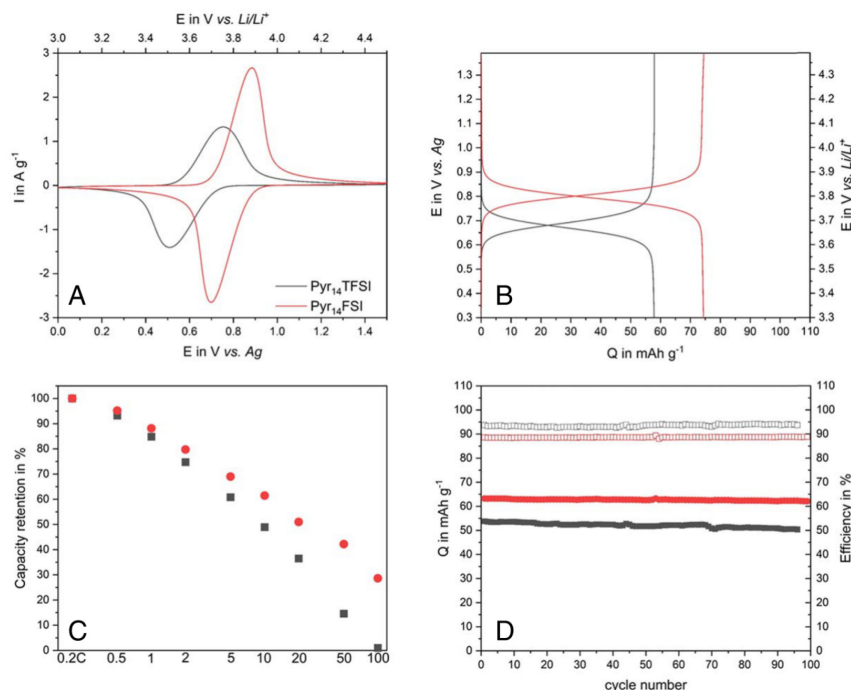


Figure 2. (a) Cyclic voltammetry at a scan rate of 2 mV s^{-1} , (b) voltage profile at 1 C, (c) rate capability from 0.2 C to 100 C and (d) cycling stability at 1 C of PTMA-based electrodes in combination with $\text{Pyr}_{14}\text{TFSI}$ and $\text{Pyr}_{14}\text{FSI}$ as electrolytes (filled dots refer to specific capacity, empty to coulombic efficiency).

PTMA-based electrodes in the two AILs as obtained by applying a current density corresponding to 1 C. As shown, also in the case of these experiments the nature of the used ILs has a strong influence on the potential at which the plateaus associated to the charge-discharge are located as well as on the specific capacity delivered by the electrodes. As a matter of fact, the electrode used in combination with $\text{Pyr}_{14}\text{TFSI}$ displays a charge plateau at 0.69 V vs Ag and delivers a specific capacity of 58 mAh g^{-1} , while those used in combination with $\text{Pyr}_{14}\text{FSI}$ display a charge plateau at 0.8 V vs Ag , and deliver a capacity of 74 mAh g^{-1} . Figure 2c compares the capacity retention of the PTMA-based electrodes utilizing current densities ranging from 0.2 C to 100 C. At 0.2 C the PTMA-based electrode cycled in $\text{Pyr}_{14}\text{TFSI}$ exhibits a specific capacity of 66 mAh g^{-1} (which has been set as the 100%). The absolute values of capacitance are reported the Supplementary Information S2). When the C-rate is increased to 1 C the electrode loses 15% of its initial capacity, and 63.5% at 20 C. At 50 C the electrode can still deliver some capacity (14% compared to the initial value), while at 100 C no capacity is accessible anymore. As expected, the use of $\text{Pyr}_{14}\text{FSI}$ improves the capacity retention of the PTMA-based electrodes. As observed above, the electrode capacity at 0.2 C is higher compared to that achievable with $\text{Pyr}_{14}\text{TFSI}$ and is equal to 76 mAh g^{-1} (which has been set as the 100%). The absolute values of capacitance are reported the Supplementary Information S2). At 1 C and 20 C the electrode displays a capacity of 67 mAh g^{-1} (88%) and 39 mAh g^{-1} (51%), respectively. At 100 C the PTMA-based electrode displays a capacity of 22 mAh g^{-1} , which corresponds to ca. 29% of the initial capacity. From these results it is evident that $\text{Pyr}_{14}\text{FSI}$ is a very promising electrolyte in view of high-power applications. Nevertheless, it is important to notice that in both

AILs, which have a very high viscosity compared to state-of-the-art organic electrolytes, the PTMA-based electrodes are able to deliver high capacity also at very high C-rates. After the rate capability tests, also the cycling stability at 1 C of PTMA-based electrodes has been investigated. As shown in Fig. 2d, the PTMA-based electrodes display an initial capacity of 54 mAh g^{-1} in $\text{Pyr}_{14}\text{TFSI}$, which decreases to 50 mAh g^{-1} after 100 cycles. In $\text{Pyr}_{14}\text{FSI}$ the electrodes have an initial capacity of 63 mAh g^{-1} , which is fully maintained after 100 cycles at 1 C. Therewith in both ILs the electrodes display high cycling stability. However, it has to be noticed that during the cycling process the coulombic efficiency of the charge-discharge process appears lower compared to the observed in the previous experiments, most likely due to the occurrence of some side reactions.

As mentioned in the introduction, the self-discharge of PTMA-based electrodes, and in general of ORPs is one of the drawbacks of these active materials. This process can be caused by the dissolution of active material into the electrolyte¹² and in a recent work we showed that the nature of the electrolytes has a strong influence on the self-discharge.^{40,41} Therefore, also the impact of $\text{Pyr}_{14}\text{TFSI}$ and $\text{Pyr}_{14}\text{FSI}$ on this process has been evaluated. Figure 3a compares the self-discharge curves of the PTMA-based electrodes in the two electrolytes. From these curves it is possible to qualitatively evaluate the capacity retention of the electrodes over the time. If the potential of the electrodes remains at the redox potential of PTMA (0.7 to 0.8 V vs Ag), charge is kept inside the active material of the electrode. As soon as the voltage drops below this value the electrodes are completely discharged. Furthermore, the slope of the voltage curve indicates how fast the active polymer is discharged. The smaller the slope, the lower the self-discharge, the higher the capacity retention. In

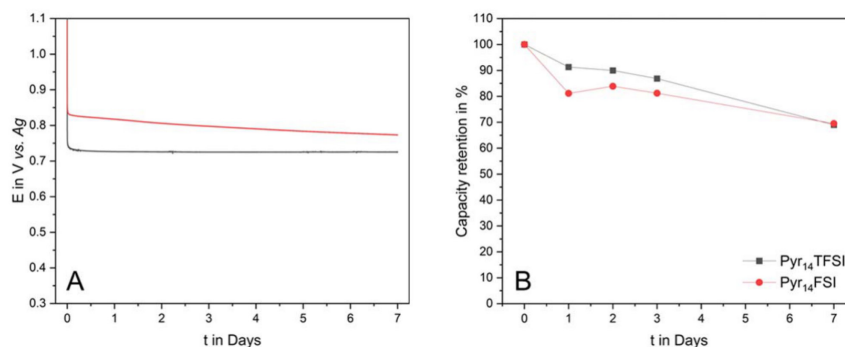


Figure 3. (a) Voltage excursion of PTMA in Pyr₁₄TFSI and Pyr₁₄FSI during 7 d of self-discharge and (b) Self-discharge of PTMA in Pyr₁₄TFSI and Pyr₁₄FSI at 1 C after 1, 2, 3 and 7 d.

Fig. 3a a very stable potential is observed for PTMA in Pyr₁₄TFSI at ca. 0.73 V vs Ag, which indicates an excellent capacity retention. Compared to this graph the potential of PTMA in Pyr₁₄FSI is set to a higher value (0.8 V vs Ag). However, the slope of the voltage loss is higher than for Pyr₁₄TFSI, which suggests a higher self-discharge for PTMA in this electrolyte. This is verified in Fig. 3b, which displays the capacity retention with respect to the time. Within the first three days PTMA shows a high capacity retention of ca. 90% when used in combination with Pyr₁₄TFSI. In the meantime, ca. 81% are kept with Pyr₁₄FSI as electrolyte. However, in both ILs the PTMA-based electrodes were able to keep ca. 70% of their initial capacity after seven days of self-discharge. This value is significantly higher than that observed in electrolytes containing organic solvents, indicating the use of ILs might significantly reduce the self-discharge of PTMA-based electrodes.

After the self-discharge, also float tests have been carried out. These aging tests are widely used to determine the stability of supercapacitors (electrodes and/or devices) at a certain potential. Although they are not often used for the investigation of ORP-based electrodes, they represent valuable experiments to evaluate the stability over time also of these types of polymeric electrodes. Figure 4 compares the variation of the capacity of PTMA-based electrodes which have been hold at 1.1 V vs Ag for several days. The

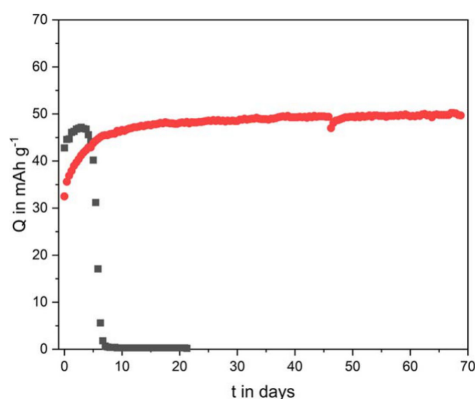


Figure 4. Capacity retention of PTMA in Pyr₁₄TFSI and Pyr₁₄FSI at 5 C after 70 d of stable potential steps at 1.1 V vs Ag.

details of the experiments are reported in the experimental section. As shown, the PTMA-based electrode used in combination with Pyr₁₄TFSI displays an initial specific capacity of 40 mAh g⁻¹, which is a value comparable to that reported in Fig. 2c. During the first three days of float, the electrode in combination with Pyr₁₄TFSI experienced an increase in capacity (up to 47 mAh g⁻¹). Starting from the fourth day, however, a rapid decrease of capacity was observed and after eight days the electrode was no longer able to deliver any capacity. A very different behavior was observed for the PTMA-based electrodes cycled in Pyr₁₄FSI. In this case, the electrode delivers an initial capacity of 32 mAh g⁻¹, which is 20 mAh less than the values from Fig. 2c. A possible explanation for this is low capacity value could be the occurrence of some degradation process during the self-discharge test. However, very interestingly, the electrode capacity increased over time, and after 20 d a stable value of ca. 50 mAh g⁻¹ is reached, which was then maintained (and even slightly increasing) for 50 d. These tests are clearly indicating that PTMA-based electrodes display an extremely high stability when used in combination with Pyr₁₄FSI (corresponding to over 9300 cycles carried out at 5 C assuming a specific capacity of ca. 50 mAh g⁻¹).

After the investigation of AIL-based systems, the use of PILs in combination with PTMA-based electrodes has been investigated for the first time. As mentioned above, PIL-based electrolytes have been successfully used in supercapacitors and LIBs. The results of these studies indicate that the proton(s) present in the structure of these ILs can strongly influence the storage process taking place in these systems.⁴⁵ The use of PILs in combination with PTMA-based electrodes appears therefore interesting to verify whether these electrodes can be cycled in a non-aqueous protic environment. As shown in Fig. 5, this is indeed the case. Figure 5a is comparing the CVs carried out at 2 mV s⁻¹ of PTMA-based electrodes in Pyr₁₄TFSI and Pyr₁₄FSI. As shown, the use of both PILs enables a highly reversible charge-discharge process. However, it is interesting to notice that the cathodic and anodic peaks of these CVs are shifted towards lower potentials compared to the results observed in AILs. Specifically, in Pyr₁₄TFSI the PTMA-based electrode displays a cathodic redox peak at 0.47 V vs Ag and an anodic peak at 0.3 V vs Ag. These values are ca. 0.2 V lower compared to that obtained in Pyr₁₄FSI. When Pyr₁₄FSI is used, the cathodic and anodic peaks are set to 0.56 V and 0.48 V vs Ag, respectively, which are values ca. 0.3 V lower than those observed in Pyr₁₄FSI. This significant peak shift indicates that not only the viscosity and conductivity of the electrolyte are affecting the potential and the intensity of the redox reactions taking place in PTMA-based electrode, but that also ion-ion interactions and/or ion-electrode surface interactions are affecting these processes. This is an important aspect, which need to be further investigated in the future in order to understand the impact of the

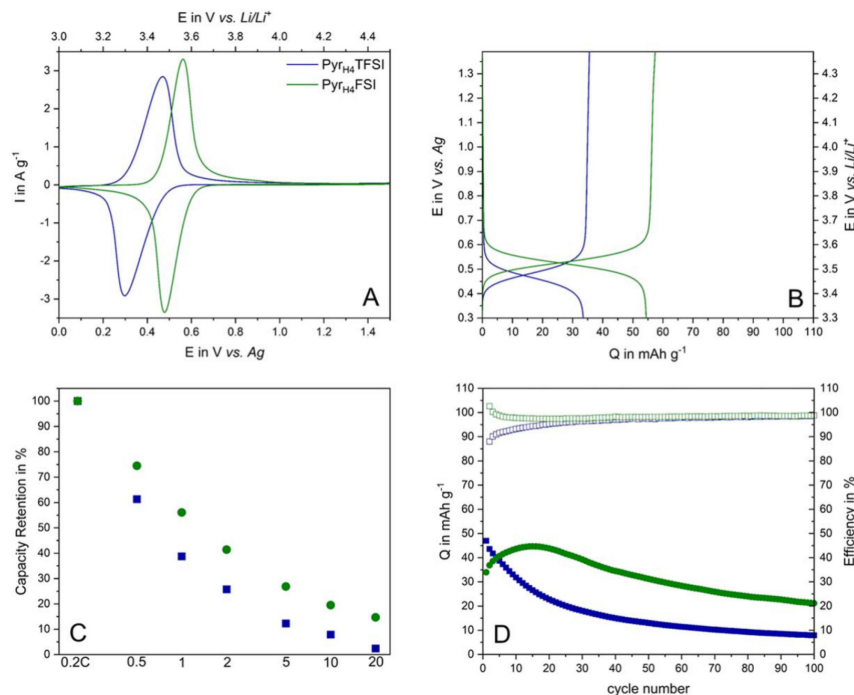


Figure 5. (a) Cyclic voltammetry at a scan rate of 2 mV s^{-1} , (b) voltage profile at 1 C, (c) rate capability from 0.2 C to 100 C and (d) cycling stability at 1 C of PTMA-based electrodes in combination with $\text{PyTfH}_4\text{TFSI}$ and PyTfH_4FSI as electrolytes (filled dots refer to specific capacity, empty to coulombic efficiency), all measurements for $\text{PyTfH}_4\text{TFSI}$ at 40°C .

proton of the PIL on the storage process of PTMA-based electrodes. This investigation, however, is out of the scope of this work and it will not be further considered in the following. As shown in Fig. 5b, when the PTMA-based electrodes are cycled in combination with PyTfH_4FSI they deliver higher capacity (55 mAh g^{-1}) than in combination with $\text{PyTfH}_4\text{TFSI}$ (24 mAh g^{-1}). This result is in line with the results observed for the AILs. However, it has to be noticed that the capacities of the PTMA-based electrodes in PILs are overall lower than the ones reached in AILs. Furthermore, the efficiency of the charge-discharge process is lower in PILs than in AILs. This lower efficiency reduces the stability of the electrodes during the cycling process. Figure 5c compares the current rate capability of PTMA in the protic ILs. As shown, in these electrolytes the PTMA-based electrodes do not perform as well as in the AILs, and they display a constant decrease of capacity when the C-rate is increased. At 20 C the electrode cycled in PyTfH_4FSI retains ca. 20% of its initial capacity, while the one cycled in $\text{PyTfH}_4\text{TFSI}$ does not deliver any significant capacity (The absolute values of capacitance are reported the Supplementary Information S2). vAs shown in Fig. 5d, the electrode cycled in $\text{PyTfH}_4\text{TFSI}$ is losing more than 80% of its initial capacity after 100 cycles at 1 C. The electrode cycled in PyTfH_4FSI displays a better stability and retains more than 62% of its maximum capacity (after an initial increase) after 100 cycles. These results indicate that although it is possible to cycle PTMA-based electrodes in PIL, the stability of these electrodes in these protic electrolytes is significantly lower than the one observed in aprotic electrolytes. It is reasonable to suppose that this difference is caused by the presence of the proton of PILs, which might interact with the PTMA structure, reducing its stability.

To further investigate the behavior of PTMA-based electrode in PIL, also the impact of these electrolytes on the electrode self-discharge has been investigated. Figure 6a displays the self-discharge curves of the PTMA-based electrodes in $\text{PyTfH}_4\text{TFSI}$ and PyTfH_4FSI . As visible, the electrode self-discharge is significantly higher in these ILs than in their aprotic counterparts. The electrode cycled in combination with $\text{PyTfH}_4\text{TFSI}$ loses all its capacity after one day. In the meantime, the electrode cycled in PyTfH_4FSI is able to deliver ca. 20% of its initial capacity. This high self-discharge could be caused by the dissolution of the active material into the electrolyte, the occurrence of side reactions involving the proton of the PILs and the presence of a high amount of redox shuttles in the ionic liquids provided by dissolved polymer.

To gain information about the degree of irreversibility of the capacity loss observed during the self-discharge tests, also float tests at 1.1 V vs Ag have been carried out. As shown in Fig. 7, the PTMA electrode cycled in $\text{PyTfH}_4\text{TFSI}$ was not able to deliver any significant capacity during this test, indicating that the electrode capacity was practically irreversibly lost. In the case of the electrode cycled in PyTfH_4FSI the situation was different. At the beginning of the test the electrode cycled in this electrolyte displays 11 mAh g^{-1} . After the application of the constant potential a strong continuous increase of capacity was obtained, and after 4.5 days a capacity of ca. 44 mAh g^{-1} was delivered by this electrode. It has to be noticed that in between the constant potential periods, when the electrode was charged and discharged (at 5 C), a fade of capacity over the cycling was observed. Nevertheless, it is interesting to notice that during a subsequent float test the capacity could be always recovered. The

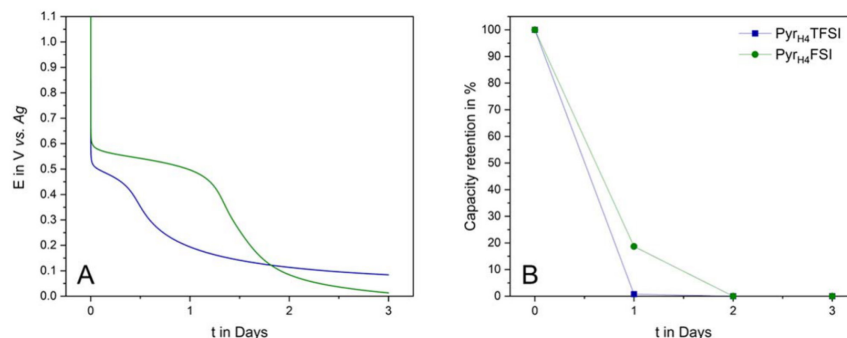


Figure 6. (a) Voltage excursion of PTMA in Pyr₁₄TFSI and Pyr₁₄FSI during 3 d of self-discharge and (b) Self-discharge of PTMA in Pyr₁₄TFSI and Pyr₁₄FSI at 1 C after 1, 2 and 3 d, respectively.

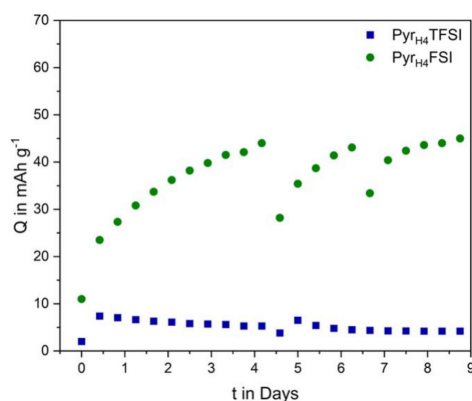


Figure 7. Floating behavior of PTMA in Pyr₁₄TFSI and Pyr₁₄FSI at 5 C after 9 d of stable potential at 1.1 V vs Ag.

results of this test are clearly indicating that the presence of the proton of the PIL has a strong influence on the stability and on the electrochemical behavior of PTMA-based electrodes.

In order to clarify in which way the presence of the proton causes the inferior performance of PTMA, post mortem analysis (SEM) of the here shown composite electrodes as well as pristine electrodes of the same kind have been carried out, which is reported in the supplementary information (S3 and S4). However, in this analysis no significant differences in the surface or the composition of the cycled electrodes has been found. This indicates that the application of PILs does not cause a structural failure of the electrodes, but more likely interferes with the redox active TEMPO moiety of the used active material. In the future, it will be therefore necessary to investigate and understand the interactions taking place between PILs and organic redox active materials in order to clarify the behavior observed above.

Conclusions

In this work, we reported a systematic investigation about the impact of AILs and PILs on the electrochemical behavior of PTMA-based electrodes. We showed that the use of aprotic ILs based on the FSI⁻ anion, such as Pyr₁₄FSI, enables the realization of

electrodes able to display high capacity, good capacity retention at high current density (42% at 50 C) and very low self-discharge. Furthermore, PTMA-based electrodes used in combination with Pyr₁₄FSI display very high stability in float tests and are able to keep all their capacity over 70 d (corresponding to over 9300 cycles at 5 C). We also reported, for the first time, that it is possible to successfully use PTMA-based electrodes in combination with PILs. The use of this protic electrolytes enables the achievement of good capacity. However, the cycling stability of PTMA electrodes in these electrolytes need to be significantly improved.

Overall, this work confirms that ILs represent very interesting candidates for the realization of high performance PTMA-based electrodes. In the future, it will be necessary to intensify the studies dedicated to the interactions taking place between ILs and organic active materials in order to better tune the properties of these promising electrolytes for an application in ORP-based energy storage systems.

Acknowledgments

The authors wish to thank the Deutsche Forschungsgemeinschaft (DFG) within the project "Redox-active ionic liquids in redox-flow-batteries" (BA4956/10-1) for the financial support.

ORCID

A. Balducci  <https://orcid.org/0000-0002-2887-8312>

References

- S. Muench, A. Wild, C. Friebe, B. Haupler, T. Janoschka, and U. S. Schubert, *Chem. Rev.*, **116**, 9438 (2016).
- C. Friebe and U. S. Schubert, *Topics in current chemistry (Journal)*, **375**, 19 (2017).
- T. Suga, Y.-J. Pu, K. Oyaizu, and H. Nishide, *BCSJ*, **77**, 2203 (2004).
- K. Nakahara, K. Oyaizu, and H. Nishide, *Chem. Lett.*, **40**, 222 (2011).
- K. Nakahara, S. Iwasa, M. Satoh, Y. Morioka, J. Iriyama, M. Suguro, and E. Hasegawa, *Chem. Phys. Lett.*, **359**, 351 (2002).
- S. Lee, G. Kwon, K. Ku, K. Yoon, S.-K. Jung, H.-D. Lim, and K. Kang, *Adv. Mater.*, **30**, e1704682 (2018).
- P. Gerlach and A. Balducci, *Chem. Electro. Chem.*, **7**, 2364 (2020).
- J.-K. Kim, J.-H. Ahn, G. Cheruvally, G. S. Chauhan, J.-W. Choi, D.-S. Kim, H.-J. Ahn, S. H. Lee, and C. E. Song, *Met. Mater. Int.*, **15**, 77 (2009).
- J.-K. Kim, G. Cheruvally, J.-H. Ahn, Y.-G. Seo, D. S. Choi, S.-H. Lee, and C. E. Song, *J. Ind. Eng. Chem.*, **14**, 371 (2008).
- J. Kim, G. Cheruvally, J. Choi, J. Ahn, S. Lee, D. Choi, and C. Song, *Solid State Ionics*, **178**, 1546 (2007).
- K. Nakahara, J. Iriyama, S. Iwasa, M. Suguro, M. Satoh, and E. J. Cairns, *J. Power Sources*, **163**, 1110 (2007).
- K. Nakahara, J. Iriyama, S. Iwasa, M. Suguro, M. Satoh, and E. J. Cairns, *J. Power Sources*, **165**, 398 (2007).
- K. Nakahara, J. Iriyama, S. Iwasa, M. Suguro, M. Satoh, and E. J. Cairns, *J. Power Sources*, **165**, 870 (2007).
- H. Nishide, S. Iwasa, Y.-J. Pu, T. Suga, K. Nakahara, and M. Satoh, *Electrochim. Acta*, **50**, 827 (2004).

15. Y. Liang, Z. Tao, and J. Chen, *Adv. Energy Mater.*, **2**, 742 (2012).
16. T. Suga, H. Konishi, and H. Nishide, *Chem. Commun.*, 1730 (2007).
17. L. Bugnon, C. J. H. Morton, P. Novak, J. Vetter, and P. Nesvadba, *Chem. Mater.*, **19**, 2910 (2007).
18. Z. Song and H. Zhou, *Energy Environ. Sci.*, **6**, 2280 (2013).
19. Y. Liang and Y. Yan, *Gen. Chem.*, **3**, 207 (2017).
20. R. Chen, D. Bresser, M. Saraf, P. Gerlach, A. Balducci, S. Kunz, D. Schröder, S. Passerini, and J. Chen, *Chem. Sus. Chem.*, **13**, 2205 (2020).
21. C. Guo, K. Zhang, Q. Zhao, L. Pei, and J. Chen, *Chem. Commun.*, **51**, 10244 (2015).
22. Y. Huang, C. Fang, W. Zhang, Q. Liu, and Y. Huang, *Chemical Communications (Cambridge, England)*, **55**, 608 (2019).
23. Z. Xu, H. Ye, H. Li, Y. Xu, C. Wang, J. Yin, and H. Zhu, *ACS Omega*, **2**, 1273 (2017).
24. X. Dong, H. Yu, Y. Ma, J. L. Bao, D. G. Truhlar, Y. Wang, and Y. Xia, *Chem. Eur. J.*, **23**, 2560 (2017).
25. Y. Liang, Y. Jing, S. Gheyhani, K.-Y. Lee, P. Liu, A. Facchetti, and Y. Yao, *Nat. Mater.*, **16**, 841 (2017).
26. L. Suo, O. Borodin, T. Gao, M. Olguin, J. Ho, X. Fan, C. Luo, C. Wang, and K. Xu, *Science*, **350**, 938 (2015).
27. S. Phadke, M. Cao, and M. Anouti, *Chem. Sus. Chem.*, **11**, 965 (2018).
28. T. Yokoji, Y. Kameyama, S. Sakaida, N. Maruyama, M. Satoh, and H. Matsubara, *Chem. Lett.*, **44**, 1726 (2015).
29. X. Wang, Z. Shang, A. Yang, Q. Zhang, F. Cheng, D. Jia, and J. Chen, *Chem.*, **5**, 364 (2019).
30. R. C. Agrawal and G. P. Pandey, *J. Phys. D: Appl. Phys.*, **41**, 223001 (2008).
31. W. Huang, Z. Zhu, L. Wang, S. Wang, H. Li, Z. Tao, J. Shi, L. Guan, and J. Chen, *Angew. Chem. Int. Ed.*, **52**, 9162 (2013).
32. J.-K. Kim, A. Matic, J.-H. Ahn, and P. Jacobsson, *RSC Adv.*, **2**, 9795 (2012).
33. I. Osada, H. de Vries, B. Scrosati, and S. Passerini, *Angewandte Chemie (International ed. in English)*, **55**, 500 (2016).
34. B. Scrosati and C. A. Vincent, *MRS Bull.*, **25**, 28 (2000).
35. Z. Zhu, M. Hong, D. Guo, J. Shi, Z. Tao, and J. Chen, *J. Am. Chem. Soc.*, **136**, 16461 (2014).
36. W. Wei, L. Li, L. Zhang, J. Hong, and G. He, *Electrochem. Commun.*, **90**, 21 (2018).
37. Y. Hanyu and I. Honma, *Sci. Rep.*, **2**, 453 (2012).
38. X. Zhu, R. Zhao, W. Deng, X. Ai, H. Yang, and Y. Cao, *Electrochim. Acta*, **178**, 55 (2015).
39. Y.-Y. Cheng, C.-C. Li, and J.-T. Lee, *Electrochim. Acta*, **66**, 332 (2012).
40. P. Gerlach, R. Burges, A. Lex-Balducci, U. S. Schubert, and A. Balducci, *J. Power Sources*, **405**, 142 (2018).
41. P. Gerlach, R. Burges, A. Lex-Balducci, U. S. Schubert, and A. Balducci, *Electrochim. Acta*, **306**, 610 (2019).
42. L. Wylie, Z. L. Seeger, A. N. Hancock, and E. I. Izgorodina, *Phys. Chem. Chem. Phys.*, **21**, 2882 (2019).
43. S. Menne, T. Vogl, and A. Balducci, *Physical chemistry chemical physics: PCCP*, **16**, 5485 (2014).
44. A. Balducci, R. Dugas, P. L. Taberna, P. Simon, D. Plé, M. Mastragostino, and S. Passerini, *J. Power Sources*, **165**, 922 (2007).
45. G. T. Kim, S. S. Jeong, M. Joost, E. Rocca, M. Winter, S. Passerini, and A. Balducci, *J. Power Sources*, **196**, 2187 (2011).
46. R.-S. Kühnel, N. Böckenfeld, S. Passerini, M. Winter, and A. Balducci, *Electrochim. Acta*, **56**, 4092 (2011).
47. R.-S. Kühnel and A. Balducci, *J. Power Sources*, **249**, 163 (2014).
48. S. Leyva-García, D. Lozano-Castelló, E. Morallón, T. Vogl, C. Schütter, S. Passerini, A. Balducci, and D. Cazorla-Amorós, *J. Power Sources*, **336**, 419 (2016).
49. S. Menne, T. Vogl, and A. Balducci, *Chemical communications (Cambridge, England)*, **51**, 3656 (2015).
50. T. Stettner, S. Gehrke, P. Ray, B. Kirchner, and A. Balducci, *ChemSusChem*, **12**, 3827 (2019).
51. T. Vogl, S. Menne, and A. Balducci, *Physical chemistry chemical physics: PCCP*, **16**, 25014 (2014).
52. T. Janoschka, A. Teichler, B. Häupler, T. Jähnert, M. D. Hager, and U. S. Schubert, *Adv. Energy Mater.*, **3**, 1025 (2013).
53. C. Schütter, T. Husch, V. Viswanathan, S. Passerini, A. Balducci, and M. Korth, *J. Power Sources*, **326**, 541 (2016).
54. X. Dong, Z. Guo, Z. Guo, Y. Wang, and Y. Xia, *Joule*, **2**, 902 (2018).
55. J.-E. Lim and J.-K. Kim, *Korean J. Chem. Eng.*, **35**, 2464 (2018).
56. J. Qin, Q. Lan, N. Liu, Y. Zhao, Z. Song, and H. Zhan, *Energy Storage Mater.*, **26**, 585 (2020).
57. S. Renault, J. Geng, F. Dolhem, and P. Poizat, *Chem. Commun.*, **47**, 2414 (2011).
58. M. Ishikawa, T. Sugimoto, M. Kikuta, E. Ishiko, and M. Kono, *J. Power Sources*, **162**, 658 (2006).
59. J. Reiter, E. Paillard, L. Grande, M. Winter, and S. Passerini, *Electrochim. Acta*, **91**, 101 (2013).
60. A. Noda, K. Hayamizu, and M. Watanabe, *J. Phys. Chem. B*, **105**, 4603 (2001).

2.4 Publication 5: The influence of current density, rest time and electrolyte composition on the self-discharge of organic radical polymers

The results of the previous works illustrated the strong influence of the electrolyte composition on the electrochemical performance of PTMA electrodes in different electrolyte environments. In addition, especially the self-discharge behavior was found to be heavily influenced by the transport properties of the utilized electrolyte. The high self-discharge rate of PTMA and other ROMP materials is considered as one of the major drawbacks of these materials. However, so far not much research effort has been spent to elucidate the mechanisms of this charge loss. Only few works, which mention the high self-discharge rate, suggest a redox shuttle process caused by the dissolution of active material in the electrolyte. Obviously, the understanding of these processes is crucial to address and overcome this drawback for PTMA and ROMPs for application purposes.

Therefore, to further investigate this poorly addressed aspect, we performed a detailed investigation on the self-discharge of PTMA-based electrodes in two different electrolytes namely neat Pyr₁₄TFSI (IL) and 1M Pyr₁₄TFSI in PC (organic electrolyte). The aim of the study was to clarify the influence of the used current density (in particular charging current) and the applied rest time, in which the self-discharge can occur.

In order to carry out this investigation we applied a specifically tailored test schedule, which is illustrated in publication 5 (Fig. 1). This schedule consists of a charging step including five different C-rates (0.1C, 0.5C, 1C, 2C or 10C), followed by four different rest times (10 min, 1 h, 10 h or 24 h) in which the self-discharge occurs. After the rest step, the residual charge within the PTMA electrodes is measured by a discharge step with the same current as used in the charge step (- 0.1C, - 0.5C, - 1C, - 2C, - 10C). This residual charge is in the following discussion referred to as capacity retention and given in %. The described schedule yields to 20 values of capacity retention for each used electrolyte. With the use of this test schedule, we aim for a deep insight into the processes, which lead to the loss of charge within PTMA-based electrodes and of which so far only suggestions have been made.

The results of the self-discharge test matrix show a strong influence of the applied C-rate on the capacity retention of PTMA in pure Pyr₁₄TFSI. At 0.1C an average capacity retention of more than 90 % is obtained independent of the used rest time. Every increase of the charging current led to a decrease in capacity retention for every rest time, which means a higher self-discharge rate. For PTMA cycled in the 1M Pyr₁₄TFSI in PC such dependency on the C-rate from 0.1C to 10C was not found. However, measurements at 20C showed a significant increase in the charge loss. This leads to the first conclusion of this study. For every system there is a threshold current above which no sufficiently stable charged state can be reached. The value of this threshold current depends on the transport properties of the system. When no stable charged state is achieved, a more rapid self-discharge process is to be expected.

For the clarification of the self-discharge mechanisms in this process the voltage curve recorded during the rest steps was again plotted with respect to $\log t$ and \sqrt{t} . Therewith in most cases, a combination of an activation-controlled faradic reaction and a charge redistribution process was found for most charge/rest/discharge combinations. This means that the application of high currents during charging, leads to subsequent faradic reactions (e.g. rearrangement of TFSI⁻ anions) on the surface of the electrode, followed by a resistance-limited charge redistribution between the surface and the bulk material of the electrodes.

Only for PTMA in 1M Pyr₁₄TFSI in PC charged at 0.1C such behavior was not found. Instead, here the presence of a diffusion-limited process was observed. This suggests that for this electrolyte with good transport properties, charged sufficiently at low C-rate, no rearrangement of ions on the electrode takes place. Due to the absence of this redistribution, the shuttling of dissolved moieties in the electrolyte becomes the limiting factor for the self-discharge.

The work described in publication 5 shows that not only a diffusion-limited process, but also an activation-controlled faradic process with a subsequent charge redistribution is occurring during the self-discharge of PTMA-based electrodes. These findings highlight the complexity of the self-discharge processes, which can be heavily influenced by the electrolyte properties as well as the applied charging conditions.

Every organic active material/ electrolyte combination needs a very careful selection of charging conditions in order to minimize the self-discharge of PTMA and ROMPs in general. In the light of these results, it is evident that for future investigations on the topic researchers should not define the self-discharge performance of innovative ROMPs and/or electrolytes by the conditions of previous materials, but by conditions fitting for the considered system. On the other hand, the meaningful selection of the electrolyte in a ROMP-based system is a powerful tool to improve the self-discharge behavior with fixed charging currents.

Last but not least the variation of the electrolyte should be understood as a tool to investigate complex processes inside EES devices, as proved by the concept and results of publication 5.



ELSEVIER

Contents lists available at ScienceDirect

Electrochimica Acta

journal homepage: www.elsevier.com/locate/electacta

The influence of current density, rest time and electrolyte composition on the self-discharge of organic radical polymers

P. Gerlach^{a,b}, A. Balducci^{a,b,*}^a Institute for Technical Chemistry and Environmental Chemistry, Friedrich-Schiller-University Jena, Philosophenweg 7a, Jena 07743, Germany^b Center for Energy and Environmental Chemistry Jena (CEEC Jena), Friedrich-Schiller-University Jena, Philosophenweg 7a, Jena 07743, Germany

ARTICLE INFO

Article history:

Received 4 January 2021

Revised 9 February 2021

Accepted 27 February 2021

Available online 3 March 2021

Keywords:

Self-discharge

Electrolyte

Radical polymer

PTMA

Ionic Liquid

ABSTRACT

In this work we report a systematic study about the influence of the charging current density and the rest time on the self-discharge of poly(2,2,6,6-tetramethylpiperidinyloxy methacrylate) (PTMA) based electrodes in two model electrolytes, namely 1-butyl-1-methylpyrrolidinium bis(trifluoromethanesulfonyl)imide (Pyr₁₄TFSI, IL) and 1 M Pyr₁₄TFSI in propylene carbonate (PC). We show that for each electrolyte it is possible to identify a threshold of current density (and thus C-rate) which can be safely applied without increasing the electrode self-discharge. Furthermore, we show that the self-discharge of the PTMA-based electrodes is originated by a combination of activation controlled faradic processes, charge redistribution and diffusion limited processes. The use of current densities above the threshold is causing an improper charging process, which leads to faradic reactions on the surface of the electrode followed by the redistribution of charge on the surface of the electrodes and causes a fast energy loss when a current is no longer applied. When current densities below the threshold are used, the diffusion of redox shuttles becomes the driving force of self-discharge taking place in PTMA based electrodes.

© 2021 Elsevier Ltd. All rights reserved.

1. Introduction

Organic radical polymers (ORPs) are nowadays regarded as promising materials for energy storage applications due to their low cost, mechanical flexibility and high power density [1–7]. One of the first and most investigated representative ORP is the poly(2,2,6,6-tetramethylpiperidinyloxy methacrylate) (PTMA), which was proposed by Nakahara et al. in 2002 [8]. PTMA holds a (2,2,6,6-tetramethylpiperidin-1-oxyl)- (TEMPO-) group attached to the polymer scaffold, which can be charged and discharged through a fast one electron exchange reaction [4]. During this process, the TEMPO unit alternates between an electroneutral uncharged radical state and a positively charged (oxoammonium cation) state. Thus, PTMA is a p-type active material, in which anions are introduced into the polymeric structure during the charge-discharge process in order to compensate the generated positive charge [9]. The nature and concentration of the anions within the electrolyte are therefore heavily affecting the electrochemical behavior of PTMA [10].

In the last years PTMA has been widely investigated as electrode battery material. Thereby, it was shown that electrodes based on this ORP display a stable voltage plateau (3.5 V vs. Li/Li⁺), deliver specific capacities close to the theoretic value (111 mAh/g) and high rate capability [11–17]. PTMA electrodes, however, are suffering from a rather strong self-discharge [15,18–20]. The occurrence of this process represents a serious drawback for the implementation of this material, but more in general of ORPs, in practical devices.

Self-discharge is a spontaneous loss of energy occurring in an idle storage device that is caused by a transition from a higher to a lower free energy state within the system [21]. This loss of energy leads to a reduction of the cell voltage and can be caused by three different processes: (1) activation controlled faradic processes; (2) diffusion controlled faradic processes and (3) ohmic leakage [22]. These processes can take place simultaneously. However, one of them might become the rate determining step for the self-discharge [21].

Recent works addressing the self-discharge in batteries suggest that processes like electrode/ electrolyte reactions, dissolution of the active material, SEI formation, redox shuttling and internal electron leakage as possible reasons for the charge loss in batteries [23–29]. To date, on the other hand, only few works investigated in detail the self-discharge of ORPs [30–32]. It has been

* Corresponding author at: Institute for Technical Chemistry and Environmental Chemistry, Friedrich-Schiller-University Jena, Philosophenweg 7a, Jena 07743, Germany.

E-mail address: andrea.balducci@uni-jena.de (A. Balducci).

suggested that the strong self-discharge occurring in PTMA-based electrodes is mainly caused by diffusion controlled redox shuttles of the TEMPO moieties between the electrode and the electrolyte [15,33]. It is important to mention, nevertheless, that most of the investigations considering the self-discharge of PTMA-based electrodes have been carried out utilizing lithium-ion battery (LIB) electrolytes, e.g. 1 M lithium hexafluorophosphate in ethylene carbonate/ dimethyl carbonate (1 M LiPF₆ in EC/DMC). These electrolytes, which can be considered the state-of-the-art electrolyte also for ORP-based batteries [10], display good transport properties, but they are favoring the occurrence of redox shuttles in the ORP-based electrodes since they contain solvents with high dielectric constants. Thus, their use is promoting the self-discharge of the PTMA electrodes [10,15,34]. Consequently, to reduce the self-discharge of PTMA-based electrodes, but more in general of ORP-based electrodes, the selection of alternative electrolytes appears of great importance.

Recently, our group showed that the use of highly concentrated organic electrolytes [35] or neat ionic liquids (ILs) significantly reduces the self-discharge of PTMA-based electrodes, as a decreased dissolution of the active material and a reduction of mobility of the redox shuttles are possible through their use [36,37]. These studies are indicating that a careful selection of the electrolyte can indeed reduce the self-discharge of PTMA-based electrodes. Nevertheless, it is important to point out that several aspects related to the self-discharge of PTMA-based electrodes, e.g., the influence of the "charging conditions", are still unclear. These aspects should be clarified, as they are of importance for the use of these polymeric materials in real application.

In this study we report a systematic investigation about the influence of charging current density and rest time on the self-discharge of PTMA-based electrodes. The aim of this work was to gain information about the impact of the "charging conditions" on the self-discharge of these electrodes when used in combination with two model electrolytes, namely 1-butyl-1-methylpyrrolidinium bis(trifluoromethanesulfonyl)imide (Pyr₁₄TFSI, IL) and 1 M Pyr₁₄TFSI in propylene carbonate (PC).

2. Experimental

PTMA (with a radical content of 90%) was synthesized as described in Ref. [38]. The electrodes investigated in this work have been prepared as indicated in Ref. [28] and contained 60% active material (crosslinked PTMA), 35% conducting agent (SuperP®, Alfa Aesar) and 5% binder (polyvinylidene fluoride (PVdF, Sigma Aldrich)). The electrode area was equal to 1.13 cm² and the mass loading was on average 0.7 mg cm⁻². Activated carbon-based electrodes were prepared as reported in Ref. [39].

The Pyr₁₄TFSI utilized in this investigation was purchased from IoLiTec (Ionic Liquids Technology, Germany), while PC was purchased from Sigma Aldrich. Pyr₁₄TFSI and PC were stored in a glove box (LabMaster, MBRAUN GmbH) under argon atmosphere with a water and oxygen content below 0.1 ppm. The water content of all electrolytes was lower than 20 ppm, as measured by Karl Fischer titration.

All electrochemical tests reported in this study have been carried out utilizing a Swagelok-cell type with a 3-electrodes configuration, containing a PTMA-based working electrode, an oversized activated carbon counter electrode and Ag wire as a quasi-reference. A glass fiber sheet (Whatmann), drenched with 160 μ l of electrolyte, was used as separator.

All electrochemical measurements were carried out at 20 °C using a VMP multichannel potentiostatic-galvanostatic workstation (Biologic Science Instruments, VMP 3) at room temperature. Before starting the "self-discharge" tests, 3 h of open circuit voltage (OCV) were recorded to set the systems into an equilibrium. Afterwards,

50 cyclic voltammetry (CV) and 50 galvanostatic charge-discharge were carried out between 0.3–1.4 V vs. Ag using a scan rate of 2 mV/s and a C-rate of 1C, (1C was defined considering a theoretical capacity of 111 mAh/g for the PTMA), respectively. These cycles have been carried out with the aim to assure full accessibility for the electrolyte to all active sites of the electrodes before the self-discharge test. From previous works it is known that this number of cycles does not negatively affect the electrode behavior [36].

3. Results and discussion

The electrolytes utilized in this work, Pyr₁₄TFSI and 1 M Pyr₁₄TFSI in PC, have been already used in supercapacitors [30,31] as well as in combination with PTMA-based electrodes [36]. These electrolytes have been selected because they contain the same cation and anion, but have significantly different viscosities and conductivities: at 20 °C the neat Pyr₁₄TFSI (which is an ionic liquid) displays a viscosity of 90 mPa s and a conductivity of 2.2 mS cm⁻¹ [40]. At the same temperature, the viscosity and the conductivity of 1 M Pyr₁₄TFSI in PC are 5.1 mPa s and 7.3 mS cm⁻¹, respectively [41]. Due to their different properties, these electrolytes can be considered as very good model electrolytes to gain insight about the self-discharge of PTMA. It has to be mentioned that the potential of the redox peaks (and plateaus) displayed by the PTMA-based electrodes are slightly different in the two electrolytes (see also Fig. S1) [36].

Fig. 1 illustrates the test schedule utilized in this work to investigate the self-discharge of the PTMA-based electrodes. As shown, the schedule consisted of 3 subsequent steps: (I) charge; (II) rest and (III) discharge. In step I the electrodes were charged from 0.3 to 1.4 V vs. Ag utilizing different C-rates (0.1C, 0.5C, 1C, 2C or 10C). In step II no current was applied over a defined interval of time (10 min, 1 h, 10 h or 1 day) and the variation of the electrode potential, representing the electrode self-discharge, was monitored. In the following, this step will be indicated as "rest time". Finally, in step III, the electrodes were completely discharged (till 0.3 vs. Ag) utilizing the same C-rate applied in step I in order to evaluate the capacity left in the electrode after the self-discharge. In the following, this latter capacity will be indicated as "capacity retention". The combination of the 5 different charge/discharge C-rates and the 4 different intervals of time resulted in a matrix of 20 different "charging-rest-discharging" conditions. This matrix was utilized to evaluate the impact of the current as well as the rest time on the self-discharge on the investigated electrodes. It is important to mention some points about the protocol described above: (1) Previous works showed that for all investigated C-rates the PTMA-based electrodes display high charge-discharge efficiency (close to 100%) [36]; (2) Experiments with no rest time have been already carried out [36] and therefore have not been considered in this work; (3) The values of capacitance retention reported in the following figures should not be taken as absolute values, but rather as indication of a reproducible trend displayed by the PTMA-electrodes.

Fig. 2 shows the capacity retention of PTMA-based electrodes, with respect to different rest times, for every applied current density in Pyr₁₄TFSI (Fig. 2A) and in 1 M Pyr₁₄TFSI in PC (Fig. 2B). As shown, the type of electrolyte used in this experiment is significantly influencing the capacity retention of the electrodes (the values of capacity displayed by the electrodes are given in the Tables S2 and S3 of the supplementary information). When Pyr₁₄TFSI is used, the capacity retention of the electrode appears to be mainly influenced by the applied C-rate of charge, while the rest time plays a subordinated role for the resulting self-discharge. As visible in Fig. 2A, the lower the applied C-rate for the charge process, the higher is the capacity retention of the electrode. At 0.1 C the electrodes are able to retain more than 90% of their initial charge,

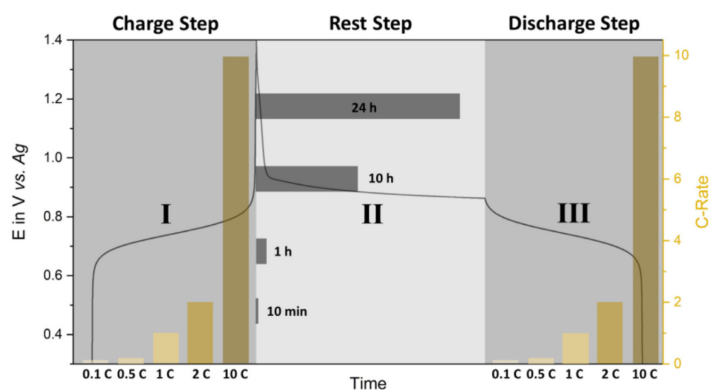


Fig. 1. Schematic illustration of the test schedule utilized to investigate the self-discharge of the PTMA-based electrodes. The combination of the 5 different charge/discharge C-rates and the 4 different intervals of time resulted in a matrix of 20 different “charging-rest-discharging” conditions.

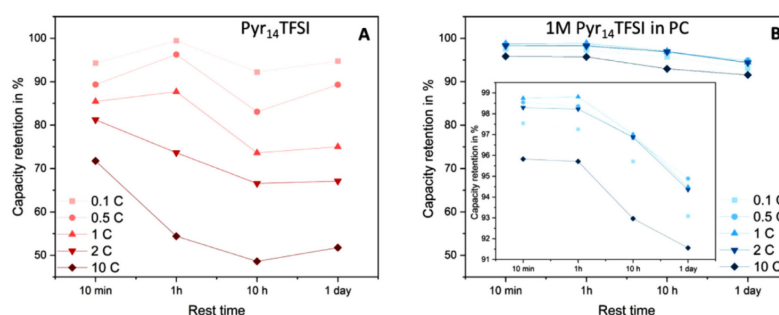


Fig. 2. Capacity retentions of PTMA-based electrodes with respect to the rest time at different current density in (A) Pyr₁₄TFSI and (B) 1 M Pyr₁₄TFSI in PC.

independent of the rest time. Every increase of the applied C-rate for the charge process leads to a decrease of the capacity retention, which becomes larger when longer rest time are applied. At 10C, when a rest time of 10 min is applied, the electrodes are retaining 70% of their initial capacity. When the rest time is increased to 1 day, the capacity retention of the electrodes drops to 50%. Taking these results into account, it is reasonable to suppose that when high C-rates are applied for the charging process, due to the relatively high viscosity and low conductivity of Pyr₁₄TFSI, the PTMA-based electrodes are not able to reach a stable charged state, most likely because of an insufficient insertion of counter ions (TFSI⁻) within the electrode material. When longer rest times are used, the capacity retention is decreasing because the electrodes are spending longer time in an unstable condition. On the other hand, the use of low C-rates has a beneficial effect on the charging of the PTMA-based electrodes. In this case, the transport properties of Pyr₁₄TFSI appears adequate to the time frame of the charging process and the electrodes are able to display high capacity retention, also when long rest times are considered. The use of 1 M Pyr₁₄TFSI in PC, which displays low viscosity and high conductivity with respect to the neat Pyr₁₄TFSI, leads to a completely different behavior. As shown in Fig. 2B, when this electrolyte is used neither the C-rate applied for the charging process, nor the length of the rest time, are affecting the capacity retention of the PTMA electrodes in a way comparable to that observed in Pyr₁₄TFSI. In all investigated

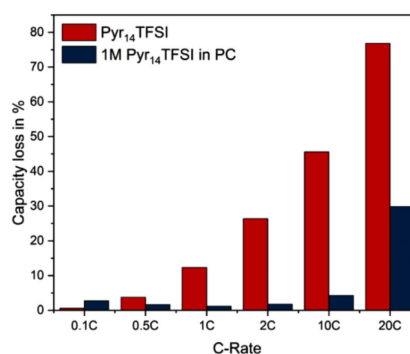


Fig. 3. Comparison of the capacity loss of PTMA-based electrodes at different C-rates (rest time of 1 h) in Pyr₁₄TFSI and 1 M Pyr₁₄TFSI in PC.

conditions the electrodes are able to retain more than 90% of their initial charge and, as visible in the inset of the figure, a minor decrease is observed only at long rest time (10 h and 1 days). Taking these results into account, it is evident that the transport prop-

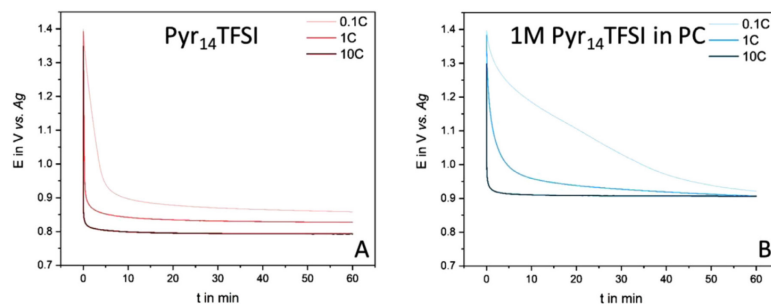


Fig. 4. Self-discharge (over 1 h) of PTMA-based electrodes charged at 0.1C, 1C and 10C in Pyr₁₄TFSI (A) and 1 M Pyr₁₄TFSI (B).

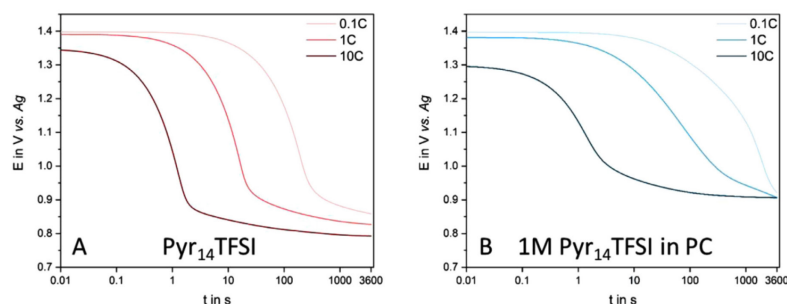


Fig. 5. Variation of the electrode potential vs. logarithm of time of PTMA-based electrodes charged at 0.1C, 1C and 10C in Pyr₁₄TFSI (A) and 1 M Pyr₁₄TFSI (B).

erties of 1 M Pyr₁₄TFSI in PC appears suitable for all investigated charging conditions. To clarify whether high charging C-rate can affect the self-discharge of the electrodes in this electrolyte, also experiments at 20C have been carried out (see Fig. S4 in supplementary information and Fig. 3). When this high C-rate is applied, the capacity retention of the electrodes decreases significantly. At a rest time of 10 min, the electrodes are able to retain only 70% of their initial capacity. When the rest time is increased to 1 day, the electrodes are not able to deliver any significant capacity.

The results discussed above are clearly indicating that the transport properties of the investigated electrolytes are significantly affecting the self-discharge of PTMA-based electrodes. For every electrolyte, there seems to be a threshold of current density, i.e., C-rate, above which a proper charge process for the electrodes cannot take place. When C-rates above this threshold are used, the electrode self-discharge increases considerably. This effect can be well visualized by comparing the capacity loss (instead of the retention) of the PTMA-electrodes at the selected rest time of 1 h and corresponding C-rates up to 20C (Fig. 3). Obviously, the better the transport properties the higher is the “limit C-rate” which can be safely applied without increasing the self-discharge. Nevertheless, it is important to remark here that also other properties of the electrolyte, e.g., dielectric constant, are affecting the electrode self-discharge as shown for LIB electrolytes (see introduction).

Fig. 4 compares the potential decay over time (self-discharge) displayed by the PTMA-based electrodes charged at 0.1, 1 and 10C in Pyr₁₄TFSI (Fig. 4A) and in 1 M Pyr₁₄TFSI in PC (Fig. 4B). A rest time of 1 h was chosen as representative time for the comparison of the behavior of the electrodes in the two electrolytes. As shown, when Pyr₁₄TFSI was used (Fig. 4A), a strong potential drop

was measured within the first 5 min of rest time. The higher the applied C-rate, the higher was this drop. When 1 M Pyr₁₄TFSI in PC was used, a different behavior was observed (Fig. 4B). In this case, the electrode charged at 0.1C displays only a small drop to 1.3 V vs. Ag. Afterwards, an almost linear decrease in potential to ca. 0.9 V vs. Ag for the time of the measure was observed. With higher C-rates, a much bigger ohmic drop occurs within the first 10 min of the measurement. However, also in these cases a potential of 0.9 V vs. Ag was reached after 60 min.

In Fig. 5A and B the potential decays discussed above are plotted versus the time in logarithmic scale. As visible, in these graphs it is possible to distinguish 2 regions: An initial plateau followed by an (almost) linear potential drop. The simultaneous presence of a plateau and a potential drop indicates that the self-discharge process occurring in the electrodes is a combination of activation controlled faradaic reactions (plateau) and resistance-limited charge redistribution (linear drop) [42]. The initial plateau could be originated by the occurrence of faradic reactions on the surface of the PTMA electrodes, caused by the rearrangement of improperly inserted anions in the organic redox material, which leads to discharged active species on the surface of the electrodes. Interestingly, the duration of these reactions heavily depends on the applied current density for Pyr₁₄TFSI (Fig. 5A) as well as 1 M Pyr₁₄TFSI in PC (Fig. 5B). At 10C, 1C and 0.1C this process takes place in 0.1 s, 1 s and 10 s, respectively, indicating an indirect correlation of charge current and duration of the initial faradic self-discharge reactions. In the second region, a resistance-limited charge redistribution between the surface and the bulk material of the electrodes takes place. This process is displayed by a rapid linear drop of the potential in the second part of the graphs, which

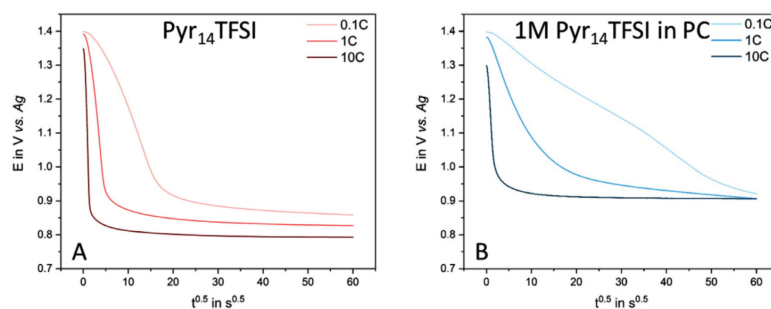


Fig. 6. Variation of the electrode potential vs. square root of time of PTMA-based electrodes charged at 0.1, 1 and 10C in Pyr₁₄TFSI (A) and 1 M Pyr₁₄TFSI in PC (B).

is more pronounced in Pyr₁₄TFSI than in 1 M Pyr₁₄TFSI in PC. In this latter, no linearity is observed for the potential drop at 0.1C, which suggest that no charge redistribution limitation is present in this system. The second part of the discharge curves can be investigated more in detail by plotting the potential decay versus the square root of the time (Fig. 6A and B). As shown, the potential profiles of the electrodes cycled in neat Pyr₁₄TFSI are characterized by a strong initial drop, followed by a plateau at low potential. As visible, the higher the C-rate applied for the charge, the lower is the potential at which the plateau is located. The absence of a linear part within the curves is indicating once more that in these electrodes the charge redistribution is the main driving force for the self-discharge. The behavior of the electrodes cycled in 1 M Pyr₁₄TFSI in PC was different. As shown, when the electrodes were charged at 1C and 10C the charge redistribution was the main driving force of the self-discharge also in the case of this electrolyte. When the electrodes were charged at 0.1C, however, the self-discharge of PTMA was mostly limited by a diffusion controlled process, as here the electrodes have been charged properly [42]. This different behavior could be originated by redox shuttles of organic active species dissolved in the organic electrolyte due to similar polarities.

4. Conclusions

In this work we reported a systematic study about the influence of the charging current density and the rest time on the self-discharge of PTMA based electrodes in two model electrolytes (Pyr₁₄TFSI and 1 M Pyr₁₄TFSI in PC).

We showed that for each electrolyte is possible to identify a threshold of current density (and thus C-rate) which can be safely applied without increasing the electrode self-discharge. This threshold is determined by the transport properties of the electrolyte, and the better the transport properties the higher is the current threshold. Furthermore, we showed that the self-discharge of the PTMA-based electrodes is originated by a combination of activation controlled faradic processes with subsequent charge redistribution and diffusion limited processes. The use of current densities above the threshold is causing an improper charging process, which leads to faradic reactions on the surface of the electrodes. This is followed by the redistribution of charge in the electrodes and causes a fast energy loss when current is no longer applied. When current densities below the threshold are used, the diffusion of redox shuttles becomes the driving force of self-discharge taking place in PTMA based electrodes.

The results of this work are indicating that a careful selection of the electrolyte, as well as of the current density applied for the

charging process, can reduce the self-discharge of PTMA electrodes significantly. In the future it will be necessary to better understand the electrolyte-electrode interplay and to verify if, through a proper electrode design, it is possible to increase the threshold of the current density usable for an electrolyte.

Credit author statement

Patrick Gerlach carried out all the experimental work reported in the manuscript and wrote the article draft.

Andrea Balducci wrote/finalized the article and supervised the work of Patrick Gerlach.

Declaration of Competing Interest

The authors declare that they have no known competing financial interests or personal relationships that could have appeared to influence the work reported in this paper.

The authors declare the following financial interests/personal relationships which may be considered as potential competing interests.

Acknowledgments

The authors wish to thank the Deutsche Forschungsgemeinschaft (DFG) within the project "Redox-active ionic liquids in redox-flow-batteries" (BA4956/10-1) for the financial support. The authors would like to thank you R. Burgos, A. Lex-Balducci and U.S. Schubert for supplying the PTMA electrodes.

Supplementary materials

Supplementary material associated with this article can be found, in the online version, at doi:10.1016/j.electacta.2021.138070.

References

- [1] C. Friebe, U.S. Schubert, High-Power-Density Organic Radical Batteries, *Top. Curr. Chem.* 375 (2017) 19.
- [2] T. Janoschka, M.D. Hager, U.S. Schubert, Radical polymers for battery applications, *Adv. Mater.* 24 (2012) 6397–6409.
- [3] S. Muench, A. Wild, C. Friebe, B. Hapler, T. Janoschka, U.S. Schubert, Polymer-Based Organic Batteries, *Chem. Rev.* 116 (2016) 9438–9484.
- [4] K. Nakahara, K. Oyaizu, H. Nishide, Organic Radical Battery Approaching Practical Use, *Chem. Lett.* 40 (2011) 222–227.
- [5] K. Oyaizu, H. Nishide, A Radical Departure from Conjugated Polymers? *Adv. Mater.* 21 (2009) 2339–2344.
- [6] M.E. Speer, M. Kolek, J.J. Jassoy, J. Heine, M. Winter, P.M. Bieler, B. Esser, Thi-anthrene-functionalized polynorbornenes as high-voltage materials for organic cathode-based dual-ion batteries, *Chem. Commun.* 51 (2015) 15261–15264.

- [7] T. Suga, H. Ohshiro, S. Sugita, K. Oyaizu, H. Nishide, Emerging N-Type Redox-Active Radical Polymer for a Totally Organic Polymer-Based Rechargeable Battery, *Adv. Mater.* 21 (2009) 1627–1630.
- [8] K. Nakahara, S. Iwasa, M. Satoh, Y. Morioka, J. Iriyama, M. Suguro, E. Hasegawa, Rechargeable batteries with organic radical cathodes, *Chem. Phys. Lett.* 359 (2002) 351–354.
- [9] S. Lee, G. Kwon, K. Ku, K. Yoon, S.K. Jung, H.D. Lim, K. Kang, Recent Progress in Organic Electrodes for Li and Na Rechargeable Batteries, *Adv. Mater.* 30 (2018) 1704682.
- [10] P. Gerlach, A. Balducci, A Critical Analysis about the Underestimated Role of the Electrolyte in Batteries Based on Organic Materials, *ChemElectroChem* 7 (2020) 1–13.
- [11] J.K. Kim, J.H. Ahn, G. Cheruvally, G.S. Chauhan, J.W. Choi, D.S. Kim, H.J. Ahn, S.H. Lee, C.E. Song, Electrochemical properties of rechargeable organic radical battery with PTMA cathode, *Met. Mater. Int.* 15 (2009) 77–82.
- [12] J.K. Kim, G. Cheruvally, J.H. Ahn, Y.G. Seo, D.S. Choi, S.H. Lee, C.E. Song, Organic radical battery with PTMA cathode: Effect of PTMA content on electrochemical properties, *J. Ind. Eng. Chem.* 14 (2008) 371–376.
- [13] J.K. Kim, G. Cheruvally, J.W. Choi, J.H. Ahn, S.H. Lee, D.S. Choi, C.E. Song, Effect of radical polymer cathode thickness on the electrochemical performance of organic radical battery, *Solid State Ion.* 178 (2007) 1546–1551.
- [14] K. Nakahara, J. Iriyama, S. Iwasa, M. Suguro, M. Satoh, E.J. Cairns, Al-laminated film packaged organic radical battery for high-power applications, *J. Power Sources* 163 (2007) 1110–1113.
- [15] K. Nakahara, J. Iriyama, S. Iwasa, M. Suguro, M. Satoh, E.J. Cairns, Cell properties for modified PTMA cathodes of organic radical batteries, *J. Power Sources* 165 (2007) 398–402.
- [16] K. Nakahara, J. Iriyama, S. Iwasa, M. Suguro, M. Satoh, E.J. Cairns, High-rate capable organic radical cathodes for lithium rechargeable batteries, *J. Power Sources* 165 (2007) 870–873.
- [17] H. Nishide, S. Iwasa, Y.J. Pu, T. Suga, K. Nakahara, M. Satoh, Organic radical battery: Nitroxide polymers as a cathode-active material, *Electrochim. Acta* 50 (2004) 827–831.
- [18] Y. Liang, Z. Tao, J. Chen, Organic Electrode Materials for Rechargeable Lithium Batteries, *Adv. Energy Mater.* 2 (2012) 742–769.
- [19] T. Suga, H. Konishi, H. Nishide, Photocrosslinked nitroxide polymer cathode-active materials for application in an organic-based paper battery, *Chem. Commun.* (2007) 1730–1732.
- [20] G. Hauffman, A. Vlad, T. Janoschka, U.S. Schubert, J.F. Gohy, Nanostructured organic radical cathodes from self-assembled nitroxide-containing block copolymer thin films, *J. Mater. Chem. A* 3 (2015) 19575–19581.
- [21] Brian E. Conway, Diagnostic analyses for mechanisms of self-discharge of electrochemical capacitors and batteries, *J. Power Sources* 65 (1997) 53–59.
- [22] J. Black, H.A. Andreas, Effects of charge redistribution on self-discharge of electrochemical capacitors, *Electrochim. Acta* 54 (2009) 3568–3574.
- [23] R. Yazami, Y. Reynier, F. van, Mechanism of self-discharge in graphite–lithium anode, *Electrochim. Acta* 47 (2002) 1217–1223.
- [24] T. Utsunomiya, O. Hatozaki, N. Yoshimoto, M. Egashira, M. Morita, Self-discharge behavior and its temperature dependence of carbon electrodes in lithium-ion batteries, *J. Power Sources* 196 (2011) 8598–8603.
- [25] S.E. Sloop, J.B. Kerr, K. Kinoshita, The role of Li-ion battery electrolyte reactivity in performance decline and self-discharge, *J. Power Sources* 119–121 (2003) 330–337.
- [26] K. Ohue, T. Utsunomiya, O. Hatozaki, N. Yoshimoto, M. Egashira, M. Morita, Self-discharge behavior of polyacenic semiconductor and graphite negative electrodes for lithium-ion batteries, *J. Power Sources* 196 (2011) 3604–3610.
- [27] V. Knap, D.I. Stroe, M. Swierczynski, R. Teodorescu, E. Schaltz, Investigation of the Self-Discharge Behavior of Lithium-Sulfur Batteries, *J. Electrochem. Soc.* 163 (2016) A911–A916.
- [28] M. Ikoma, Y. Hoshina, I. Matsumoto, C. Iwakura, Self-Discharge Mechanism of Sealed-Type Nickel/Metal-Hydride Battery, *J. Electrochem. Soc.* 143 (1996) 1904–1907.
- [29] H.Y. Chiaki Iwakura, Self-Discharge Mechanism of Nickel-Hydrogen Batteries Using Metal Hydride Anodes, *J. Electrochem. Soc.* 136 (1989) 1351–1355.
- [30] P. Sun, P. Bai, Z. Chen, H. Su, J. Yang, K. Xu, Y. Xu, A Lithium-Organic Primary Battery, *Small* 16 (2020) e1906462.
- [31] H. Olsson, M. Strömme, L. Nyholm, M. Sjödin, Activation Barriers Provide Insight into the Mechanism of Self-Discharge in Polypyrrole, *J. Phys. Chem. C* 118 (2014) 29643–29649.
- [32] M. Kolek, F. Otteny, P. Schmidt, C. Mück-Lichtenfeld, C. Einholz, J. Becking, E. Schleicher, M. Winter, P. Bieker, B. Esser, Ultra-high cycling stability of poly(vinylphenothiazine) as a battery cathode material resulting from π - π interactions, *Energy Environ. Sci.* 10 (2017) 2334–2341.
- [33] S. Iwasa, T. Nishi, H. Sato, S. Nakamura, Flexibility and High-Rate Discharge Properties of Organic Radical Batteries with Gel-State Electrodes, *J. Electrochem. Soc.* 164 (2017) A884–A888.
- [34] R. Chen, D. Bresser, M. Saraf, P. Gerlach, A. Balducci, S. Kunz, D. Schröder, S. Passerini, J. Chen, A Comparative Review of Electrolytes for Organic-Material-Based Energy-Storage Devices Employing Solid Electrodes and Redox Fluids, *ChemSusChem* 13 (2020) 1–16.
- [35] P. Gerlach, R. Burges, A. Lex-Balducci, U.S. Schubert, A. Balducci, Influence of the salt concentration on the electrochemical performance of electrodes for polymeric batteries, *Electrochim. Acta* 306 (2019) 610–616.
- [36] P. Gerlach, R. Burges, A. Lex-Balducci, U.S. Schubert, A. Balducci, The influence of the electrolyte composition on the electrochemical behaviour of cathodic materials for organic radical batteries, *J. Power Sources* 405 (2018) 142–149.
- [37] P. Gerlach, R. Burges, A. Lex-Balducci, U.S. Schubert, A. Balducci, Aprotic and Protic Ionic Liquids as Electrolytes for Organic Radical Polymers, *J. Electrochem. Soc.* 167 (2020) 120546.
- [38] T. Janoschka, A. Teichler, B. Häupler, T. Jähnert, M.D. Hager, U.S. Schubert, Reactive Inkjet Printing of Cathodes for Organic Radical Batteries, *Adv. Energy Mater.* 3 (2013) 1025–1028.
- [39] C. Schütter, T. Husch, V. Viswanathan, S. Passerini, A. Balducci, M. Korth, Rational design of new electrolyte materials for electrochemical double layer capacitors, *J. Power Sources* 326 (2016) 541–548.
- [40] R.S. Kühnel, A. Balducci, Comparison of the anodic behavior of aluminum current collectors in imide-based ionic liquids and consequences on the stability of high voltage supercapacitors, *J. Power Sources* 249 (2014) 163–171.
- [41] S. Pohlmann, R.S. Kühnel, T.A. Centeno, A. Balducci, The Influence of Anion-Cation Combinations on the Physicochemical Properties of Advanced Electrolytes for Supercapacitors and the Capacitance of Activated Carbons, *ChemElectroChem* 1 (2014) 1301–1311.
- [42] H.A. Andreas, J.M. Black, A.A. Oickle, Self-discharge in Manganese Oxide Electrochemical Capacitor Electrodes in Aqueous Electrolytes with Comparisons to Faradaic and Charge Redistribution Models, *Electrochim. Acta* 140 (2014) 116–124.

3 Conclusion

This thesis presents a series of investigations carried out to elucidate the influence of the electrolyte composition, electrolyte concentration and nature of ionic liquid-based electrolytes on the performance PTMA-based electrodes with special attention towards the self-discharge behavior.

Publication 1 clarified the importance of the chosen electrolyte for every ROMP in EES application. Furthermore, a lack of investigations of novel electrolytes for ROMPs has been found and the need for new electrolyte systems for the optimization of organic battery performance has been highlighted. This optimization was addressed for PTMA-based electrodes by publication 2-5.

In publication 2, the impact of the nature of the solvent and salt of the electrolyte on the performance of PTMA was considered. The results of this study show that PTMA-based electrodes display good performance in organic electrolytes (especially in 1M Pyr₁₄TFSI in PC) in terms of specific capacity and rate capability. It is noteworthy here that, although 1M Pyr₁₄TFSI in PC and 1M Et₄N⁺TFSI⁻ in PC are both organic electrolytes and display comparable transport properties (1M Et₄N⁺TFSI⁻ in PC even more favorable conductivity and viscosity), a far better performance was found for PTMA electrodes in combination with 1M Pyr₁₄TFSI in PC. This indicates an impact of the chosen cation of the electrolyte on the electrochemical behavior, although for P-type materials like PTMA mostly only the insertion/release of the anions during the charge/discharge process is obvious to have an influence. Furthermore, in the context of this thesis, publication 2 presents a first beneficial impact of high concentrated electrolytes like neat Pyr₁₄TFSI on the performance in regard of self-discharge and stability.

In the matter of high concentrated electrolytes, publication 3 targeted the influence of the concentration of the electrolyte on the behavior of PTMA electrodes with the use of 1, 2 and 3M Pyr₁₄BF₄ in PC. In this study, PTMA in 2M Pyr₁₄BF₄ in PC as electrolyte shows the best performance with respect to the specific capacity and cycling stability at low currents. However, with increasing currents the limitation of the reduced ion mobility due to higher viscosity becomes visible. On the other side, this reduced mobility has a

beneficial effect on self-discharge performance of PTMA, since the lowest loss in charge was found in 3M Pyr₁₄BF₄ in PC. This behavior can be explained by the reduction of diffusion, which was found to be the driving force for the self-discharge in this system. There, redox active groups dissolved into the electrolyte are suggested for working as redox shuttles during the cell rest. The process of dissolution and diffusion is found to be reduced in highly concentrated systems. The same reduction of dissolution and diffusion is obtained at low temperature tests at 0°C at which self-discharge performance as well as cycling stability are improved.

Because of our interest in the performance of PTMA electrodes in high concentrated electrolytes, PTMA was tested in combination with four different ionic liquids (aprotic and protic) as electrolytes in publication 4. In this work, a good compromise between electrode performance and electrode stability was found for the use of aprotic ionic liquids, especially considering the results of PTMA in Pyr₁₄FSI. On the other side, the first successful use of protic ionic liquids as electrolytes for PTMA was accomplished in this study. However, these protic electrolytes were not able to compete with their AIL counterparts in terms of cell potential, capacity, self-discharge and stability, since a clear interaction of the proton of PILs with the active material and therewith accompanying parasitic reactions are evident.

At last, there was a great interest in the self-discharge behavior of PTMA in different electrolyte systems. Therefore, in publication 5 the effect of the applied current density during charging and the applied rest time in which the self-discharge can occur was investigated for PTMA-based electrodes in 1M Pyr₁₄TFSI in PC (organic electrolyte) and neat Pyr₁₄TFSI (ionic liquid). Thereby, it was found that for each electrolyte there is a threshold current, which is appropriate to use. If the system is charged with C-rates higher than this current, an unstable charged state is generated, which causes activation-controlled faradic reactions on the surface of the electrode followed by a charge redistribution process. These processes govern the self-discharge in the electrode. The threshold is highly dependent on the transport properties of the electrolyte. The faster the transport the higher the threshold. When currents well below the threshold are used, which causes a stable charged state to be reached, the self-discharge of PTMA is

again diffusion-controlled. Therefore, a thorough selection of electrolytes and charge conditions is needed in order to minimize self-discharge in PTMA-based electrodes.

In the works of this thesis, the number of electrolytes used for investigations on PTMA has been systematically increased. It has been proven that the performance of PTMA is significantly dependent on the used electrolyte, which was to be expected from the theoretical considerations of the introduction. Thus, it can be said that the optimal electrolyte for the application of PTMA depends on the application itself. Systems with a need for high specific capacity and rate capability should be used in combination with low concentrated electrolytes with high transport properties. On the other hand, for applications, which require low self-discharge and high stability performance at low rates or elevated stable potentials, highly concentrated electrolytes should be used. An all-round system needs a careful optimization of concentration and choice of ions in order to provide a trade-off of both aspects.

Furthermore, as shown in these works the electrolyte can be understood as a tool to tailor the cell performance and additionally to understand chemical and physical mechanisms and processes within the cell system.

4 Outlook

With the results of this work the knowledge about the important influence of the electrolyte on the electrochemical behavior of PTMA-based electrodes has been significantly expanded. Therein, it was possible to tune the performance of PTMA and as well study mechanisms inside the cell.

However, after this work the number of possible investigations for PTMA is still large. It has been found that high concentrated, highly viscous electrolytes have a beneficial effect on the stability and self-discharge performance. Therefore, a way to continue the work in this regard is the application of other electrolyte concepts like solid state, gel polymer or water-in-salt electrolytes. Furthermore, the electrochemical measurements presented here gave many indications about possible processes inside the cell especially during the self-discharge of PTMA. In order to fully understand these processes in-situ measurements like in-situ infrared spectroscopy or in-situ Raman spectroscopy should be carried out.

The investigations presented here for PTMA-based electrodes can be regarded as a model case study, which gives an indication about the complex interactions of ROMPs and utilized electrolytes. Since each ROMP/electrolyte combination is unique, each combination will result to different interactions inside the cell. Therefore, each test concept applied to PTMA in this thesis and more could and should be applied as well to other redox active organic molecules and polymers. This would allow the task-specific optimization of new and established organic battery materials beyond the state-of-the-art performance in the standard electrolytes.

Furthermore, the results of this work illustrate that the electrolyte can be seen as a tool to understand the mechanisms occurring inside EES devices by promoting or preventing certain processes inside a storage device. This aspect should be utilized by researchers in future studies.

Also, it must be stated here that the half-cell setup of this thesis focuses on the electrochemical behavior of one working electrode (PTMA). In the real application full-cells are

used, of course. Therefore, in the case of PTMA in combination with other active materials, especially other organics, even more optimization and research interest have to be spent on the careful selection of the right electrolyte in order to achieve best performance for the EES device.

Only with the view on the electrolyte as a third active component in the EES system a successful implementation of ROMPs for sustainable energy storage application can be achieved.

References

- [1] D. Larcher, J.-M. Tarascon, *Nat. Chem.* 7 (2015) 19–29.
- [2] O. Publishing, *World Energy Outlook 2010*, 1. Aufl., OECD, s.l., 2010.
- [3] G. Zubi, R. Dufo-López, M. Carvalho, G. Pasaoglu, *Renewable Sustainable Energy Rev.* 89 (2018) 292–308.
- [4] K. Xu, *Chem. Rev.* 104 (2004) 4303–4418.
- [5] E.A. Olivetti, G. Ceder, G.G. Gaustad, X. Fu, *Joule* 1 (2017) 229–243.
- [6] P.C.K. Vesborg, T.F. Jaramillo, *RSC Adv.* 2 (2012) 7933.
- [7] C. Wadia, P. Albertus, V. Srinivasan, *J. Power Sources* 196 (2011) 1593–1598.
- [8] R.B. Sandler, *U.S. Geological Survey* (2019).
- [9] European Commission, *European Commission Enterprise and Industry* (2010).
- [10] P.C.K. Vesborg, T.F. Jaramillo, *RSC Adv.* 2 (2012) 7933.
- [11] Y. Liang, Y. Yao, *Joule* 2 (2018) 1690–1706.
- [12] Z. Song, H. Zhou, *Energy Environ. Sci.* 6 (2013) 2280.
- [13] Y. Liang, Z. Tao, J. Chen, *Adv. Energy Mater.* 2 (2012) 742–769.
- [14] Y. Lu, Q. Zhang, L. Li, Z. Niu, J. Chen, *Chem* 4 (2018) 2786–2813.
- [15] S. Muench, A. Wild, C. Friebe, B. Häupler, T. Janoschka, U.S. Schubert, *Chem. Rev.* 116 (2016) 9438–9484.
- [16] V. Dieterich, J.D. Milshtein, J.L. Barton, T.J. Carney, R.M. Darling, F.R. Brushett, *Transl. Mater. Res.* 5 (2018) 34001.
- [17] C. Friebe, A. Lex-Balducci, U.S. Schubert, *ChemSusChem* 12 (2019) 4093–4115.
- [18] P. Poizot, J. Gaubicher, S. Renault, L. Dubois, Y. Liang, Y. Yao, *Chemical reviews* 120 (2020) 6490–6557.
- [19] Y. Liang, Y. Yan, *Gen. Chem.* 3 (2017) 207–212.
- [20] K. Nakahara, J. Iriyama, S. Iwasa, M. Suguro, M. Satoh, E.J. Cairns, *J. Power Sources* 165 (2007) 398–402.
- [21] M. Kolek, F. Otteny, J. Becking, M. Winter, B. Esser, P. Bieker, *Chem. Mater.* 30 (2018) 6307–6317.
- [22] M. Winter, R.J. Brodd, *Chem. Rev.* 104 (2004) 4245–4270.
- [23] R. Gracia, D. Mecerreyes, *Polym. Chem.* 4 (2013) 2206.
- [24] P. Novák, K. Müller, K.S.V. Santhanam, O. Haas, *Chem. Rev.* 97 (1997) 207–282.

- [25] B. Häupler, A. Wild, U.S. Schubert, *Adv. Energy Mater.* 5 (2015) 1402034.
- [26] S. Lee, J. Hong, K. Kang, *Adv. Energy Mater.* 10 (2020) 2001445.
- [27] S. Komaba, C. Takei, T. Nakayama, A. Ogata, N. Yabuuchi, *Electrochem. Commun.* 12 (2010) 355–358.
- [28] P.K. Nayak, L. Yang, W. Brehm, P. Adelhelm, *Angew. Chem. Int. Ed.* 57 (2018) 102–120.
- [29] D.L. Williams, J.J. Byrne, J.S. Driscoll, *J. Electrochem. Soc.* 116 (1969) 2.
- [30] H. Shirakawa, E. J. Louis, A. G. MacDiarmid, C. K. Chiang, A. J. Heeger, *J., Chem. Soc. Chem. Commun.* (1977) 578–580.
- [31] C.K. Chiang *J. Electrochem. Soc.* 128 (1981) 1454–1456.
- [32] Paul J. Nigrey, David MacInnes, Jr., David P. Nairns, Alan G. MacDiarmid and Alan J. Heeger, *J. Electrochem. Soc.* 128 (1981) 1651–1654.
- [33] B. Broich, J. Hocker, *Berichte der Bunsengesellschaft für physikalische Chemie* 88 (1984) 497–503.
- [34] T. Nagatomo, C. Ichikawa, O. Omoto, *J. Electrochem. Soc.* 134 (1987) 305–308.
- [35] D. Aradilla, F. Estrany, F. Casellas, J.I. Iribarren, C. Alemán, *Organic Electronics* 15 (2014) 40–46.
- [36] A.C. Baptista, I. Ropio, B. Romba, J.P. Nobre, C. Henriques, J.C. Silva, J.I. Martins, J.P. Borges, I. Ferreira, *J. Mater. Chem. A* 6 (2018) 256–265.
- [37] Y. Chen, J. Lüder, M.-F. Ng, M. Sullivan, S. Manzhos, *Physical chemistry chemical physics PCCP* 20 (2017) 232–237.
- [38] Y. Chen, S. Manzhos, *Journal of Power Sources* 336 (2016) 126–131.
- [39] M. Zhou, Y. Xiong, Y. Cao, X. Ai, H. Yang, *J. Polym. Sci. B Polym. Phys.* 51 (2013) 114–118.
- [40] J. Tang, Z.-P. Song, N. Shan, L.-Z. Zhan, J.-Y. Zhang, H. Zhan, Y.-H. Zhou, C.-M. Zhan, *J. Power Sources* 185 (2008) 1434–1438.
- [41] Yasuo Kudoh, Kenji Akami, Yasue Matsuya, *Synth. Met.* (1999) 973–974.
- [42] L. Zhan, Z. Song, J. Zhang, J. Tang, H. Zhan, Y. Zhou, C. Zhan, *Electrochim. Acta* 53 (2008) 8319–8323.
- [43] A.J. Heeger, *Polym J* 17 (1985) 201–208.
- [44] A. Moliton, R.C. Hiorns, *Polym. Int.* 53 (2004) 1397–1412.
- [45] J.F. Mike, J.L. Lutkenhaus, *J. Polym. Sci. B Polym. Phys.* 51 (2013) 468–480.

- [46] M. Mueller, M. Fabretto, D. Evans, P. Hojati-Talemi, C. Gruber, P. Murphy, *Polymer* 53 (2012) 2146–2151.
- [47] G.A. Snook, P. Kao, A.S. Best, *Journal of Power Sources* 196 (2011) 1–12.
- [48] T. Janoschka, M.D. Hager, U.S. Schubert, *Adv. Mater.* 24 (2012) 6397–6409.
- [49] K. Shinozaki, Y. Tomizuka, A. Nojiri, *Jpn. J. Appl. Phys.* 23 (1984) L892-L894.
- [50] B. Krische, M. Zagorska, *Synthetic Metals* 28 (1989) 257–262.
- [51] D.M. de Leeuw, M. Simenon, A.R. Brown, R. Einerhand, *Synthetic Metals* 87 (1997) 53–59.
- [52] M.D. Levi, D. Aurbach, *Journal of Power Sources* 180 (2008) 902–908.
- [53] L.W. Shacklette, J.E. Toth, N.S. Murthy, R.H. Baughman, *J. Electrochem. Soc.* 132 (1985) 1529–1535.
- [54] P.J. Nigrey, D. MacInnes, D.P. Nairns, A.G. MacDiarmid, A.J. Heeger, *J. Electrochem. Soc.* 128 (1981) 1651–1654.
- [55] H. Alt, H. Binder, A. Köhling and G. Sanstede (1971).
- [56] K. Oyaizu, A. Hatemata, W. Choi, H. Nishide, *J. Mater. Chem.* 20 (2010) 5404.
- [57] A. Vizintin, J. Bitenc, A. Kopač Lautar, K. Pirnat, J. Grdadolnik, J. Stare, A. Randon-Vitanova, R. Dominko, *Nat. Commun.* 9 (2018) 661.
- [58] M. Miroshnikov, K.P. Divya, G. Babu, A. Meiyazhagan, L.M. Reddy Arava, P.M. Ajayan, G. John, *J. Mater. Chem. A* 4 (2016) 12370–12386.
- [59] T. Nokami, T. Matsuo, Y. Inatomi, N. Hojo, T. Tsukagoshi, H. Yoshizawa, A. Shimizu, H. Kuramoto, K. Komae, H. Tsuyama, J. Yoshida, *J. Am. Chem. Soc.* 134 (2012) 19694–19700.
- [60] W. Wei, L. Li, L. Zhang, J. Hong, G. He, *Mater. Lett.* 213 (2018) 126–130.
- [61] Y. Wu, R. Zeng, J. Nan, D. Shu, Y. Qiu, S.-L. Chou, *Adv. Energy Mater.* 7 (2017) 1700278.
- [62] M. Yao, H. Senoh, S. Yamazaki, Z. Siroma, T. Sakai, K. Yasuda, *J. Power Sources* 195 (2010) 8336–8340.
- [63] Y. Liang, P. Zhang, S. Yang, Z. Tao, J. Chen, *Adv. Energy Mater.* 3 (2013) 600–605.
- [64] W. Deng, X. Liang, X. Wu, J. Qian, Y. Cao, X. Ai, J. Feng, H. Yang, *Scientific reports* 3 (2013) 2671.

- [65] H. Kim, J.E. Kwon, B. Lee, J. Hong, M. Lee, S.Y. Park, K. Kang, *Chem. Mater.* 27 (2015) 7258–7264.
- [66] J. Bitenc, N. Lindahl, A. Vizintin, M.E. Abdelhamid, R. Dominko, P. Johansson, *Energy Storage Mater.* 24 (2020) 379–383.
- [67] Q. Zhao, Y. Lu, J. Chen, *Adv. Energy Mater.* 7 (2017) 1601792.
- [68] S. Lee, G. Kwon, K. Ku, K. Yoon, S.-K. Jung, H.-D. Lim, K. Kang, *Advanced materials (Deerfield Beach, Fla.)* 30 (2018) e1704682.
- [69] H. Chen, M. Armand, M. Courty, M. Jiang, C.P. Grey, F. Dolhem, J.-M. Tarascon, P. Poizot, *J. Am. Chem. Soc.* 131 (2009) 8984–8988.
- [70] M. Armand, S. Grugeon, H. Vezin, S. Laruelle, P. Ribière, P. Poizot, J.-M. Tarascon, *Nature materials* 8 (2009) 120–125.
- [71] S. Wang, L. Wang, K. Zhang, Z. Zhu, Z. Tao, J. Chen, *Nano letters* 13 (2013) 4404–4409.
- [72] H. Chen, M. Armand, G. Demailly, F. Dolhem, P. Poizot, J.-M. Tarascon, *ChemSusChem* 1 (2008) 348–355.
- [73] S. Renault, J. Geng, F. Dolhem, P. Poizot, *Chemical communications (Cambridge, England)* 47 (2011) 2414–2416.
- [74] D.W. Leedy, D.L. Muck, *J. Am. Chem. Soc.* 93 (1971) 4264–4270.
- [75] Z. Song, H. Zhan, Y. Zhou, *Angewandte Chemie (International ed. in English)* 49 (2010) 8444–8448.
- [76] X. Han, C. Chang, L. Yuan, T. Sun, J. Sun, *Adv. Mater.* 19 (2007) 1616–1621.
- [77] Steven J. Visco and Lutgard C. DeJonghe, *J. Electrochem. Soc.* 135 (1988) 2905–2909.
- [78] S.J. Visco, C.C. Mailhe, L.C. de Jonghe, M.B. Armand, *J. Electrochem. Soc.* 136 (1989) 661–664.
- [79] M. Liu, S.J. Visco, L.C. de Jonghe, *J. Electrochem. Soc.* 136 (1989) 2570–2575.
- [80] S. J. Visco, M. Liu, and L. C. De Jonghe, *J. Electrochem. Soc.* 137 (1990).
- [81] Y. NuLi, Z. Guo, H. Liu, J. Yang, *Electrochemistry Communications* 9 (2007) 1913–1917.
- [82] N. Oyama, T. Tatsuma, T. Sato, T. Sotomura, *Nature* 374 (1995) 196.
- [83] S.-R. Deng, L.-B. Kong, G.-Q. Hu, T. Wu, D. Li, Y.-H. Zhou, Z.-Y. Li, *Electrochimica Acta* 51 (2006) 2589–2593.

- [84] K. Naoi, K. Kawase, Y. Inoue, J. Electrochem. Soc. 144 (1997) L170-L172.
- [85] M. Wu, Y. Cui, A. Bhargava, Y. Losovyj, A. Siegel, M. Agarwal, Y. Ma, Y. Fu, Angew. Chem. 128 (2016) 10181–10185.
- [86] J.Y. Zhang, L.B. Kong, L.Z. Zhan, J. Tang, H. Zhan, Y.H. Zhou, C.M. Zhan, J. Power Sources 168 (2007) 278–281.
- [87] M.E. Speer, M. Kolek, J.J. Jassoy, J. Heine, M. Winter, P.M. Bieker, B. Esser, Chem. Commun. 51 (2015) 15261–15264.
- [88] M. Kolek, F. Otteny, P. Schmidt, C. Mück-Lichtenfeld, C. Einholz, J. Becking, E. Schleicher, M. Winter, P. Bieker, B. Esser, Energy Environ. Sci. 10 (2017) 2334–2341.
- [89] F. Otteny, M. Kolek, J. Becking, M. Winter, P. Bieker, B. Esser, Adv. Energy Mater. 8 (2018) 1802151.
- [90] V. Perner, D. Diddens, F. Otteny, V. Küpers, P. Bieker, B. Esser, M. Winter, M. Kolek, ACS applied materials & interfaces 13 (2021) 12442–12453.
- [91] K. Nakahara, K. Oyaizu, H. Nishide, Chem. Lett. 40 (2011) 222–227.
- [92] C. Friebe, U.S. Schubert, Top. Curr. Chem. 375 (2017) 19.
- [93] K. Oyaizu, H. Nishide, Adv. Mater. 21 (2009) 2339–2344.
- [94] T. Suga, Y.-J. Pu, K. Oyaizu, H. Nishide, BCSJ 77 (2004) 2203–2204.
- [95] K. Nakahara, S. Iwasa, M. Satoh, Y. Morioka, J. Iriyama, M. Suguro, E. Hasegawa, Chem. Phys. Lett. 359 (2002) 351–354.
- [96] H. Nishide, S. Iwasa, Y.-J. Pu, T. Suga, K. Nakahara, M. Satoh, Electrochim. Acta 50 (2004) 827–831.
- [97] J.-K. Kim, G. Cheruvally, J.-W. Choi, J.-H. Ahn, S.H. Lee, D.S. Choi, C.E. Song, Solid State Ionics 178 (2007) 1546–1551.
- [98] K. Nakahara, J. Iriyama, S. Iwasa, M. Suguro, M. Satoh, E.J. Cairns, J. Power Sources 163 (2007) 1110–1113.
- [99] K. Nakahara, J. Iriyama, S. Iwasa, M. Suguro, M. Satoh, E.J. Cairns, J. Power Sources 165 (2007) 870–873.
- [100] J.-K. Kim, G. Cheruvally, J.-H. Ahn, Y.-G. Seo, D.S. Choi, S.-H. Lee, C.E. Song, Journal of Industrial and Engineering Chemistry 14 (2008) 371–376.
- [101] J.-K. Kim, J.-H. Ahn, G. Cheruvally, G.S. Chauhan, J.-W. Choi, D.-S. Kim, H.-J. Ahn, S.H. Lee, C.E. Song, Met. Mater. Int. 15 (2009) 77–82.

- [102] Y.-H. Wang, M.-K. Hung, C.-H. Lin, H.-C. Lin, J.-T. Lee, *Chemical communications* (Cambridge, England) 47 (2011) 1249–1251.
- [103] G. Hauffman, A. Vlad, T. Janoschka, U.S. Schubert, J.-F. Gohy, *J. Mater. Chem. A* 3 (2015) 19575–19581.
- [104] S. Muench, P. Gerlach, R. Burges, M. Strumpf, S. Hoepfner, A. Wild, A. Lex-Balducci, A. Balducci, J.C. Brendel, U.S. Schubert, *ChemSusChem* 14 (2021) 449–455.
- [105] T. Suga, H. Konishi, H. Nishide, *Chemical communications* (Cambridge, England) (2007) 1730–1732.
- [106] J.-K. Kim, Y. Kim, S. Park, H. Ko, Y. Kim, *Energy Environ. Sci.* 9 (2016) 1264–1269.
- [107] J.-K. Kim, J. Scheers, J.-H. Ahn, P. Johansson, A. Matic, P. Jacobsson, *J. Mater. Chem. A* 1 (2013) 2426–2430.
- [108] K. Oyaizu, T. Kawamoto, T. Suga, H. Nishide, *Macromolecules* 43 (2010) 10382–10389.
- [109] T. Ibe, R.B. Frings, A. Lachowicz, S. Kyo, H. Nishide, *Chemical communications* (Cambridge, England) 46 (2010) 3475–3477.
- [110] K. Nakahara, S. Iwasa, J. Iriyama, Y. Morioka, M. Suguro, M. Satoh, E.J. Cairns, *Electrochim. Acta* 52 (2006) 921–927.
- [111] M. Suguro, S. Iwasa, Y. Kusachi, Y. Morioka, K. Nakahara, *Macromol. Rapid Commun.* 28 (2007) 1929–1933.
- [112] T. Suga, H. Ohshiro, S. Sugita, K. Oyaizu, H. Nishide, *Adv. Mater.* 21 (2009) 1627–1630.
- [113] T. Jähnert, M.D. Hager, U.S. Schubert, *J. Mater. Chem. A* 2 (2014) 15234.
- [114] T. Jähnert, B. Häupler, T. Janoschka, M.D. Hager, U.S. Schubert, *Macromolecular rapid communications* 35 (2014) 882–887.
- [115] T. Suga, S. Sugita, H. Ohshiro, K. Oyaizu, H. Nishide, *Advanced materials* (Deerfield Beach, Fla.) 23 (2011) 751–754.
- [116] V. Aravindan, J. Gnanaraj, S. Madhavi, H.-K. Liu, *Chem. Eur. J.* 17 (2011) 14326–14346.
- [117] R. Chen, D. Bresser, M. Saraf, P. Gerlach, A. Balducci, S. Kunz, D. Schröder, S. Passerini, J. Chen, *ChemSusChem* (2020).
- [118] K. Xu, *Chemical reviews* 114 (2014) 11503–11618.

- [119] G. Zubi, R. Dufo-López, M. Carvalho, G. Pasaoglu, *Renewable and Sustainable Energy Reviews* 89 (2018) 292–308.
- [120] M. Dahbi, F. Ghamouss, F. Tran-Van, D. Lemordant, M. Anouti, *Journal of Power Sources* 196 (2011) 9743–9750.
- [121] N. Casado, D. Mantione, D. Shanmukaraj, D. Mecerreyes, *ChemSusChem* 13 (2020) 2464–2470.
- [122] B.A. Kahsay, A. Ramar, F.-M. Wang, N.-H. Yeh, P.-L. Lin, Z.-J. Luo, T.-S. Chan, C.-H. Su, *Journal of Power Sources* 428 (2019) 115–123.
- [123] A. Wild, M. Strumpf, B. Häupler, M.D. Hager, U.S. Schubert, *Adv. Energy Mater.* 7 (2017) 1601415.
- [124] B. Tian, G.-H. Ning, W. Tang, C. Peng, D. Yu, Z. Chen, Y. Xiao, C. Su, K.P. Loh, *Material. Horiz.* 3 (2016) 429–433.
- [125] N. Wang, X. Dong, B. Wang, Z. Guo, Z. Wang, R. Wang, X. Qiu, Y. Wang, *Angewandte Chemie (International ed. in English)* 59 (2020) 14577–14583.
- [126] Q. Zhao, C. Guo, Y. Lu, L. Liu, J. Liang, J. Chen, *Ind. Eng. Chem. Res.* 55 (2016) 5795–5804.
- [127] S. Phadke, M. Cao, M. Anouti, *ChemSusChem* 11 (2018) 965–974.
- [128] Y. Liang, P. Zhang, J. Chen, *Chem. Sci.* 4 (2013) 1330.
- [129] J.-E. Lim, J.-K. Kim, *Korean J. Chem. Eng.* 35 (2018) 2464–2467.
- [130] T. Yokoji, Y. Kameyama, S. Sakaida, N. Maruyama, M. Satoh, H. Matsubara, *Chem. Lett.* 44 (2015) 1726–1728.
- [131] L. Fan, R. Ma, J. Wang, H. Yang, B. Lu, *Advanced materials (Deerfield Beach, Fla.)* 30 (2018) e1805486.
- [132] C. Guo, K. Zhang, Q. Zhao, L. Pei, J. Chen, *Chem. Commun.* 51 (2015) 10244–10247.
- [133] Y. Huang, C. Fang, W. Zhang, Q. Liu, Y. Huang, *Chemical communications (Cambridge, England)* 55 (2019) 608–611.
- [134] Z. Xu, H. Ye, H. Li, Y. Xu, C. Wang, J. Yin, H. Zhu, *ACS omega* 2 (2017) 1273–1278.
- [135] X. Dong, Z. Guo, Z. Guo, Y. Wang, Y. Xia, *Joule* 2 (2018) 902–913.
- [136] J. Qin, Q. Lan, N. Liu, Y. Zhao, Z. Song, H. Zhan, *Energy Storage Mater.* 26 (2020) 585–592.

- [137] X. Dong, H. Yu, Y. Ma, J.L. Bao, D.G. Truhlar, Y. Wang, Y. Xia, *Chem. Eur. J.* 23 (2017) 2560–2565.
- [138] Liumin Suo, Oleg Borodin, Tao Gao, Marco Olguin, Janet Ho, Xiulin Fan, Chao Luo, Chunsheng Wang, Kang Xu, *Science* 350 (2015) 938–943.
- [139] Y. Liang, Y. Jing, S. Gheytani, K.-Y. Lee, P. Liu, A. Facchetti, Y. Yao, *Nat. Mater.* 16 (2017) 841–848.
- [140] A.P. Abbott, R.C. Harris, K.S. Ryder, *The journal of physical chemistry. B* 111 (2007) 4910–4913.
- [141] D.R. MacFarlane, K.R. Seddon, *Aust. J. Chem.* 60 (2007) 3.
- [142] Y.-Y. Cheng, C.-C. Li, J.-T. Lee, *Electrochimica Acta* 66 (2012) 332–339.
- [143] Jian Qin, Qing Lan, Ning Liu, Fang Men, Xin Wang, Zhiping Song, Hui Zhan, *iScience* 15 (2019) 16–27.
- [144] J.-K. Kim, A. Matic, J.-H. Ahn, P. Jacobsson, *RSC Adv.* 2 (2012) 9795.
- [145] X. Wang, Z. Shang, A. Yang, Q. Zhang, F. Cheng, D. Jia, J. Chen, *Chem* 5 (2019) 364–375.
- [146] L. Wylie, Z.L. Seeger, A.N. Hancock, E.I. Izgorodina, *Phys. Chem. Chem. Phys.* 21 (2019) 2882–2888.
- [147] A. Manthiram, X. Yu, S. Wang, *Nat. Rev. Mater.* 2 (2017) 294.
- [148] M. Lécuyer, J. Gaubicher, A.-L. Barrès, F. Dolhem, M. Deschamps, D. Guyomard, P. Poizot, *Electrochem. Commun.* 55 (2015) 22–25.
- [149] W. Li, L. Chen, Y. Sun, C. Wang, Y. Wang, Y. Xia, *Solid State Ionics* 300 (2017) 114–119.
- [150] W. Wei, L. Li, L. Zhang, J. Hong, G. He, *Electrochem. Commun.* 90 (2018) 21–25.
- [151] X. Zhu, R. Zhao, W. Deng, X. Ai, H. Yang, Y. Cao, *Electrochim. Acta* 178 (2015) 55–59.
- [152] W. Huang, Z. Zhu, L. Wang, S. Wang, H. Li, Z. Tao, J. Shi, L. Guan, J. Chen, *Angew. Chem. Int. Ed.* 52 (2013) 9162–9166.
- [153] J.-K. Kim, A. Matic, J.-H. Ahn, P. Jacobsson, *RSC Adv.* 2 (2012) 9795.
- [154] Y. Hanyu, I. Honma, *Scientific reports* 2 (2012) 453.
- [155] J.-K. Kim, G. Cheruvally, J.-W. Choi, J.-H. Ahn, D.S. Choi, C.E. Song, *J. Electrochem. Soc.* 154 (2007) A839.

- [156] S. Pohlmann, C. Ramirez-Castro, A. Balducci, *J. Electrochem. Soc.* 162 (2015) A5020-A5030.
- [157] S. Pohlmann, R.-S. Kühnel, T.A. Centeno, A. Balducci, *CHEMELECTROCHEM* 1 (2014) 1301–1311.
- [158] C. Schütter, T. Husch, V. Viswanathan, S. Passerini, A. Balducci, M. Korth, *Journal of Power Sources* 326 (2016) 541–548.
- [159] R.-S. Kühnel, A. Balducci, *Journal of Power Sources* 249 (2014) 163–171.
- [160] G. Leftheriotis, S. Papaefthimiou P. Yianoulis, *Solid State Ionics* 178 (2007) 259–263.
- [161] V. Augustyn, J. Come, M.A. Lowe, J.W. Kim, P.-L. Taberna, S.H. Tolbert, H.D. Abruña, P. Simon, B. Dunn, *Nature materials* 12 (2013) 518–522.
- [162] H.A. Andreas, *J. Electrochem. Soc.* 162 (2015) A5047-A5053.
- [163] H.A. Andreas, J.M. Black, A.A. Oickle, *Electrochim. Acta* 140 (2014) 116–124.
- [164] B. Babu, A. Balducci, *Journal of Power Sources Advances* 5 (2020) 100026.
- [165] J. Black, H.A. Andreas, *J. Power Sources* 195 (2010) 929–935.
- [166] J. Black, H.A. Andreas, *Electrochim. Acta* 54 (2009) 3568–3574.
- [167] Brian E. Conway, *J. Power Sources* 65 (1997) 53–59.
- [168] J. Niu, B.E. Conway, W.G. Pell, *J. Power Sources* 135 (2004) 332–343.
- [169] A.M. Oickle, H.A. Andreas, *J. Phys. Chem. C* 115 (2011) 4283–4288.
- [170] A. Balducci, *Topics in current chemistry (Cham)* 375 (2017) 20.
- [171] S. Menne, T. Vogl, A. Balducci, *Chemical communications (Cambridge, England)* 51 (2015) 3656–3659.

Appendix

Utilized cell setup of this work

The measurements of this work have been done in a Swagelok-type three-electrode setup where the working electrode was the PTMA composite (60 % active material PTMA, 35 % carbon black conductive additive and 5 % PVdF binder), the counter electrode was an oversized carbon electrode (85 % activated carbon, 10 % carbon black and 5 % binder PTFE), and a silver wire was used as a quasi-reference (Standard potential of Ag vs. Li⁺/Li at approximately 3V). Glass fiber was used as separator, which was drenched with 150 μ l of electrolyte. This cell design is also referred to as half-cell setup and is illustrated in Figure A1.

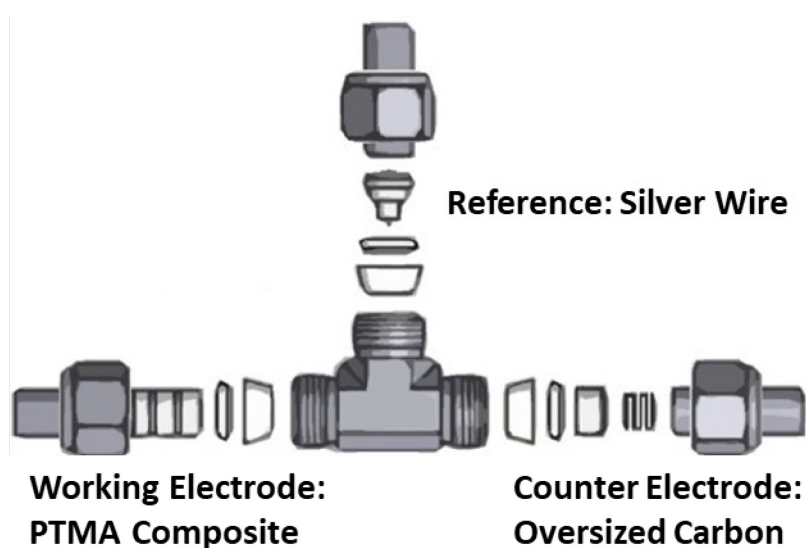


Figure A1: Three-electrode-setup utilized in this work.

List of Publications

In this thesis

- P1** Gerlach, P., & Balducci, A. (2020). *A critical analysis about the underestimated role of the electrolyte in batteries based on organic materials*. ChemElectroChem, 7(11), 2364-2375.
- P2** Gerlach, P., Burges, R., Lex-Balducci, A., Schubert, U. S., & Balducci, A. (2018). *The influence of the electrolyte composition on the electrochemical behaviour of cathodic materials for organic radical batteries*. Journal of Power Sources, 405, 142-149.
- P3** Gerlach, P., Burges, R., Lex-Balducci, A., Schubert, U. S., & Balducci, A. (2019). *Influence of the salt concentration on the electrochemical performance of electrodes for polymeric batteries*. Electrochimica Acta, 306, 610-616.
- P4** Gerlach, P., Burges, R., Lex-Balducci, A., Schubert, U. S., & Balducci, A. (2020). *Aprotic and Protic Ionic Liquids as Electrolytes for Organic Radical Polymers*. Journal of The Electrochemical Society, 167(12), 120546.
- P5** Gerlach, P., & Balducci, A. (2021). *The influence of current density, rest time and electrolyte composition on the self-discharge of organic radical polymers*. Electrochimica Acta, 377, 138070.

Not included

- 1** Chen, R., Bresser, D., Saraf, M., Gerlach, P., Balducci, A., Kunz, S., & Chen, J. (2020). *A comparative review of electrolytes for organic material-based energy storage devices employing solid electrodes and redox fluids*. ChemSusChem.

- 2 Muench, S., Gerlach, P., Burges, R., Strumpf, M., Hoeppener, S., Wild, A., ... & Schubert, U. S. (2021). *Emulsion polymerizations for a sustainable preparation of efficient TEMPO-based electrodes*. *ChemSusChem*, 14(1), 449.

List of Conference Presentations

- 1 Patrick Gerlach, Rene Burges, Alexandra Lex-Balducci, Ulrich S. Schubert, Andrea Balducci, *The influence of the electrolyte composition on the electrochemical behaviour of organic radical polymers*, presented at 69th Annual Meeting of the International Society in Bologna, Italy, 2018
- 2 Patrick Gerlach, Rene Burges, Alexandra Lex-Balducci, Ulrich S. Schubert, Andrea Balducci, *The influence of the electrolyte composition on the electrochemical behaviour of organic radical polymers*, presented at Bunsentagung - 118th General Assembly of the German Bunsen Society for Physical Chemistry in Jena, Germany, 2019
- 3 Patrick Gerlach, Rene Burges, Alexandra Lex-Balducci, Ulrich S. Schubert, Andrea Balducci, *The influence of the electrolyte composition on the electrochemical behaviour of organic radical polymers*, presented at Electrochemical Conference on Energy and the Environment: Bioelectrochemistry and Energy Storage (ECEE) in Glasgow, Scotland, 2019
- 4 Patrick Gerlach, Rene Burges, Alexandra Lex-Balducci, Ulrich S. Schubert, Andrea Balducci, *The Influence of Protic and Aprotic Ionic Liquids on the Electrochemical Behavior of Organic Radical Polymers*, presented at 71st Annual Meeting of the International Society in Belgrade Online, 2020

Supplementary Information

Publication 2

Supplementary Information - The influence of the electrolyte composition on the electrochemical behaviour of PTMA-based electrodes

P. Gerlach ^{a,b}, R. Burges ^{b,c}, A. Lex-Balducci ^{b,c}, U. S. Schubert ^{b,c}, A. Balducci ^{a,b,*}

*Corresponding author: andrea.balducci@uni-jena.de

S1)

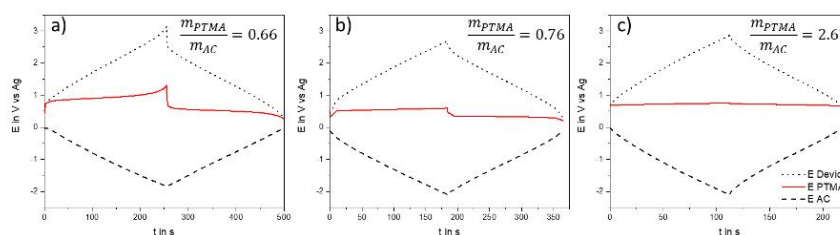


Figure 1: Voltage profiles of PTMA-based electrode; AC-based electrodes and a (not-optimized) hybrid device at cycle 10. The test has been carried out at 10C in 1M PyT₁₄TFSI in PC with a mass balancing $m_{PTMA}:m_{AC}$ equal to a) 0.66, b) 0.76 and c) 2.67.

S2)

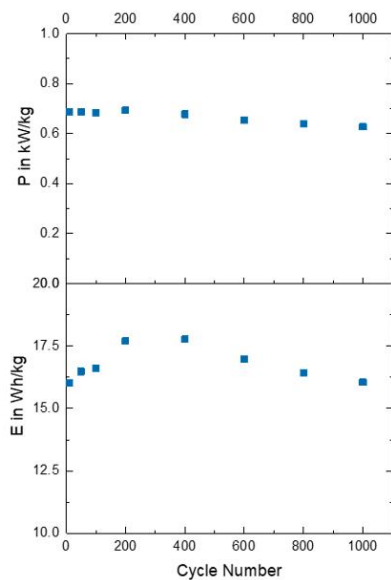


Figure 2: Variation of energy and power of a 3V device containing a PTMA-based positive electrode and an activated carbon (AC)-based negative electrode in neat Pyr₁₄TFSI with a mass balancing of $m_{PTMA}:m_{AC} = 1.2$.

S3)

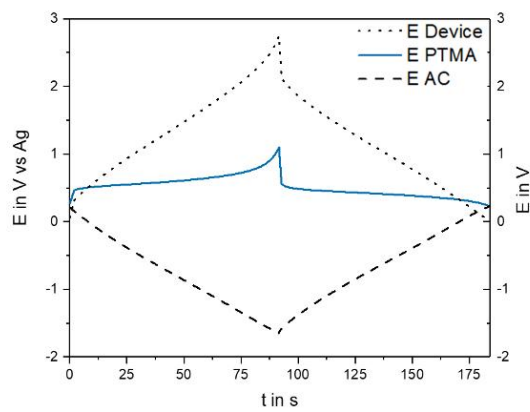


Figure 3: Voltage profile of PTMA-based electrode; AC-based electrodes and a (not-optimized) hybrid device at cycle 1000. The test has been carried out at 10C in neat PyT₁₄TFSI with a mass balancing of $m_{PTMA}:m_{AC} = 1.2$.

Publication 3

Supplementary Information - The influence of the electrolyte concentration on the electrochemical behaviour of PTMA-based electrodes

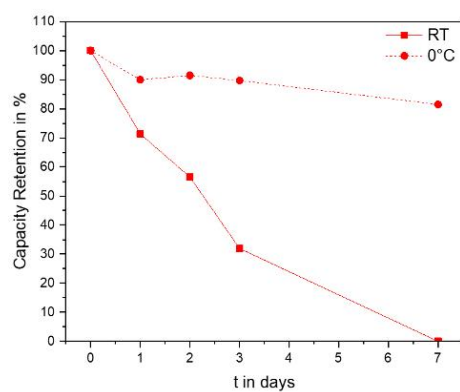
P. Gerlach ^{a,b}, R. Burges ^{b,c}, A. Lex-Balducci ^{b,c}, U. S. Schubert ^{b,c}, A. Balducci^{a,b,*}

*Corresponding author: andrea.balducci@uni-jena.de

Table 1: Remaining charge of the PTMA electrodes after 1, 2, 3 and 11 days of the self-discharge test

| Days of Self-Discharge | 1M Pyr ₁₄ BF ₄ | 2M Pyr ₁₄ BF ₄ | 3M Pyr ₁₄ BF ₄ |
|--------------------------------------|--------------------------------------|--------------------------------------|--------------------------------------|
| Capacity Retention after 1 Day in % | 86.97 | 84.91 | 84.91 |
| Capacity Retention after 2 Day in % | 81.5 | 85.19 | 85.19 |
| Capacity Retention after 3 Day in % | 75.98 | 82.33 | 82.33 |
| Capacity Retention after 11 Day in % | 0 | 0 | 2.16 |

Figure 1: Capacity Retention of PTMA-based electrodes in 1M Pyr₁₄BF₄ in PC after 7 days at room temperature as well as 0°C.



Publication 4

Supplementary Information - Aprotic and protic ionic liquids as electrolytes for organic radical polymers

P. Gerlach ^{a,b}, R. Burges ^{b,c}, A. Lex-Balducci ^{b,c}, U. S. Schubert ^{b,c}, A. Balducci ^{a,b,*}

*Corresponding author: andrea.balducci@uni-jena.de

S1)

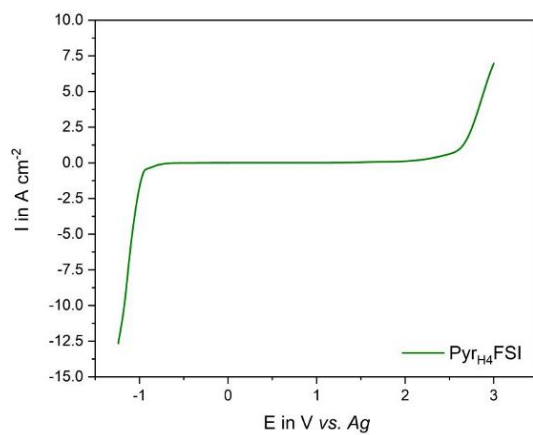


Figure S1: Electrochemical stability window of Pyr_{H4}FSI

S2)

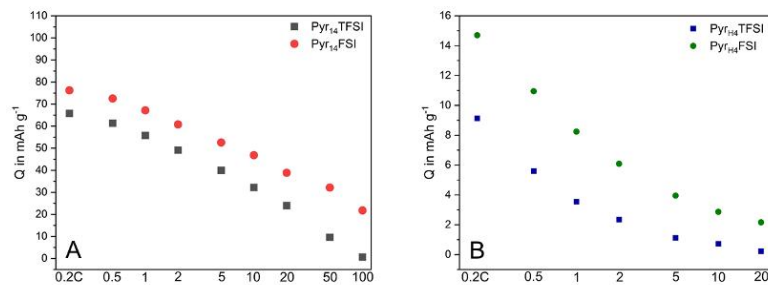


Figure S2: Rate Capability test with absolute values of retained specific capacity for all ILs from 0.2C to 100C

S3)

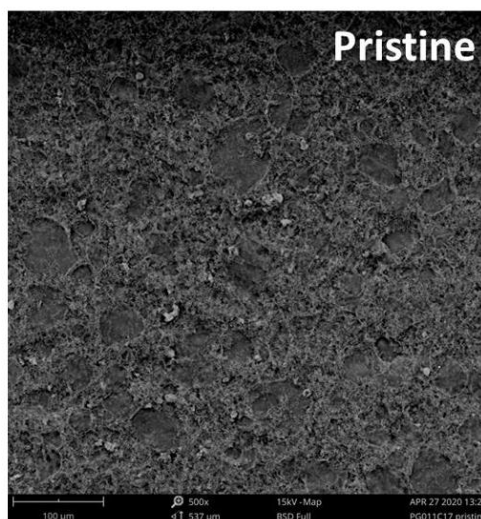


Figure S3: SEM Figures of pristine PTMA-based electrode surface with a magnification of 500 and 15 kV

S4)

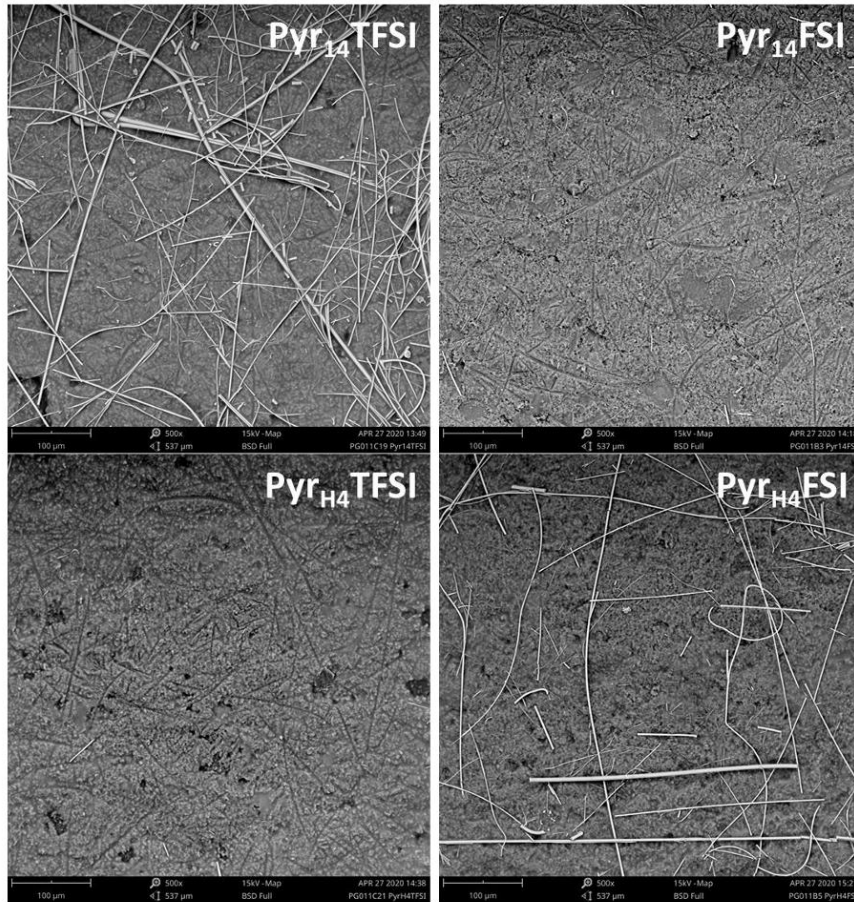


Figure S4: SEM Figures of cycled PTMA-based electrode surfaces with a magnification of 500 and 15 kV

Publication 5

Supplementary Information –

The influence of current density, rest time and electrolyte composition on the self-discharge of organic radical polymers

P. Gerlach^{a,b}, A. Balducci^{a,b,*}

*Corresponding author: andrea.balducci@uni-jena.de

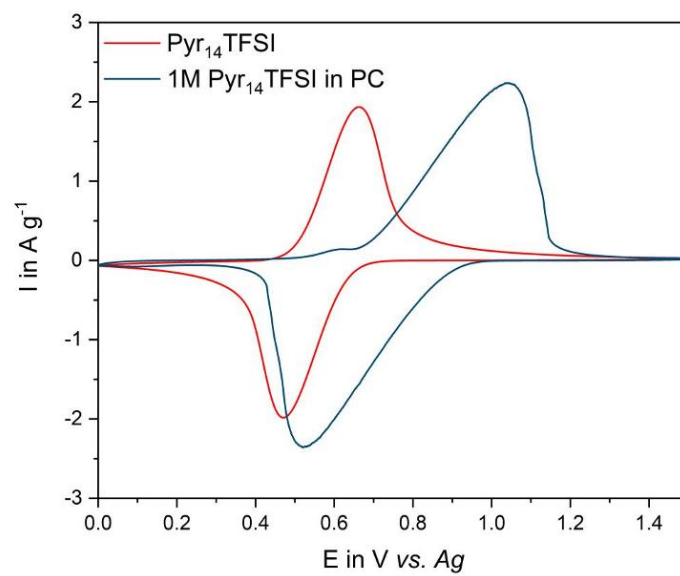


Figure S1: Cyclic voltammogram of PTMA-based electrodes at 2 mV s^{-1} in Pyr₁₄TFSI and 1M Pyr₁₄TFSI in PC

| Time | Charge (C) and Discharge (D) Capacity in mAh g ⁻¹ for every applied C-Rate | | | | | | | | | |
|--------|---|----|-------|----|----|----|----|----|-----|----|
| | 0.1 C | | 0.5 C | | 1C | | 2C | | 10C | |
| | C | D | C | D | C | D | C | D | C | D |
| 10 min | 68 | 64 | 58 | 52 | 53 | 46 | 47 | 38 | 43 | 31 |
| 1 h | 66 | 65 | 63 | 60 | 52 | 45 | 48 | 35 | 42 | 23 |
| 10 h | 69 | 65 | 56 | 46 | 53 | 39 | 48 | 32 | 42 | 21 |
| 1 day | 67 | 63 | 55 | 50 | 52 | 39 | 47 | 32 | 44 | 23 |

Table S2: Charge and discharge capacities of PTMA-based electrode in Pyr₁₄TFSI

| Time | Charge (C) and Discharge (D) Capacity in mAh g ⁻¹ for every applied C-Rate | | | | | | | | | |
|--------|---|----|-------|----|----|----|----|----|-----|----|
| | 0.1 C | | 0.5 C | | 1C | | 2C | | 10C | |
| | C | D | C | D | C | D | C | D | C | D |
| 10 min | 81 | 79 | 79 | 78 | 79 | 78 | 79 | 77 | 69 | 50 |
| 1 h | 81 | 78 | 88 | 87 | 79 | 78 | 79 | 77 | 84 | 80 |
| 10 h | 80 | 77 | 85 | 82 | 79 | 77 | 78 | 76 | 81 | 76 |
| 1 day | 80 | 74 | 88 | 83 | 78 | 74 | 78 | 73 | 80 | 74 |

Table S3: Charge and discharge capacities of PTMA-based electrode in 1M Pyr₁₄TFSI in

PC

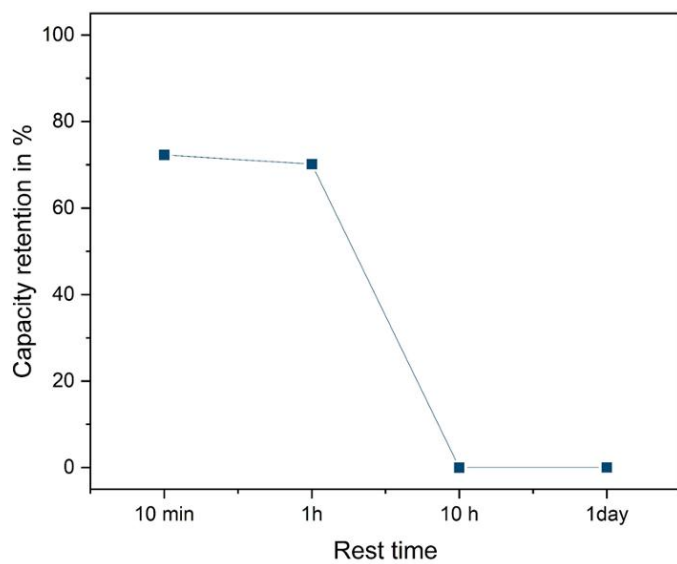


Figure S4: Capacity retention of PTMA-based electrode with respect to the rest time at a current density of 20C in 1M Py_{r14}TFSI in PC